



**POST-PROCESSING RESOLUTION ENHANCEMENT
OF OPEN SKIES PHOTOGRAPHIC IMAGERY**

THESIS

Daniel E. Sperl, Captain, USAF

AFIT/GEO/ENG/00M-03

**DEPARTMENT OF THE AIR FORCE
AIR UNIVERSITY**

AIR FORCE INSTITUTE OF TECHNOLOGY

Wright-Patterson Air Force Base, Ohio

APPROVED FOR PUBLIC RELEASE; DISTRIBUTION UNLIMITED.

DTIC QUALITY INSPECTED 4

20000815 162

The views expressed in this thesis/dissertation are those of the author and do not reflect the official policy or position of the United States Air Force, Department of Defense, or the U. S. Government

AFIT/GEO/ENG/00M-03

POST-PROCESSING RESOLUTION
ENHANCEMENT OF OPEN SKIES PHOTOGRAPHIC IMAGERY

THESIS

Presented to the Faculty

Department of Electrical and Computer Engineering

Graduate School of Engineering and Management

of the Air Force Institute of Technology

Air University

Air Education and Training Command

In Partial Fulfillment of the Requirements for the

Degree of Master of Science in Electro-Optics

Daniel E. Sperl, B.S., M.B.A.

Captain, USAF

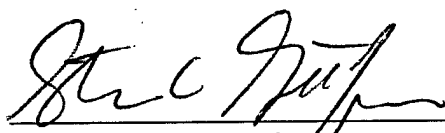
March 2000

Approved for public release; distribution unlimited

POST-PROCESSING RESOLUTION
ENHANCEMENT OF OPEN SKIES PHOTOGRAPHIC IMAGERY

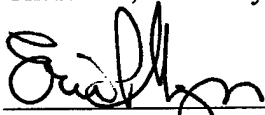
Daniel E. Sperl, B.S., M.B.A.
Captain, USAF

Approved:



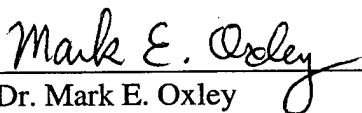
Dr. Steven C. Gustafson
Chairman, Advisory Committee

8 Mar 00
Date



Maj Eric P. Magee
Member, Advisory Committee

8 MAR 2000
Date



Dr. Mark E. Oxley
Member, Advisory Committee

8 March 2000
Date

ACKNOWLEDGMENTS

The writer wishes to express special thanks to my faculty advisors, Dr. Steve Gustafson, Maj Eric Magee, and Dr. Mark Oxley, whose encouragement, helpful counsel, and practical suggestions were crucial to the successful outcome of this thesis project. Appreciation is also due to Capt Tom Fitzgerald and Dennis Grieshop for their assistance with obtaining aerial photographs of Wright-Patterson AFB and to Capt Kelce Wilson for his help with Matlab.

This statement would be incomplete without recognizing my wife Diana, who has been so understanding during my graduate school career. She has been my scribe, my proofreader, and my encouragement. I also must recognize my three children, Leland, Sabrina, and Ryan. They have been my other source of inspiration.

Daniel E. Sperl

TABLE OF CONTENTS

ACKNOWLEDGMENTS	iv
LIST OF FIGURES	vi
LIST OF TABLES	viii
ABSTRACT	ix
I. INTRODUCTION	1
II. BACKGROUND	2
History	2
Data Collection and Aircraft Operations	3
Imaging Test Objects	6
III. REVIEW OF RELEVANT LITERATURE AND RESEARCH	13
Super-Resolution of Images: Algorithms, Principles, and Performance	13
IV. RESEARCH METHODOLOGY	15
Enhancement Using Commercial Software	15
Enhancement Using Model Fit	16
V. RESULTS	26
Enhancement Using Commercial Product	26
Enhancement Using Model Fit	28
VI. CONCLUSIONS and RECOMMENDATIONS	50
APPENDIX A. Matlab Code	52
APPENDIX B. List of Scanned Negatives	80
BIBLIOGRAPHY	81
Vita	85

LIST OF FIGURES

Figure 1. US Optical Cameras	3
Figure 2: Ground Resolution Distance	4
Figure 3. US Open Skies OC-135 Aircraft [37]	5
Figure 4. 3-Bar Target	6
Figure 5. Airstar Emblem	7
Figure 6. Aerial View of Area B, WPAFB	8
Figure 7. Extraction of 3-Bar Target from Area B Imagery	9
Figure 8. Original Image of Group 9, 3-Bar Target, 2D & 3D Views	10
Figure 9. Original Image of Group 9, 3-Bar Target, 2D & 3D Views - Enlarged	10
Figure 10. C-119 Cargo Plane	11
Figure 11. B-1A Bomber	11
Figure 12. Image of 2-Bar Target Degraded with German Filter	12
Figure 13: Bias/Variance Tradeoff	17
Figure 14. Line Scan of an Image Row	20
Figure 15: Flowchart for 3-Bar and 2-Bar Target Model Fit	21
Figure 16: Linescan Flowchart for 3-Bar and 2-Bar Target Model Fit	22
Figure 17. Line Plots of Bar Groups 13, 14, & 15	23
Figure 18: Flowchart for Airstar Model Fit	25
Figure 19. Enhancement by Commercial Software	26
Figure 20. Line Plots for Bar Groups 9, 11, & 13	27
Figure 21. Enhancement of a C-119 Cargo Plane	27
Figure 22. Original Image of Group 9, tar66a.tif, 2D & 3D Views	32

Figure 23. Optimized Image of Group 9, 2D & 3D Views	33
Figure 24. Original & Optimized Images of Group 9	34
Figure 25. Original Image of Group 12, 5.7 micron scan, tar66a.tif, 2D & 3D Views .	35
Figure 26. Optimized Image of Group 12, 2D & 3D Views	36
Figure 27. Original & Optimized Images of Group 12	37
Figure 28. Original Image of Group 12, 4 micron scan, target66u.tif, 2D & 3D Views	38
Figure 29. Optimized Image of Group 12, 2D & 3D Views	39
Figure 30. Original & Optimized Images of Group 12	40
Figure 31. Original Image of 2-Bar Target, German S1 Filter, ges1a.tif, 2D & 3 D Views	41
Figure 32. Optimized Image of 2-Bar Target, German S1 Filter, 2D & 3D Views	42
Figure 33. Original & Optimized Images of 2-Bar Target, German S1 Filter	43
Figure 34. Original Airstar, B-1A Bomber, plane55b.tif, 2D & 3D Views	44
Figure 35. Model Airstar, B-1A Bomber, 2D & 3D Views	45
Figure 36. Optimized Airstar, B-1A Bomber, 2D & 3D Views	46
Figure 37. Original Airstar, C-119 Cargo Plane, plane55a.tif, 2D & 3D Views	47
Figure 38. Model Airstar, C-119 Cargo Plane, 2D & 3D Views	48
Figure 39. Optimized Airstar, C-119 Cargo Plane, 2D & 3D Views	49

LIST OF TABLES

Table 1. Items Visible Based on the 30 Centimeter Ground Resolution Limit	2
Table 2. Generic Model Fit Procedure	19
Table 3. List of Matlab Code and Data Files	52

ABSTRACT

The Treaty on Opens Skies allows any signatory nation to fly a specifically equipped reconnaissance aircraft anywhere over the territory of any other signatory nation. For photographic images, this treaty allows for a maximum ground resolution of 30 cm. The National Air Intelligence Center (NAIC), which manages implementation of the Open Skies Treaty for the US Air Force, wants to determine if post-processing of the photographic images can improve spatial resolution beyond 30 cm, and if so, determine the improvement achievable. Results presented in this thesis show that standard linear filters (edge and sharpening) do not improve resolution significantly and that super-resolution techniques are necessary. Most importantly, this thesis describes a prior-knowledge model fitting technique that improves resolution beyond the 30 cm treaty limit. The capabilities of this technique are demonstrated for a standard 3-Bar target, an optically degraded 2-Bar target, and the USAF airstar emblem.

Post-Processing Resolution
Enhancement of Open Skies Photographic Imagery

I. INTRODUCTION

The Treaty on Open Skies is an international effort to promote goodwill and openness. The treaty allows any signatory nation to fly a specifically equipped reconnaissance aircraft anywhere over the territory of any other signatory nation [12:4]. For photographic images, the treaty allows for a maximum ground resolution of 30 cm. Unfortunately, due to advances in technology, post-processing may increase this maximum ground resolution. The goal of this research is to develop Matlab models that demonstrate post-processing resolution enhancement of Open Skies photographic imagery.

Chapter II provides background on Open Skies and the data set of aerial images used for this research. Chapter III presents some relevant previous research, results, and Chapter IV reviews super-resolution theory. Chapter V discusses results, and Chapter VI presents conclusions and recommendations.

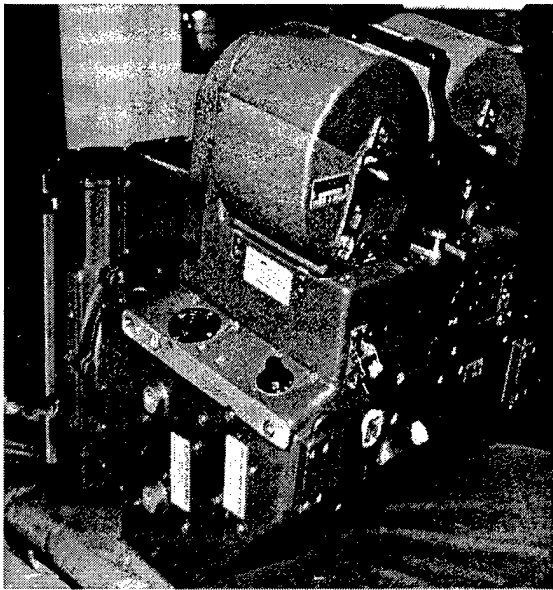
II. BACKGROUND

History

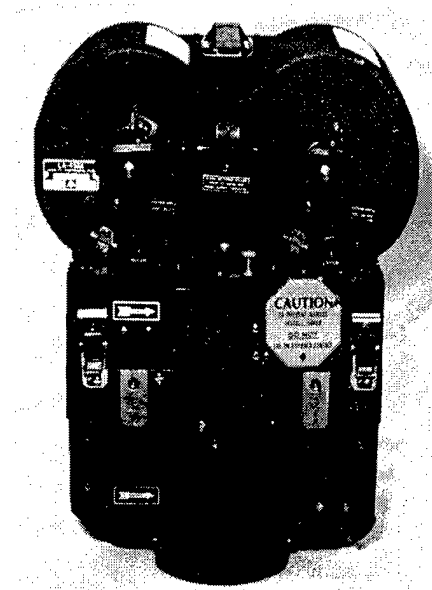
The United States, along with 26 other nations, signed the Treaty on Open Skies (OS) on 24 March 1992 as part of an international effort to promote openness and trust building; however, "The Treaty is not an arms control program [12:5]." Each country allows overflights of their entire national territory, including territorial waters and islands by other countries. The treaty enters into force (EIF) when twenty countries that include Canada, Germany, Russia, Belarus, US, France, UK, Italy, Turkey, and Ukraine ratify it; this has not happened yet [37]. Table 1 gives examples of items that are and are not visible under the treaty resolution limit of 30 cm. The OS aircraft are equipped with an approved suite of sensors.

Table 1. Items Visible Based on the 30 Centimeter Ground Resolution Limit [37]

CAN	CANNOT
Identify small aircraft by type (such as F-14s, F-15s, F-16s) when singly deployed.	Identify a specific model fighter (such as an F-16A versus F-16C) by small details such as dielectric patches on wings.
Read call letters and numbers on wings when 3 feet high.	Identify the pitot tube on a fighter aircraft.
Detect uploaded weapons on aircraft wings.	Identify a specific weapon type.
Identify an F-16 fighter from an F-16 trainer by canopy configuration.	Identify on the appropriate model fighter, wing flap actuator fairings and yaw vanes.
Detect presence of shipboard weapons and major electronics (guns, missiles, surface search radar).	Accurately identify by specific type shipboard weapons and major electronics.
Detect the presence and pattern of mooring lines.	Identify draft marks.
Detect presence of life rails when raised.	Identify mast configuration.
Accurately distinguish smaller vehicle types (for instance, pick-up trucks versus sedans).	Identify small ground support equipment by type, such as dollies, tow bars, and fire extinguisher carts.



KA-91C Panoramic Camera



KA-87E Framing Camera

Figure 1. US Optical Cameras

Data Collection and Aircraft Operations

The Treaty allows three types of sensors: optical, infrared, and Synthetic Aperture Radar (SAR). Optical cameras (Figure 1) include one vertically mounted framing camera, two obliquely mounted framing cameras, one panoramic camera, and one video camera. Infrared sensors include a line scanner and a side-looking SAR. Currently, and until EIF, the Treaty allows only optical sensors (cameras) [12:5]. The optical and SAR sensors may be used during the first three years after EIF, but the infrared (IR) may not be used until three years after EIF unless otherwise agreed. During an observation flight, sensor operation is suspended if the aircraft altitude is below the minimum altitude, or if the flight deviates more than 50 km from the planned flight path. Both parties receive copies of the data, and any other treaty signatory may get a copy by written request and

payment for reproduction. Both ground resolution distance (GRD) [12:9-10], shown in Equation 1, and safety of flight restricts the lowest operating altitude over a particular area.

$$GRD = \frac{height * resolution}{focal\ length * theta} \quad (1)$$

where *height* is the altitude difference between the camera and target, *resolution* is the distance between observable cycles on the film substrate, the *focal length* is that of the camera, and *theta* is the tangent angle when the target is not directly under the camera (Figure 2). The GRD, which is the minimum distance on the ground between two closely

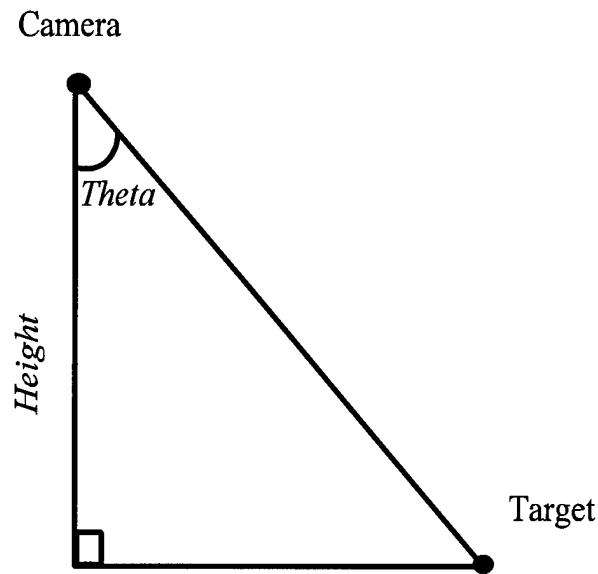


Figure 2: Ground Resolution Distance

located objects at which they are distinguishable as separate objects, defines the altitude that allows maximum resolution for the operating sensors (the lower the altitude, the better the spatial resolution because the sensor is closer to imaged objects). The aircraft's service ceiling restricts the maximum operating altitude [37]. The country being overflown has the right to supply the aircraft (taxi option), otherwise, the observing

country may use its own aircraft. In either case, an inspection at the OS point of entry ensures treaty conformance of aircraft and sensors. The United States uses OC-135B aircraft as depicted in Figure 3.



Figure 3. US Open Skies OC-135 Aircraft [37]

Imaging Test Objects

The United States Air Force (USAF) uses a 3-Bar target (Figure 4) which includes horizontal and vertical bar groups of various sizes and spacings. The two triangles show which bar group meets the treaty spatial resolution limit of 30 cm, which means that objects at least 30 cm apart on they can distinguish ground from each other [12:8-9].

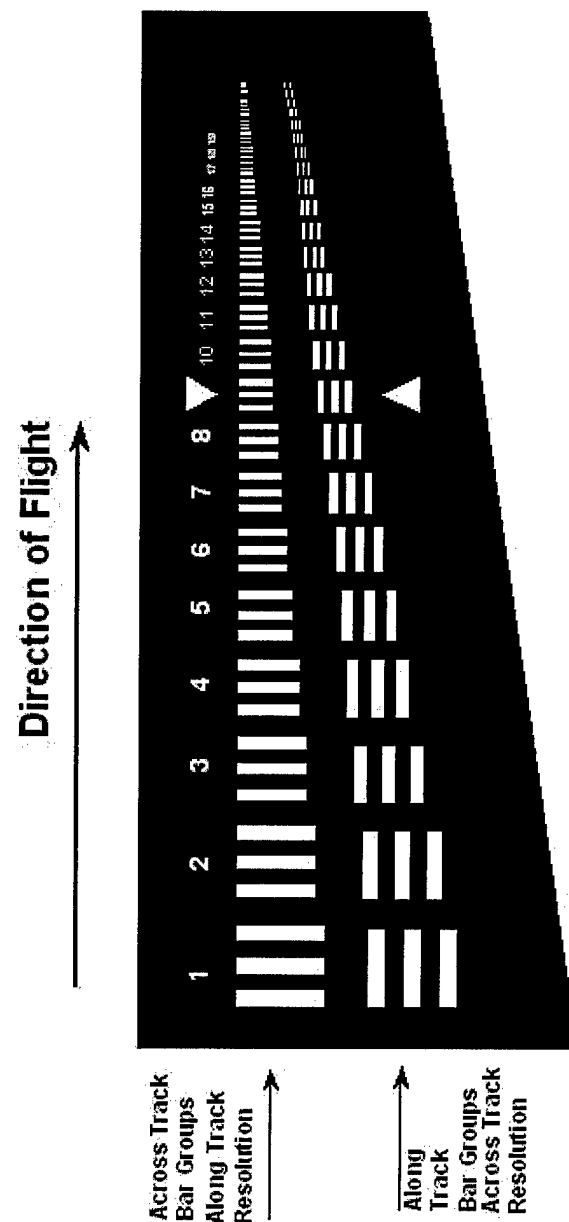


Figure 4. 3-Bar Target

The airstar emblem (Figure 5) is a painted object on all US military aircraft; it consists of a blue field with a white star and white and red stripes. This colored version of the airstar emblem has been phased out and replaced with a grayscale version to reduce visibility and increase survivability.

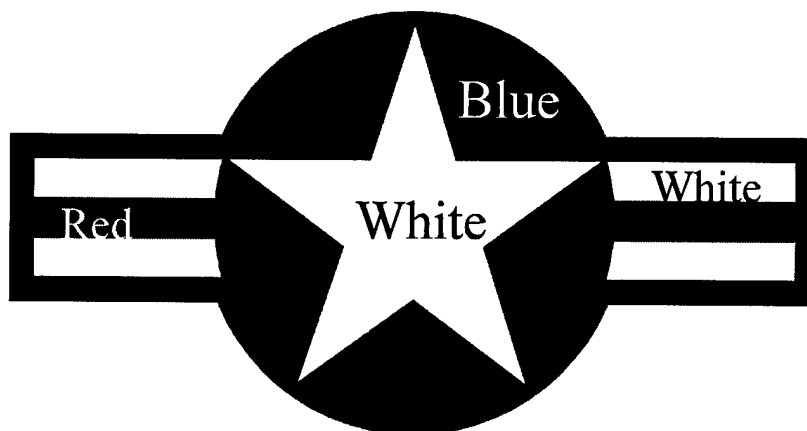


Figure 5. Airstar Emblem

For this research the data set is a series of aerial negatives from an altitude of approximately 1,250 m provided by NAIC (Appendix B). The images in these negatives are of the 3-Bar target, the USAF Museum, and surrounding area in Area B at Wright-Patterson AFB, Ohio, and a 2-Bar target located in Europe. These images were digitized using a scanner with a pixel resolution of 5.7 microns. An example of one of these images (66target.tif) is given in Figure 6. Since multi-frame resolution was not the goal of this thesis, frames were chosen (checkmarked in Appendix B) and the relevant regions of interest were extracted. For example, an area that contained the 3-Bar target was extracted from 66target.tif (Figure 7). The grain sizes on negatives are usually uniform and submicron in size, but the grain size can be up to 4 microns [30]. Since the

resolution of the negatives is much finer than the scanner's 5.7 micron resolution, the negatives were optically enlarged and digitized to provide more samples. For example, the group 9 bar group in the original negative yielded a 21 by 21 pixel matrix (Figure 8) , whereas the enlarged negative yielded a 200 by 200 pixel matrix (Figure 9). Enlarging the negatives added some noise but did not affect the results, which are discussed in

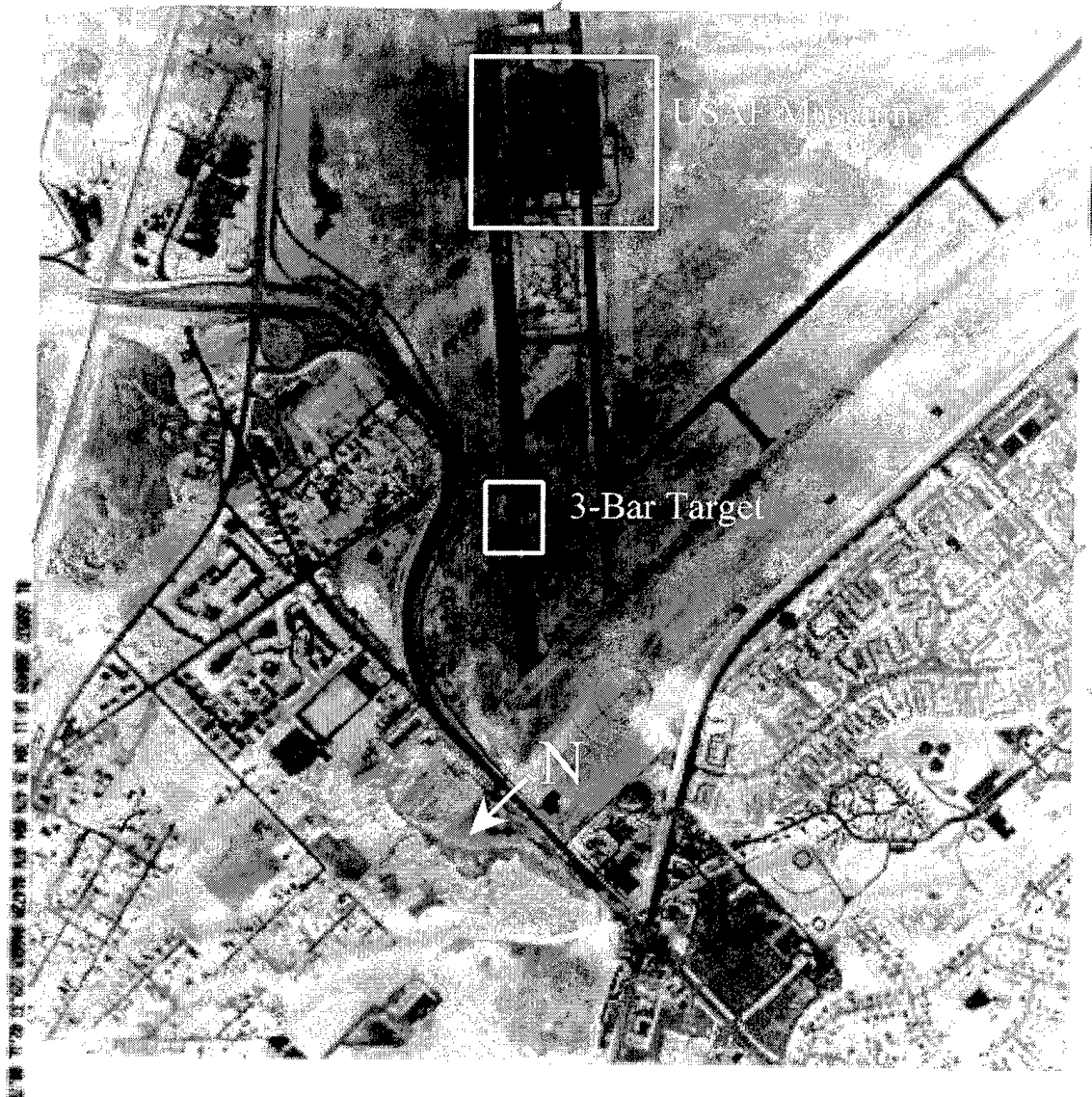


Figure 6. Aerial View of Area B, WPAFB

Chapter IV. Additionally, the data set includes images of aircraft on static display at the USAF museum, a C-119 cargo plane (Figure 10) and a B-1A bomber (Figure 11), and a 2-Bar target (Figure 12), which was optically degraded by a German phase filter [35]. For the B-1A and C-119, the measured width across the stripes in the airstar is 28.2 cm (red: 6.2 cm, white: 6.2 cm times 2, and blue: 4.8 cm times 2) and 57.8 cm (red: 13.0 cm, white: 12.8 cm times 2, and blue: 9.6 cm times 2) respectively. The bar groups next to the white rectangular region (Figure 12) are both 30 cm and satisfy the Treaty requirement. The images of the planes and the 2-Bar target were also optically enlarged to provide additional samples.

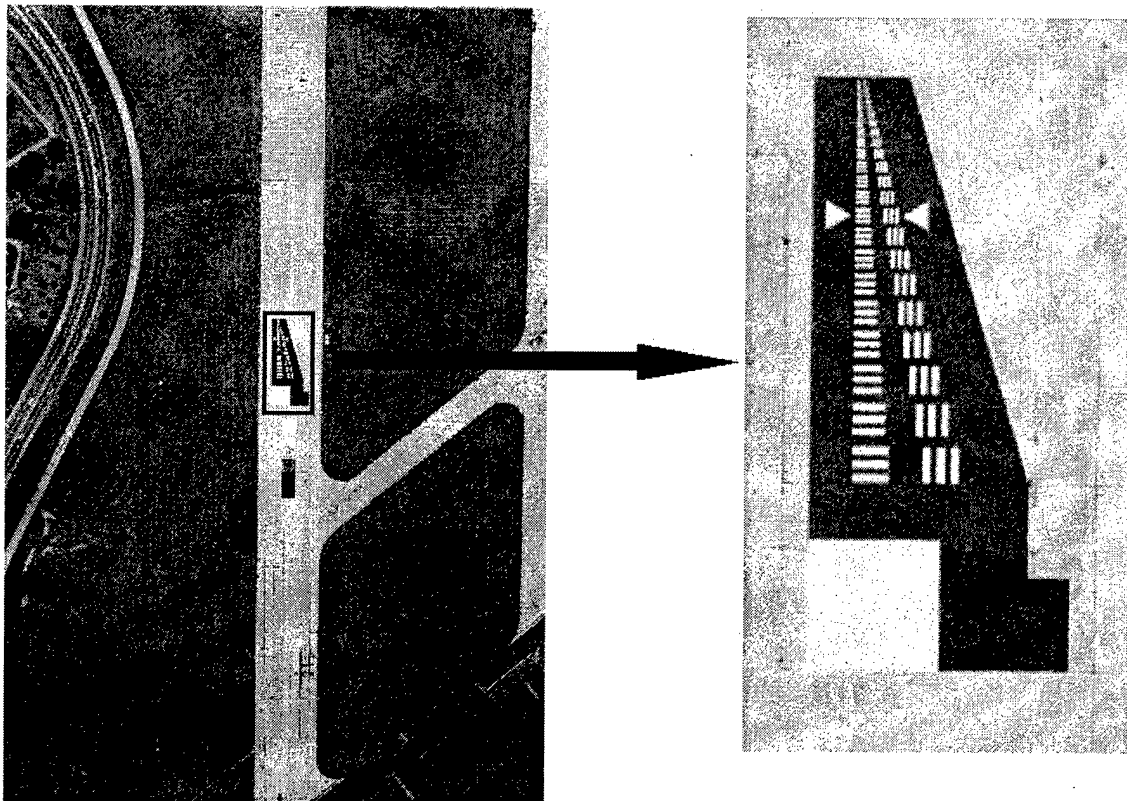


Figure 7. Extraction of 3-Bar Target from Area B Imagery

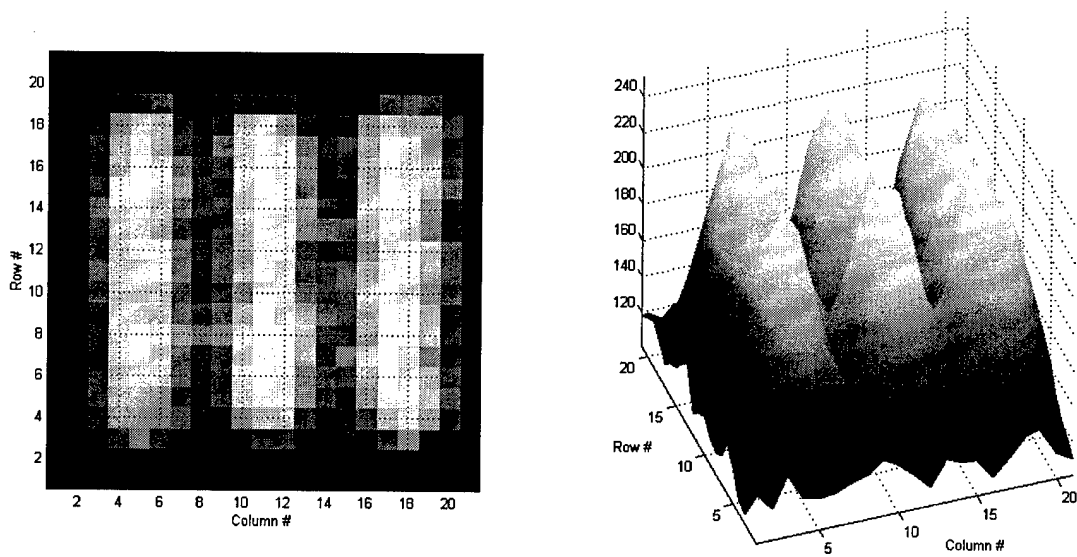


Figure 8. Original Image of Group 9, 3-Bar Target, 2D & 3D Views

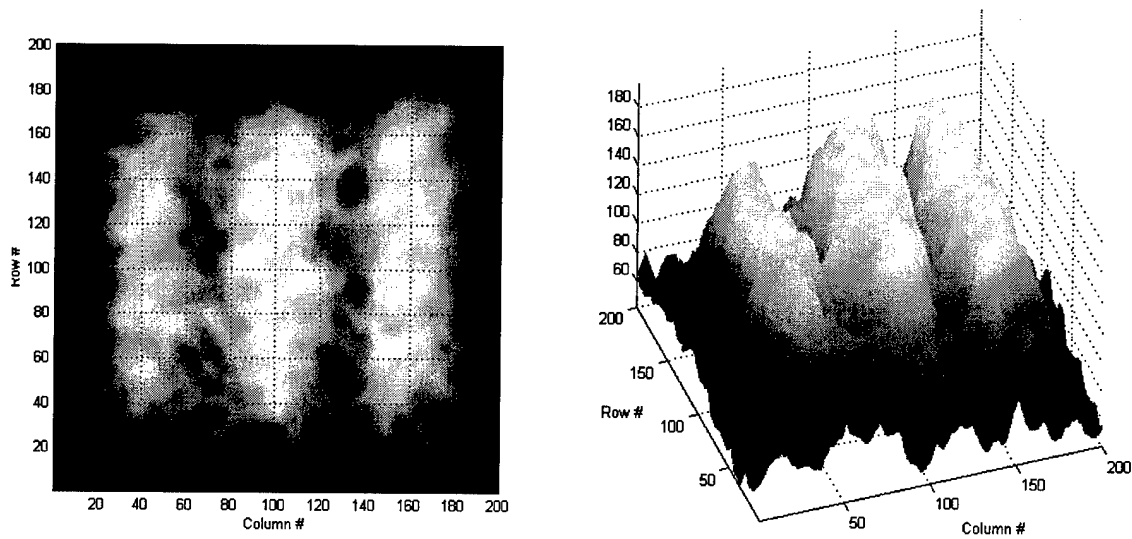


Figure 9. Original Image of Group 9, 3-Bar Target, 2D & 3D Views - Enlarged

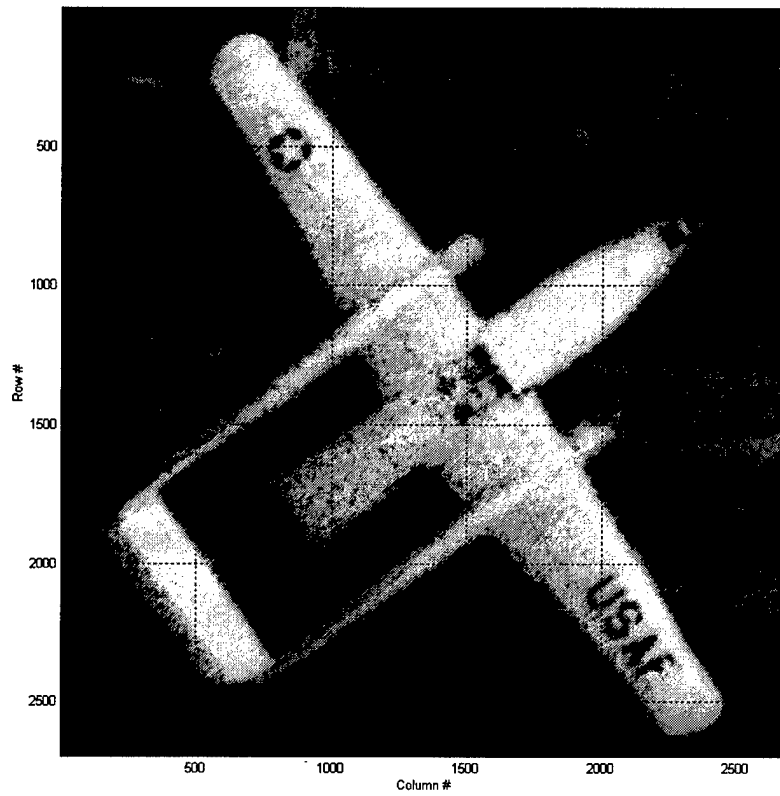


Figure 10. C-119 Cargo Plane

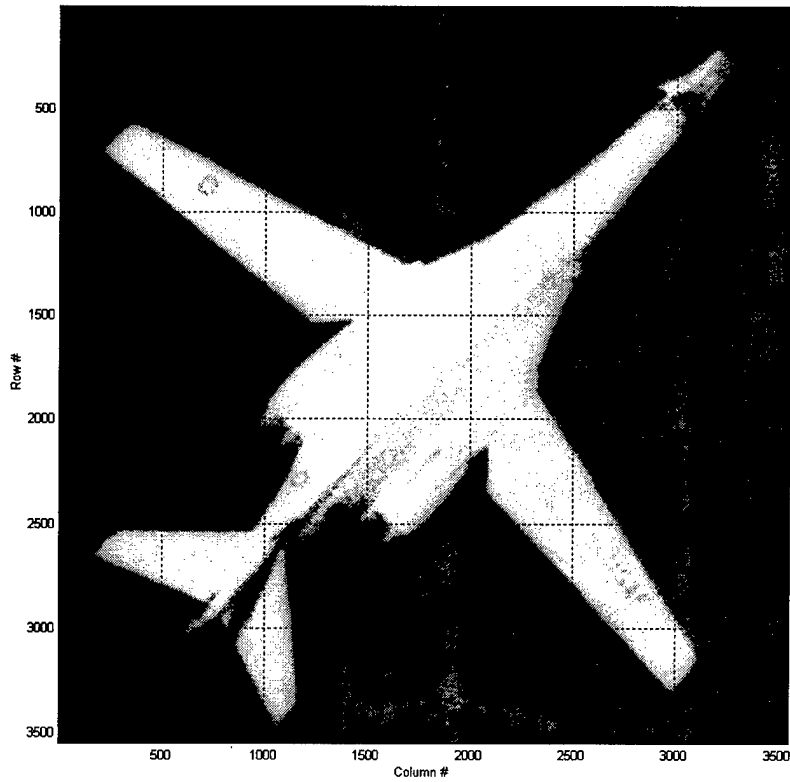


Figure 11. B-1A Bomber

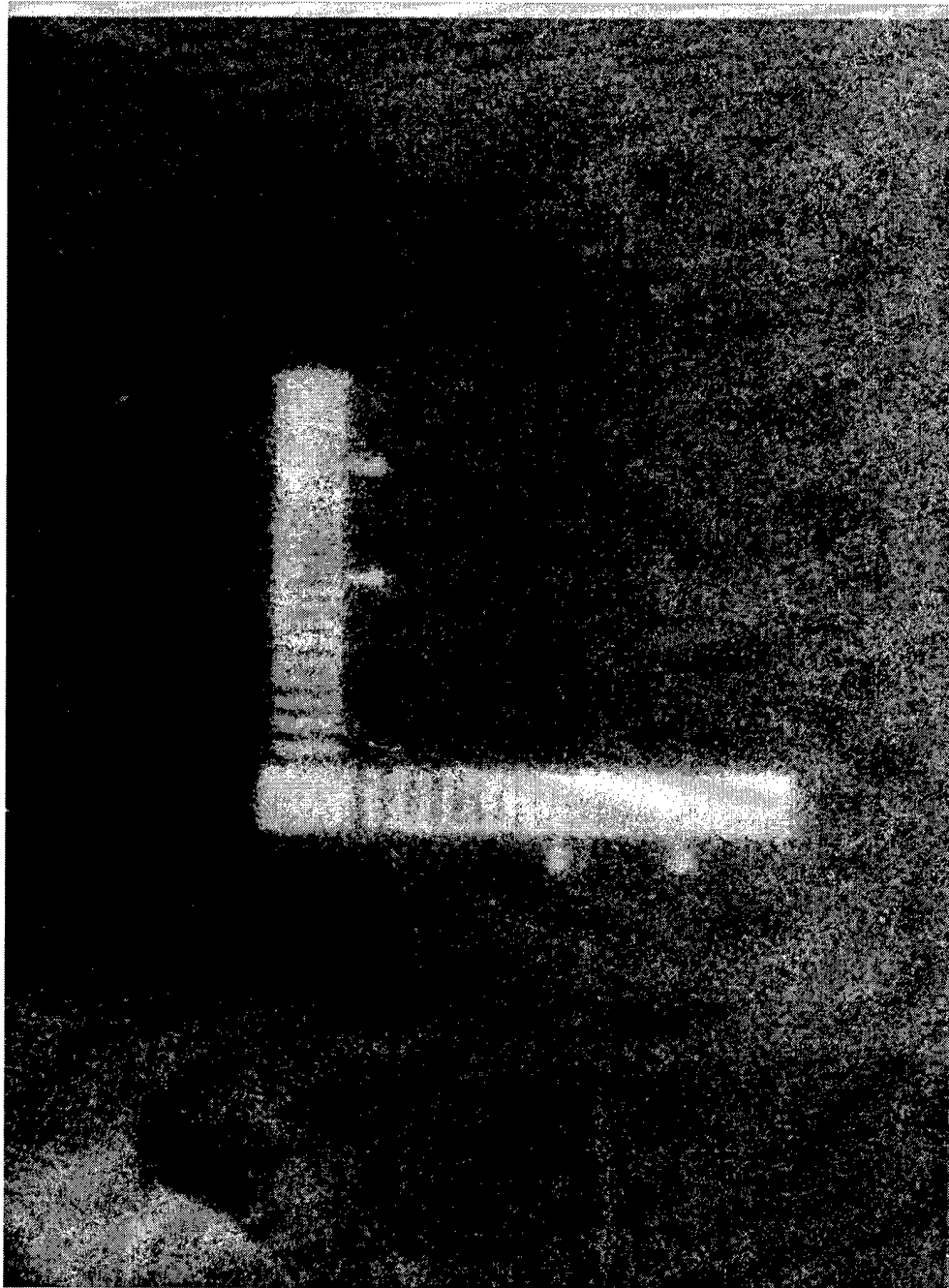


Figure 12. Image of 2-Bar Target Degraded with German Filter

III. REVIEW OF RELEVANT LITERATURE AND RESEARCH

The review given here is based upon information available from libraries, the Internet, and the National Air Intelligence Center.

Super-Resolution of Images: Algorithms, Principles, and Performance

Many technical documents relating to image enhancement [3, 4, 7, 10, 14, 15, 32, 38, 39], blind deconvolution [28, 29], and super-resolution [1, 9, 11, 17-22, 24-27, 34, 41-47] present methods for improving the resolution of multi-frame sequences.

Unfortunately, these documents do not apply to this research, because image registration [1, 8, 19, 20, 23, 26, 25-27, 43, 45] is assumed, and the data set used in this research is not registered. Image registration is an area of research beyond the scope of this thesis. From these documents, only two are relevant to this research.

The first relevant article to this research is a paper on the super-resolution of images by Hunt [22], which provides a good overview of super-resolution principles and techniques. This paper discusses diffraction as the key motivation for performing super-resolution, and it indicates that the use of prior information is one critical principle that enables super-resolution:

- “The spatial frequencies that are captured by image formation below the diffraction limit contain some of the information necessary to reconstruct spatial frequencies above the diffraction limit;
- Using additional information about the object (e.g., compact, hence possessing an analytic Fourier transform) provides a means to use the information below the diffraction limit to reconstruct information above that limit [22:298-299].”

This paper also lists some features that affect the performance of super-resolution

algorithms:

- Object, size, shape, and location - "Usually the image of an object is adequate to make an estimate of the approximate size, shape, and location of the object. The size and shape characteristics of the object can be inferred from measured size and shape of the image and optical system PSF [22:301]."
- Bounds on object intensity - "The minimum intensity level of an object is zero, because negative light is meaningless in incoherent optical image formation[22:301]."

The other article that is relevant to this research is by Matson [33] and discusses error reduction in images through use of perfect prior knowledge. The technique is based on the notion that "part of an image may be known exactly, and this can be used as a constraint to decrease noise levels in the image outside the region of perfectly known data [33]." Matson's algorithm requires multiple iterations between the spatial and frequency domains until the noise is minimized outside the region of prior knowledge. "The algorithm's steps are: (1) in the image domain, replace the measured data with the prior knowledge in the region where prior knowledge is available; (2) Fourier transform; (3) if the real (imaginary) part of the measured Fourier data is less noisy than the imaginary (real), replace the iterated real (imaginary) part of the Fourier data with the measured data, but leave the imaginary (real) part unchanged; (4) inverse-Fourier-transform; (5) go back to step (1) until the noise is minimized outside the region of prior knowledge [33]."

The use of prior information, positive image intensity, object size, error reduction, and shape relationships are the basis for the super-resolution techniques discussed in the next chapter.

IV. RESEARCH METHODOLOGY

The Open Skies treaty requires a calibration flight to be flown over a 3-Bar target before a signatory nation performs data gathering missions. Data from the calibration flight is used to set the minimum altitude and GRD at which the data gathering missions are flown. Due to weather constraints (i.e., clouds, storms, etc.), the National Air Intelligence Center wants the capability to fly at lower altitudes while still maintaining the 30 cm spatial resolution limit. Flying at lower altitudes increases spatial resolution. Therefore, the optics used to record images must be degraded to the treaty requirement. Since the optics are artificially degraded, it is also necessary to ensure that the increased spatial resolution from flying at lower altitudes cannot be recovered (e.g., by post-processing). This research demonstrates that the resolution of Open Skies photographic imagery can be increased beyond the treaty limit of 30 cm if certain a priori knowledge of the image exists. The methods reported here deal with a 3-Bar target (Figure 4) and an airstar emblem (Figure 5).

Enhancement Using Commercial Software

Resolution enhancement was attempted using three commercially available programs for editing photographs: Ulead PhotoImpact 4.2, Scion Image, and Micrografx's Picture Publisher. All three programs contain image enhancement functions for sharpening, edge detection, and contrast adjustment.

Enhancement Using Model Fit

One classic approach to increasing the resolution of an image is to use the Gerchberg algorithm [22], which requires multiple iterations and transformations between the spatial and spatial frequency domains. Since enough prior information exists about the 3-Bar target and the airstar emblem, employing a spatial domain model fit algorithm is appropriate.

Resolution enhancement using the model fit method may be justified by extending the rationale presented by Hunt [22] and Matson [33]. Suppose that a given gray level digital image consists of an underlying model plus additive noise, but that no prior knowledge is available about the model. Then the most unbiased (equivalent to maximum entropy) choice for the underlying model is the image mean (i.e., the mean of all pixel level values), and the standard deviation about this mean may be chosen as the variance in the given data. Now suppose that prior knowledge about the model exists (i.e., the model is a known object) and that the knowledge is perfect except for linear transformations. Then the only unknowns are the relative translation, rotation, and scale of the object and the linear scaling of the image intensity. Thus, six parameters may be evaluated to fit the model to the image: horizontal and vertical placement, rotation angle about the horizontal axis, size of the object, and minimum and maximum gray level values. Some of these parameters may be fixed (e.g., the rotation angle is assumed zero). The values of the six parameters that minimize the mean squared error (MSE) [5:11] between the model and given data may be chosen to specify the fitted model where the minimized quantity is:

$$MSE = \frac{\sum_{i=1}^n \sum_{j=1}^m \left[\left(Given_{ij} - Model_{ij} \right)^2 \right]}{nm} \quad (2)$$

Where *Given* represents the input data (image) matrix, *Model* represents the model data matrix, and *n* and *m* denotes the number of rows and columns in the matrices. Note that the two matrices have equal dimensions. When the MSE equals zero, the model fits the data perfectly. Depending on the situation, a perfect fit may or may not be desirable. For example, if the given (original) image of a 3-Bar target is well-defined and free of distortions (i.e., atmospheric, scanner, camera, etc.), then a MSE that equals zero is highly desired because the given data and the model are very similar. The Open Skies imagery falls is not well-defined, which means that the MSE for the best fit model cannot be equal to zero. Therefore, finding the best fit model becomes a bias/variance tradeoff

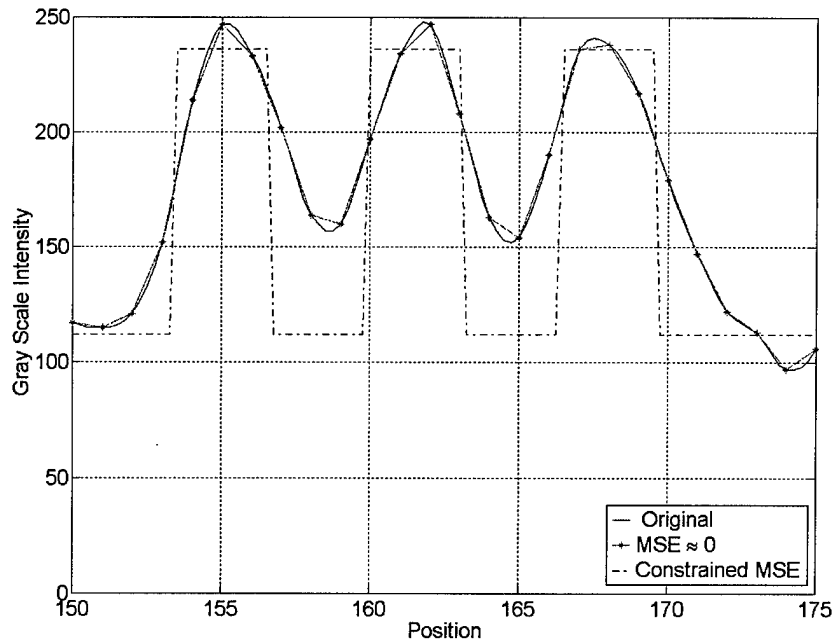


Figure 13: Bias/Variance Tradeoff

(i.e., fit vs. smoothness of fit of the model to the given data) [5, 13] with the minimum MSE contrained by prior knowledge (see Figure 13). The standard deviation about the fitted model (i.e., \sqrt{MSE}) may then be chosen as a measure of the added noise, and this standard deviation will generally be less than the standard deviation [5:34] about the image mean (\overline{Given}):

$$STD\ Given = \sqrt{\frac{\sum_{i=1}^n \sum_{j=1}^m \left[\left(Given_{ij} - \overline{Given} \right)^2 \right]}{nm}} \quad (3)$$

where

$$\overline{Given} = \frac{\sum_{i=1}^n \sum_{j=1}^m \left(Given_{ij} \right)}{nm} \quad (4)$$

Therefore, the following expression may be chosen to specify a processed image that incorporates the prior knowledge:

$$New_{ij} = Given_{ij} + \left(Model_{ij} - Given_{ij} \right) (\Gamma) \quad for\ 0 < \Gamma < 1 \quad (5)$$

where New is the processed image, and $\Gamma = \sqrt{MSE} / STD\ Given$, is the ratio of standard deviations for the given data about the fitted model to the given data (or image) mean. This ratio is a scale factor that measures the extent to which available prior knowledge reduces noise and enhances resolution. Note that Equation (5) is applied to each pixel independently, and when necessary, the new data is re-scaled for gray level

values outside the 0-255 range. The model fit method matches a model (procedure in Table 2, Matlab code in Appendix A) of the object to the given data in the spatial domain only. Finally, for modeling purposes knowing the altitude and speed of the aircraft, or the camera parameters (focal length, etc.) is not necessary; the only required information is some prior knowledge about the imaged object.

The 3-Bar target has a height to width ratio of 5:1 and equal spacing within each bar group (i.e., the widths of the white bars and the black spacing between them are equal, see Figure 4). The minimum contrast ratio (white/black) is 2:1, which means that the minimum/maximum gray levels in the optimized image should be close to the minimum/maximum gray levels in the original image. Each row of pixels across a bar group has uniform gray intensity levels, and therefore the same model. By using this prior knowledge, the model fit method can generate a model of each row or the whole bar group. In addition, since the 3-Bar target consists of simple objects (rectangles), generating the model is straight-forward because the algorithm adjusts only a few variables. Adjusting five variables (bar width, horizontal and vertical bar placement,

Table 2. Generic Model Fit Procedure

1. Extract the region of interest from the given image.
2. Estimate initial parameter values (horizontal and vertical placement, the rotation angle about the horizontal axis, the size of the object, and the minimum and maximum gray level intensity).
3. Perform an exhaustive search to minimize the mean squared error between the given data and the model (using the initial estimates from Step 2).
4. Incorporate the prior knowledge into the given data using Equation 5.

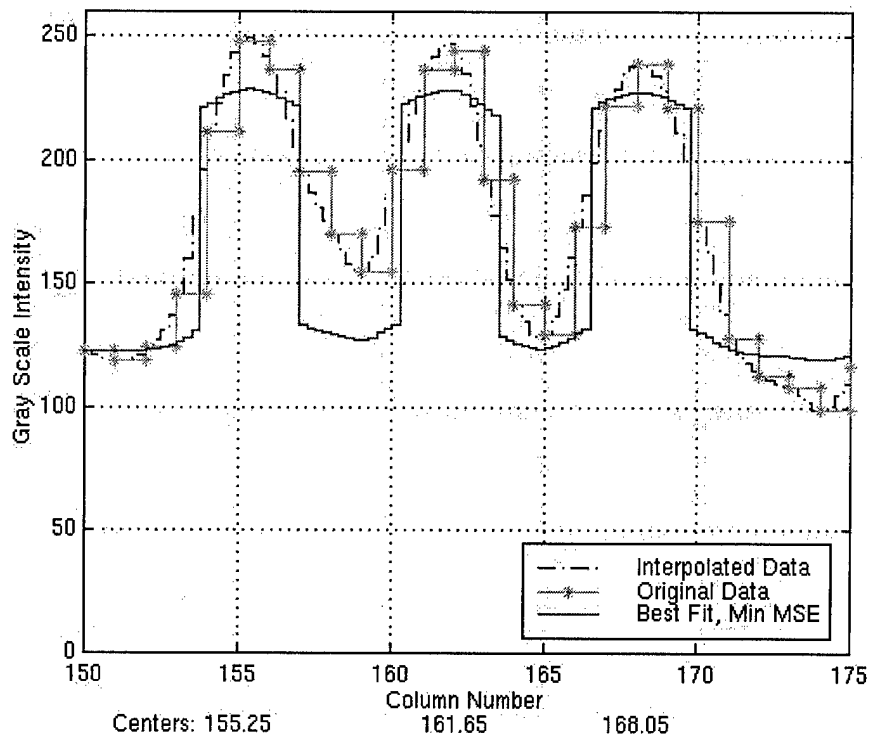


Figure 14. Line Scan of an Image Row

minimum and maximum gray value) minimizes the mean squared error (Equation 2) between the model and the given data (rotation is assumed zero for the 3-Bar target images). Since the number of bars in each group is the only difference between the 2-Bar and 3-Bar targets, modeling the 2-Bar target follows the same process. The algorithm applies two types of models to a Bar target image: an image model (Figure 15) and a line scan model (Figure 16).

The procedure for increasing resolution begins with the extraction of a square matrix. The image model begins by applying a line scan algorithm to estimate minimum and maximum gray scale values, bar width, and bar starting position (Figure 14). By

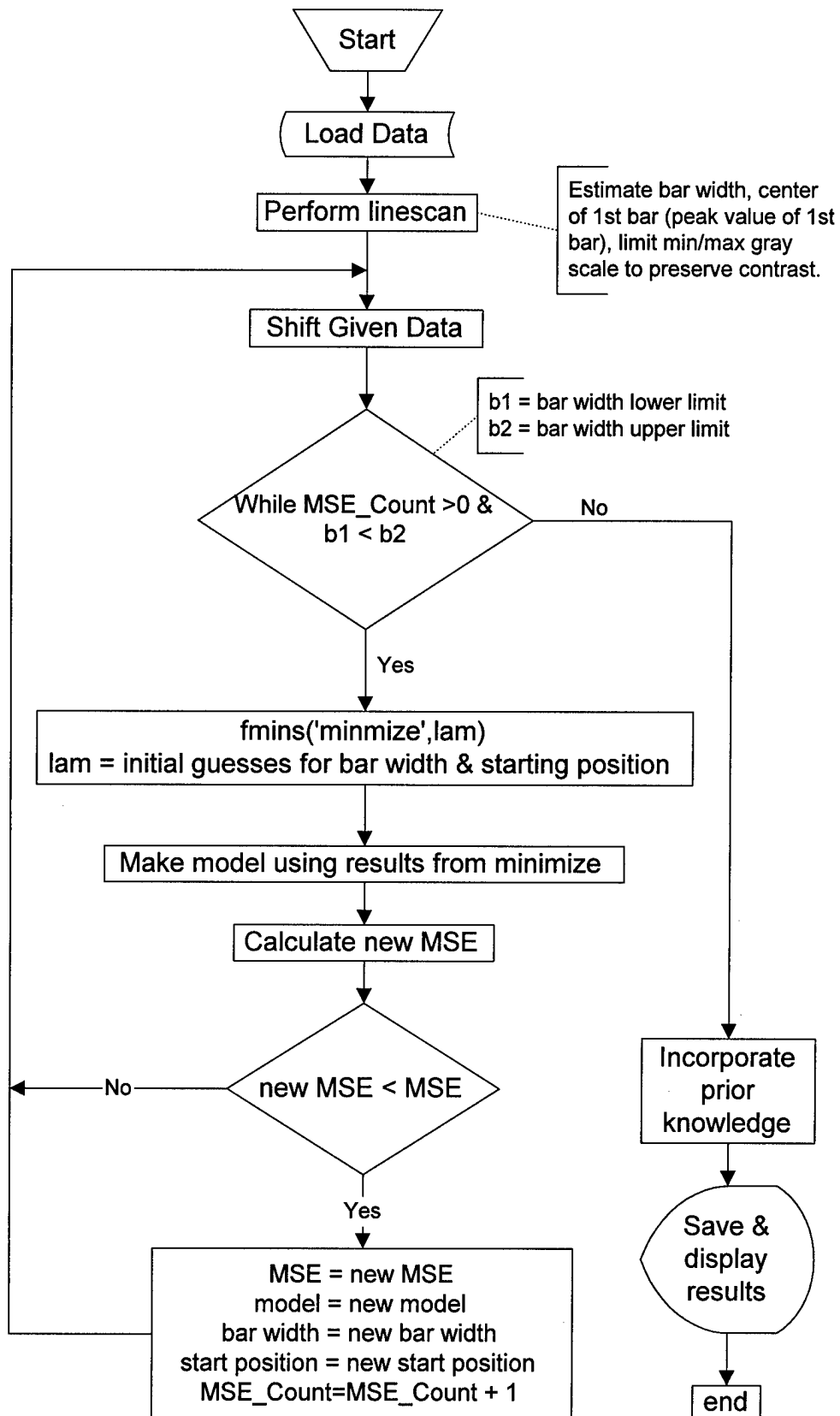


Figure 15: Flowchart for 3-Bar and 2-Bar Target Model Fit

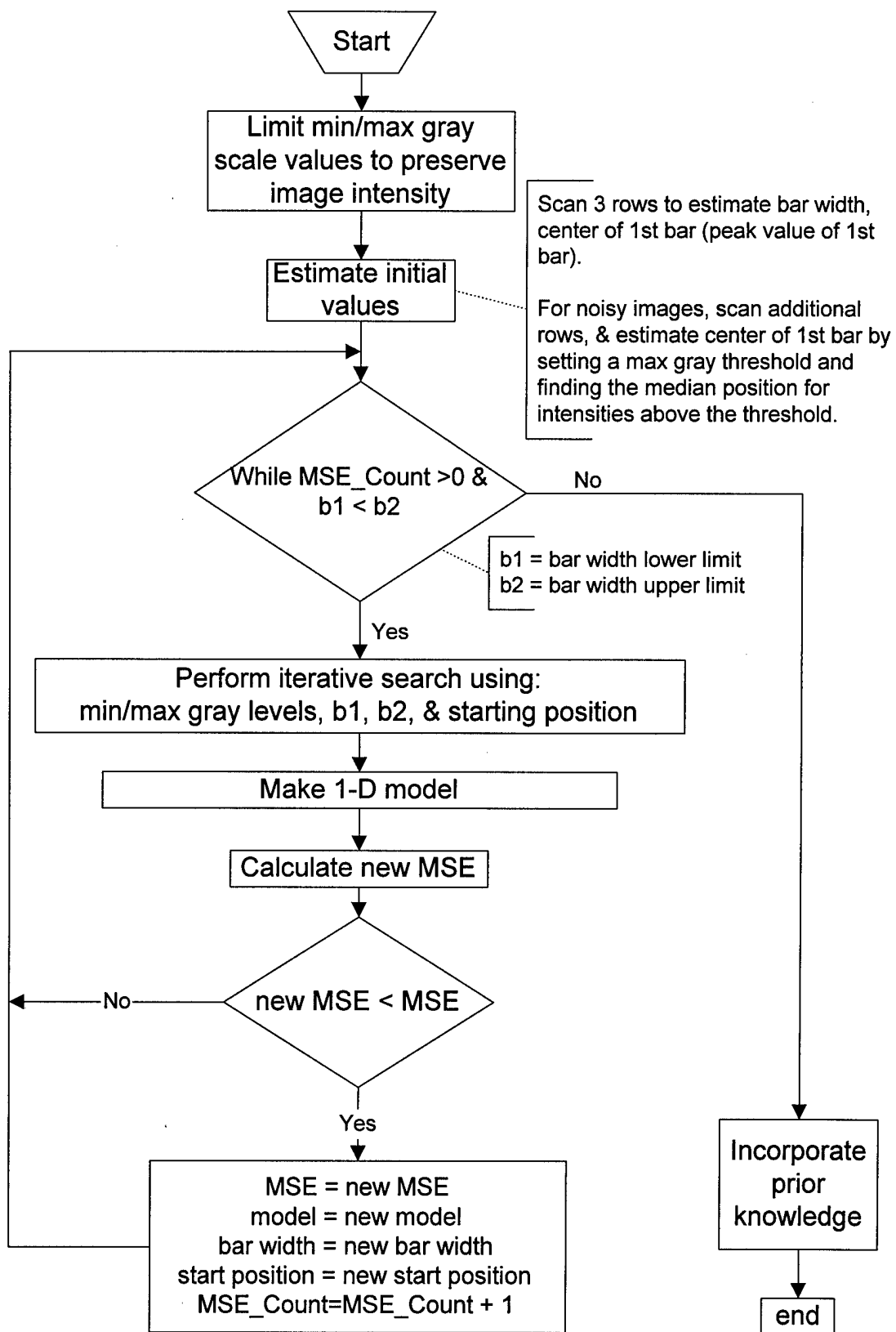


Figure 16: Linescan Flowchart for 3-Bar and 2-Bar Target Model Fit

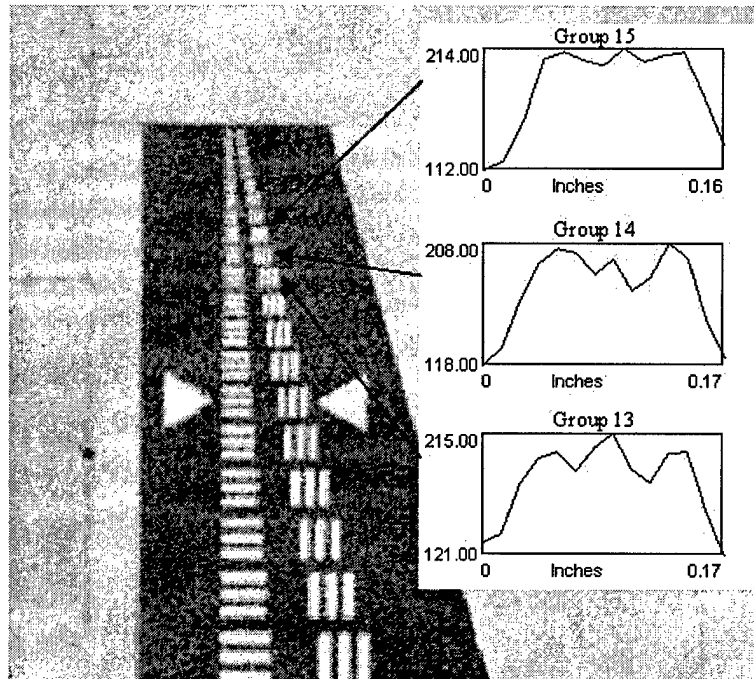


Figure 17. Line Plots of Bar Groups 13, 14, & 15

iterative search, models are generated from these estimates to minimize the MSE between the model and the given data, with Equation 5 incorporating the prior knowledge into the given data. Any of the adjustable parameters can be a source of possible fit error, but measuring this error is impossible because an original perfect image does not exist.

An optimized image could be generated for any of the smaller bar groups (13 and up) using prior knowledge. However, the accuracy or confidence level of the model fit method would be lower because the smaller bar groups do not show any distinguishable bar separation (Figure 17). Therefore, the method was not used for bar groups that do not show relative separation between bars.

Obviously, there are many more variables for complex objects such as airplanes or

buildings, and generating a model is much more difficult. For such objects, developing the model for a small region of interest (ROI) limits the number of variables. For example, instead of developing a model for a whole aircraft, or even an aircraft wing, the ROI is limited to a part of the wing. For this research the ROI was limited to the area surrounding the airstar emblem.

Modeling the airstar is much more difficult than the 3-Bar target because each row of pixels is different and there are multiple gray levels that represent the red, white, and blue colors. Although the airstar shape is more complex due to the stripes, circle, and the star, it has known characteristics. The general procedure for modeling the airstar (Figure 18) is similar to modeling the bar target. Estimates are made for rotation, minimum and maximum gray scale values, and placement. An iterative search is performed using these estimates to minimize the MSE between the model and the given data, and Equation (5) then incorporates the prior knowledge into the given data. As before, the adjustable parameters can be a source of fit error, but the use of prior knowledge allows development and application of a robust model while processing only in the spatial domain.

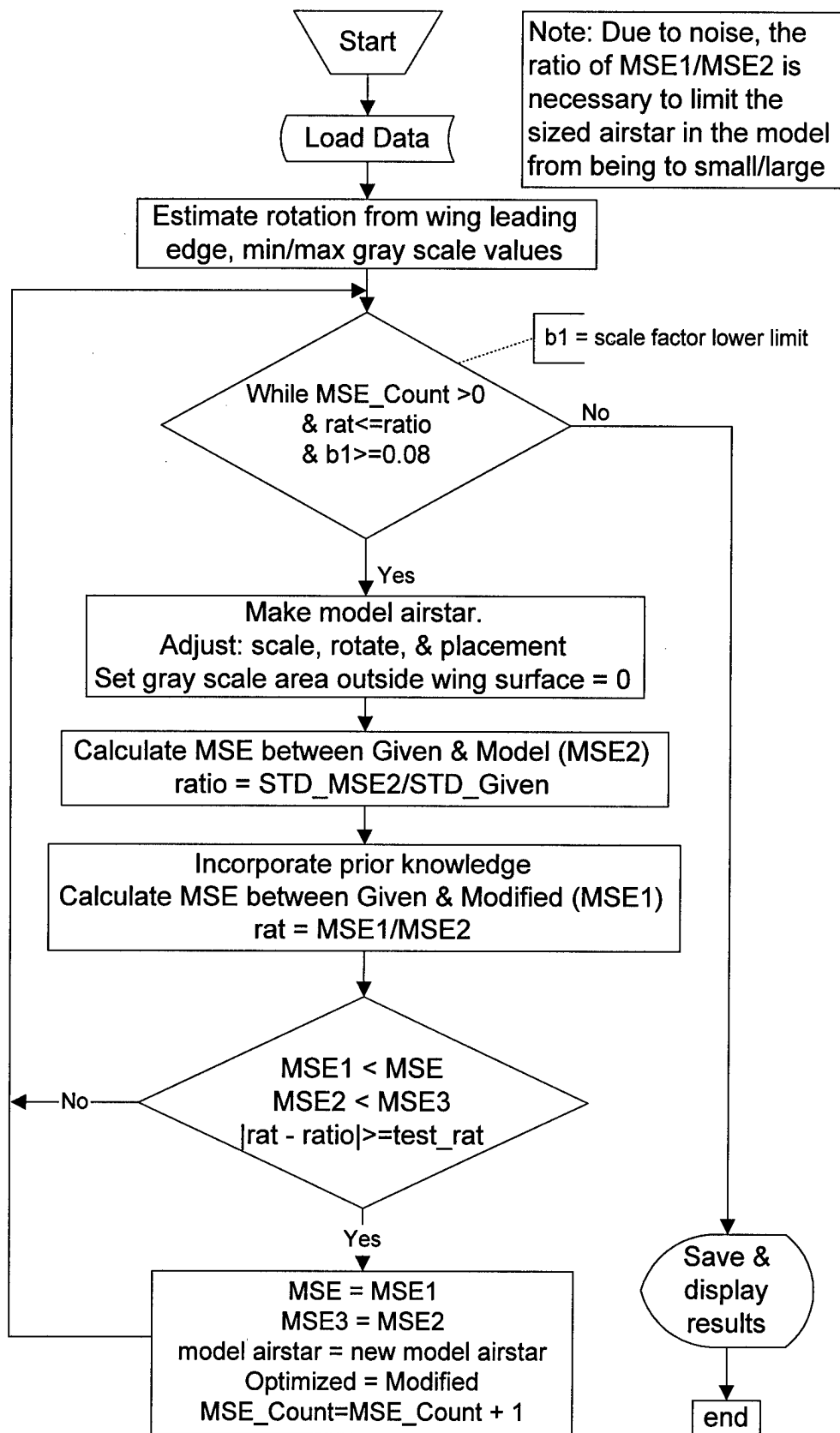


Figure 18: Flowchart for Airstar Model Fit

V. RESULTS

Enhancement Using Commercial Product

At best, the three commercial products produced marginal results (Figure 19) using the generic filters included in each product. Only two of the programs, Ulead's PhotoImpact and Scion Image, allowed for the creation and use of custom filters. The generic filters generally enhanced image resolution, but also amplified image noise as evidenced by speckling. Results also indicate that a darkening contrast adjustment had

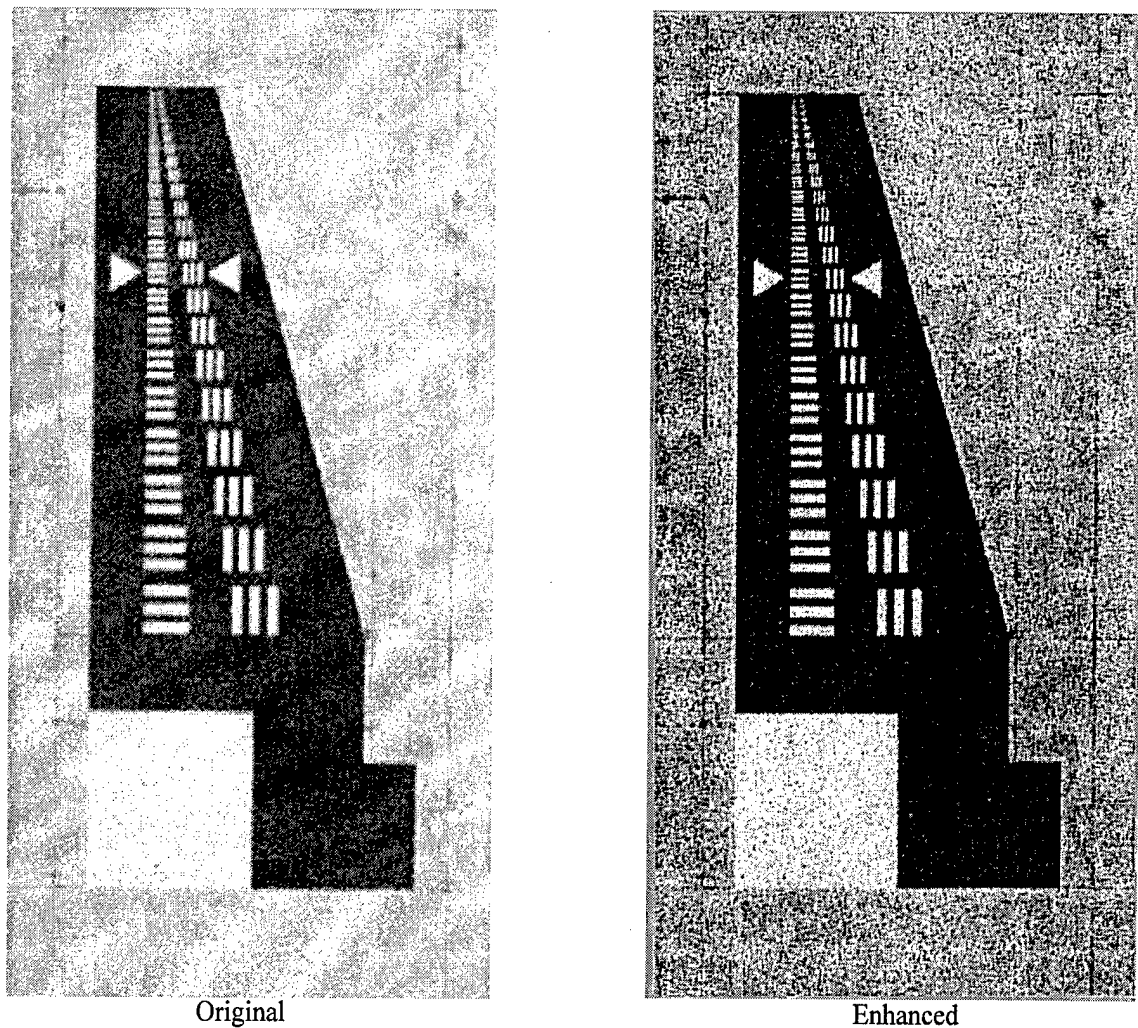


Figure 19. Enhancement by Commercial Software

the greatest enhancement effect. The bar targets in Figures 19 and 20 are the same, but the latter displays line plots for selected bar groups that show resolution before and after enhancement. Enhancement was also tried on the image of a C-119 (Figure 21) with the same noise amplification results.

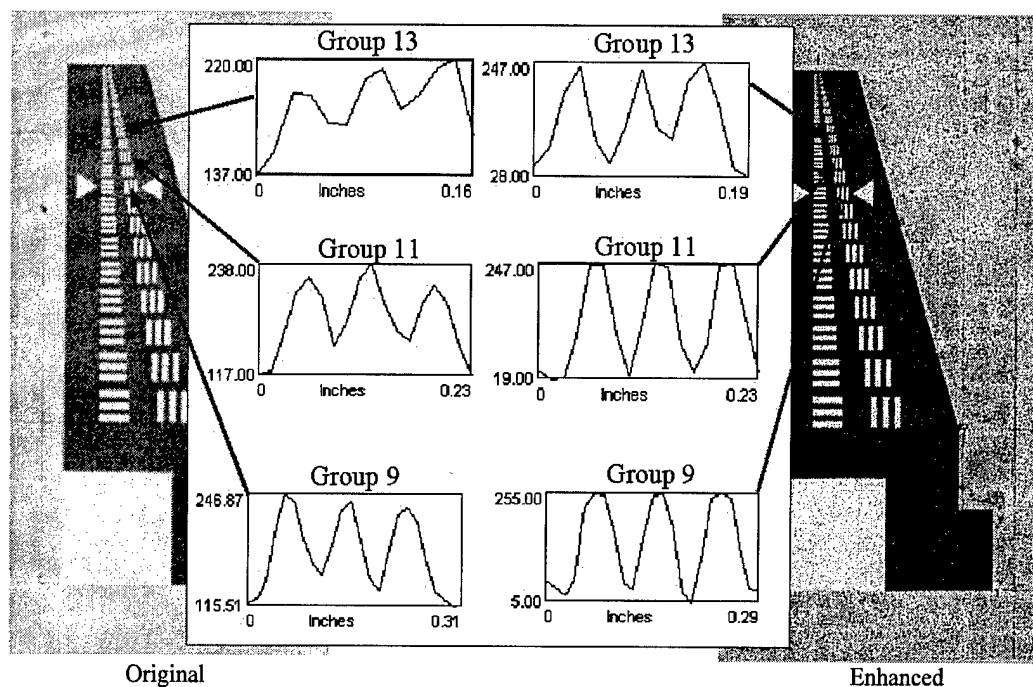


Figure 20. Line Plots for Bar Groups 9, 11, & 13

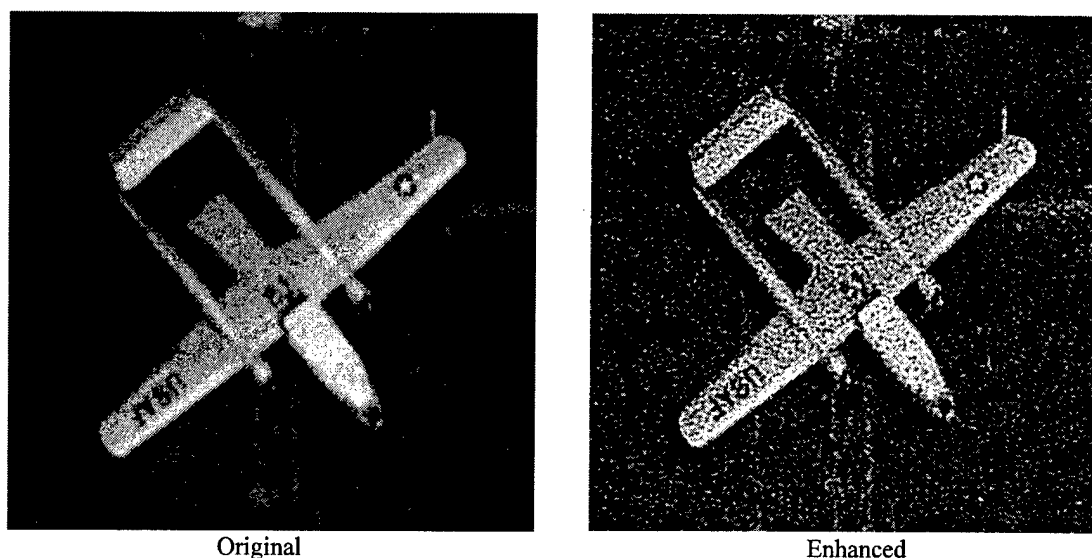


Figure 21. Enhancement of a C-119 Cargo Plane

Enhancement Using Model Fit

Results from the model fit technique were far better than the results obtained through use of the commercial software. The procedure in Table 2 was applied to the extracted group 9, bar width 30 cm[36] (Figure 22) and produced an optimized image (Figure 23). A side-by-side comparison (Figure 24) of line plots for group 9 shows that the original image does not have well defined peaks and valleys, whereas the optimized image is visually well defined. The original contains blurring due to aircraft motion and atmospheric effects not present in the optimized group 9 image. Furthermore, the line plots show that the overall intensity (62-192 vs. 67-188) did not change during the optimization process.

The same algorithm was applied to group 12, bar width of 21 cm [36] (Figure 25) of the same image with different results. A comparison of Figures 22, 25, and the first line plot in Figure 27 shows an almost nonexistent separation between bars in the bar group. Since the original enlarged negative showed some separation of the bars, suspicion arose that the scanning process undersampled some data. Consequently, application of the algorithm failed to produce a good optimized image (Figure 26). Scanning group 12 at a 5.7 micron resolution produced a 150 by 150 pixel matrix (Figure 25), while scanning at a 4 micron resolution produced a 200 by 200 pixel matrix (Figure 28). Figure 28 shows more noise (due to the scanner), but the algorithm produced a very well defined bar group (Figure 29). Here, the algorithm adjusted the noise elements and the optimized image is visually almost perfect. As before, the overall intensity (65-180 vs. 67-175) did not change. The results (Figures 27 and 30) show that the model fit

algorithm is highly dependent upon the number of available samples (i.e., scanning at 5.7 microns vs. 4 microns). In addition, the results indicate that sampling limits the amount of increased resolution (i.e., the resolution of the film used to record the original image, or the digital scanner used). For example, Figure 17 shows line plots of groups 13, 14, and 15 that are unresolved. Prior knowledge insures that the object contains three bars, but the film does not have the resolution to record three separate bars at an altitude that satisfies the Treaty limit of 30 cm. Since the image satisfies the Treaty limit and the bar group 12 width is 21 cm [36], post-processing increases the resolution by 9 cm, or a 30 percent increase.

Applying the model to the degraded image (Figure 31) introduced some new challenges due to the added noise introduced by the German phase filter. The three-dimensional plot in Figure 31 and the upper line plot in Figure 33 indicate that little or no separation exists between the two bars. Modifying the model to handle two bars instead of three was straight-forward, but handling the additional noise required a different approach to finding the center of the first bar. For example, in the undegraded 3-Bar target images (Figure 22) the bars have defined peaks and valleys, whereas the degraded 2-Bar target image (Figure 31) has much noise where the first bar should be. Therefore, modifying the algorithm was necessary to find all values above a threshold in the first 130 positions of each row to estimate the starting bar width and bar position. In addition, the algorithm used five rows instead of three to generate these estimates. Application of the modified algorithm to the degraded 2-Bar target image (Figure 31) removed or adjusted the added noise to produce an optimized image (Figure 32) for the 30 cm bar

group. Like the results from the 3-Bar target, the line plots (Figure 33) show that the overall intensity (140-200 vs. 140-196) did not change during the optimization process.

Noise in the image made the model fit of the airstar on the B-1A wing and on the C-119 wing more challenging, but produced results just as dramatic. Adding more constraints to the algorithm was necessary due to noise problems. For example, while the bar group algorithm minimized only the MSE between the given and model data, the airstar model fit algorithm minimized two different MSEs: the MSE between the given and model data ($MSE1$), and the MSE between the given and optimized data ($MSE2$). $MSE1$ decreased as the size of the airstar used in the model decreased while $MSE2$ decreased as the size of the airstar increased. Therefore, the ratio of $MSE1/MSE2$ was applied to further constrain the size of the model airstar from getting too small or too large. Part of the B-1A wing (Figure 34) extracted from an enlarged negative (plane55b.tif) shows an almost unintelligible airstar. Through application of the model fit algorithm with the necessary constraints, a model (Figure 35) generated an optimized image (Figure 36) with a well-defined airstar. Again, the image satisfies the treaty limit of 30 cm and post-processing increased the resolution by 25.2 cm to 4.8 cm (the width of the blue stripe in the airstar), or 84 percent.

The algorithm produced similar results when applied to the airstar on the C-119 wing. As before, part of the image containing the airstar (Figure 37) was extracted from an enlarged negative (plane55a.tif). After an exhaustive search, a model (Figure 38) of the wing section optimized (Figure 39) the given data with a resolution increase of 20.4 cm to 9.6 cm (the width of the blue stripe in the airstar), or 68 percent. Comparing the

original images (Figures 34 and 37) shows more definition in the C-119 airstar than the B-1A airstar. The five points of the star on the C-119 are identifiable, and a fairly uniform rectangular region on each side faintly outlines the stripes of the star. None of these features are clearly visible on the B-1A. The star on the B-1A is (for lack of a better term) a blob in the middle of what should be a blue circular background, and the stripes are not present. A comparison of the optimized images for the B-1A and C-119 with their respective original images indicates that the algorithm produced a better fit for the C-119 than the B-1A. However, this is not so: A visual inspection of Figures 34 and 36 shows that the star is centered in the optimized image just as the blob is centered on the original. Likewise, Figures 37 and 39 show that the star is centered in both the original and optimized images. Therefore, the algorithm performed correctly when minimizing the MSE.

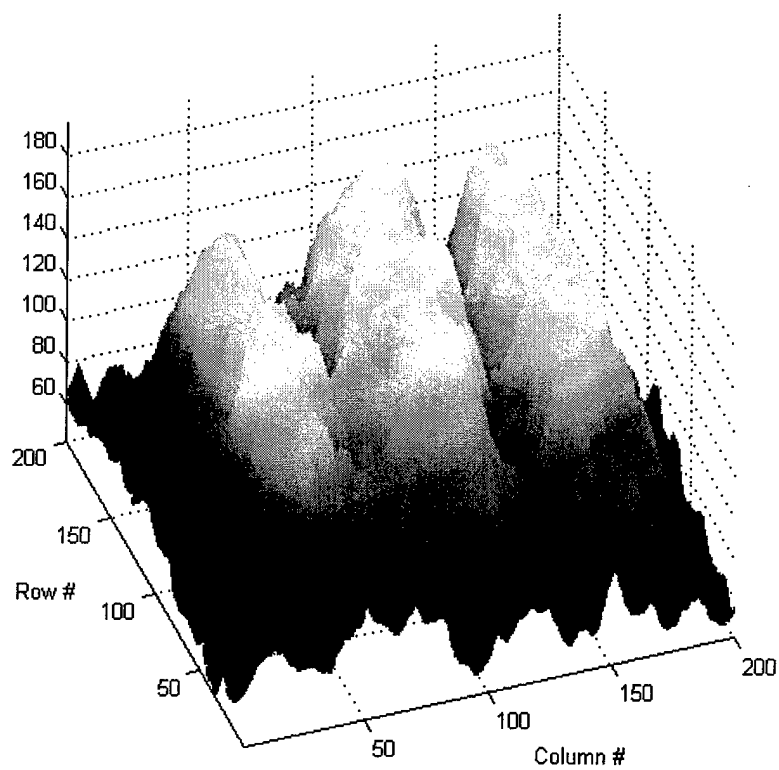
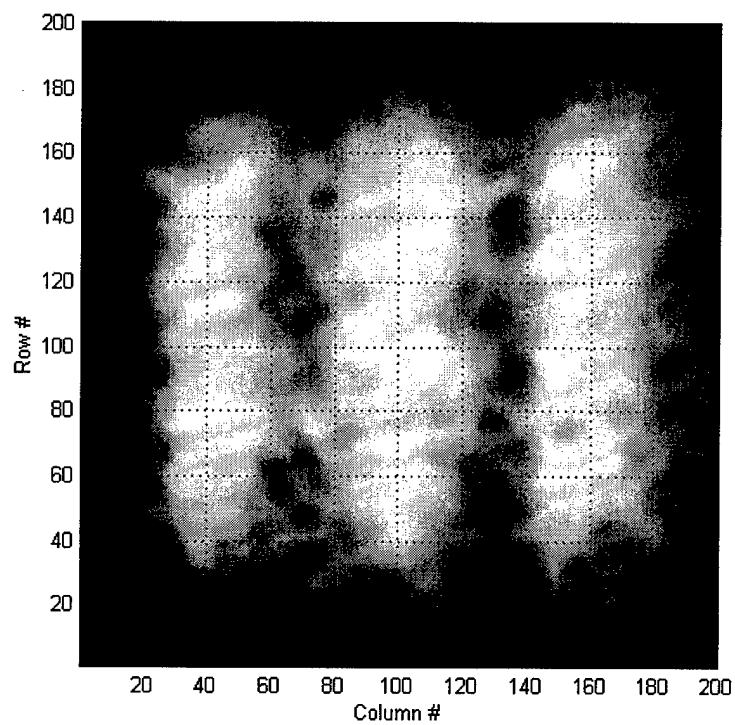


Figure 22. Original Image of Group 9, tar66a.tif, 2D & 3D Views

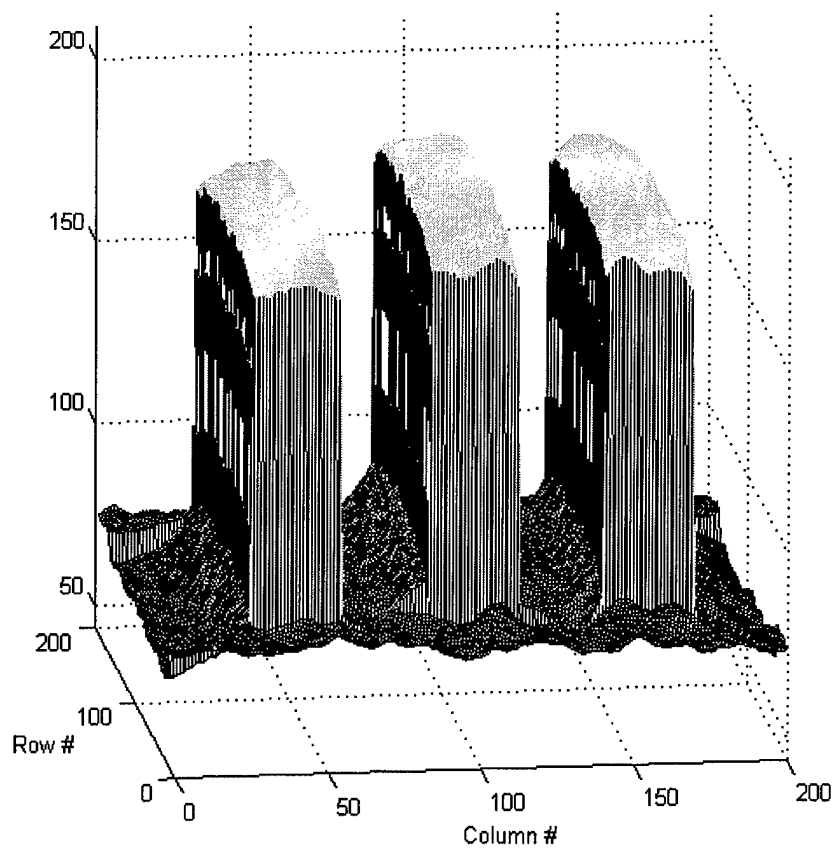
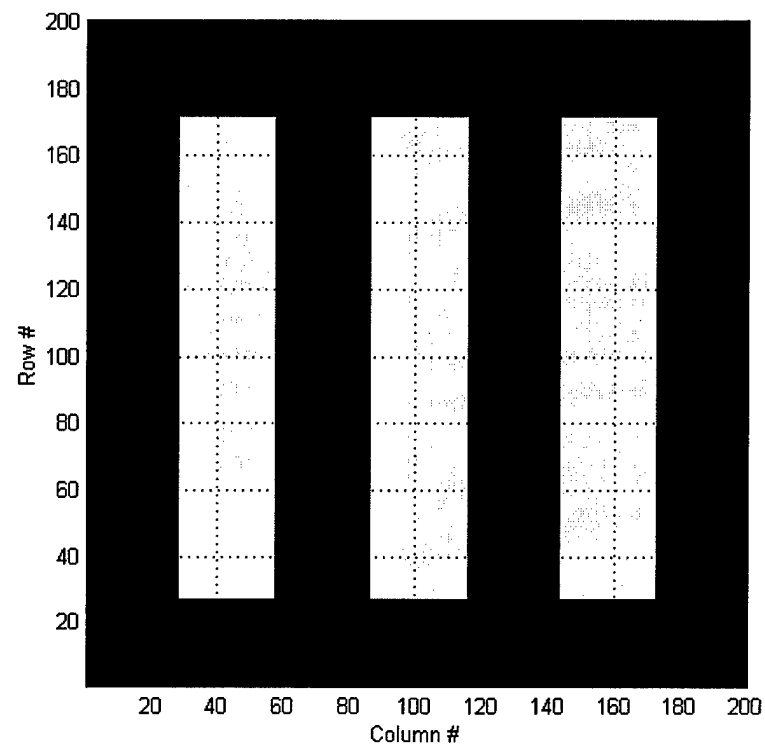


Figure 23. Optimized Image of Group 9, 2D & 3D Views

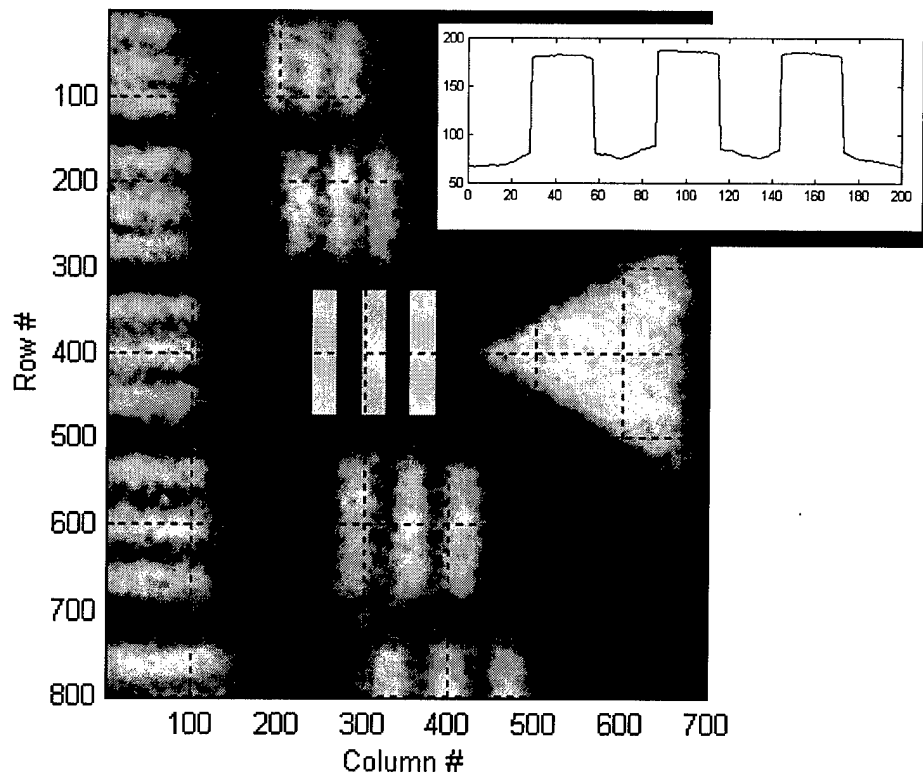
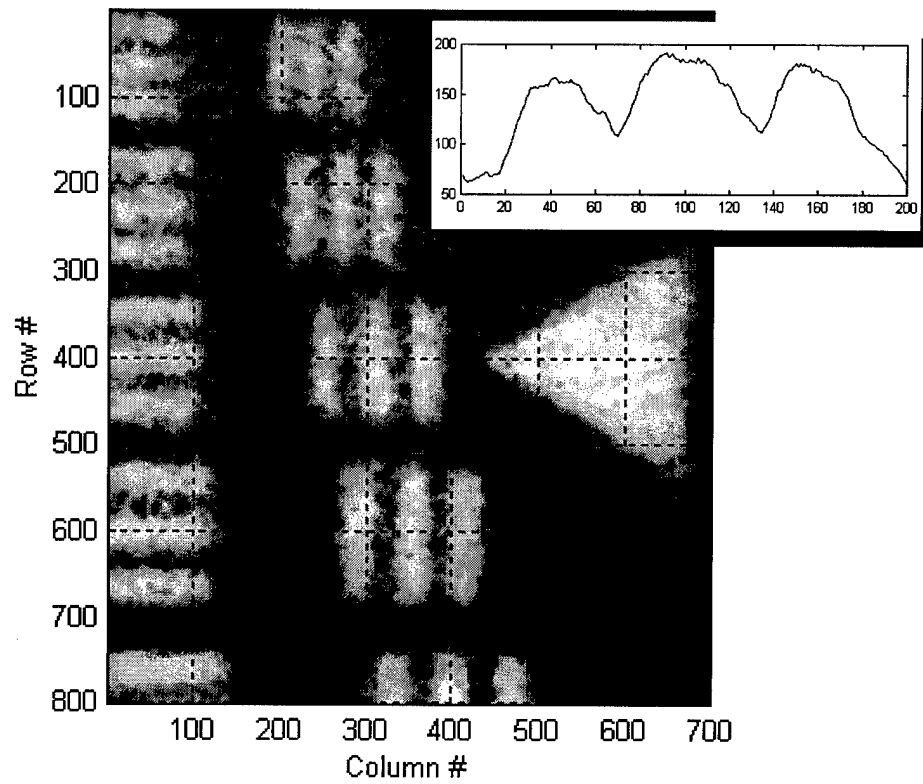


Figure 24. Original & Optimized Images of Group 9

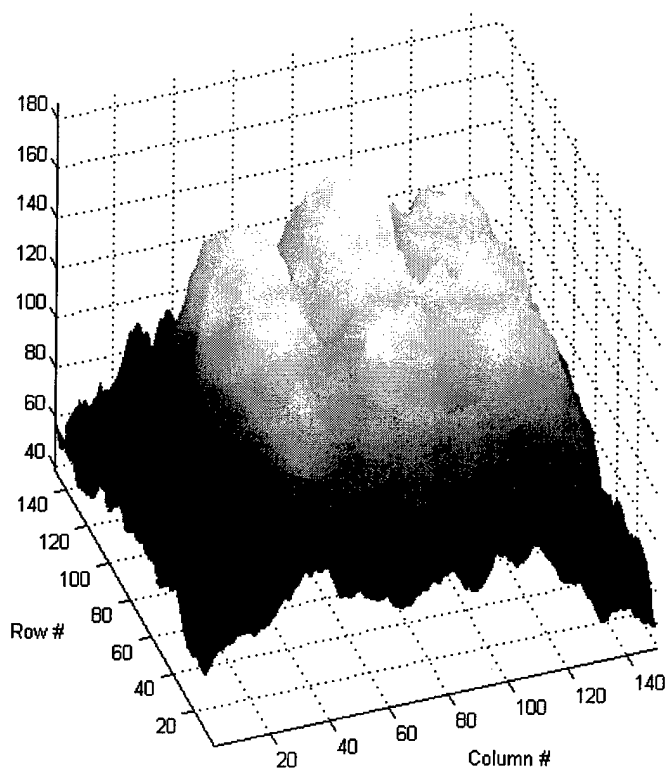
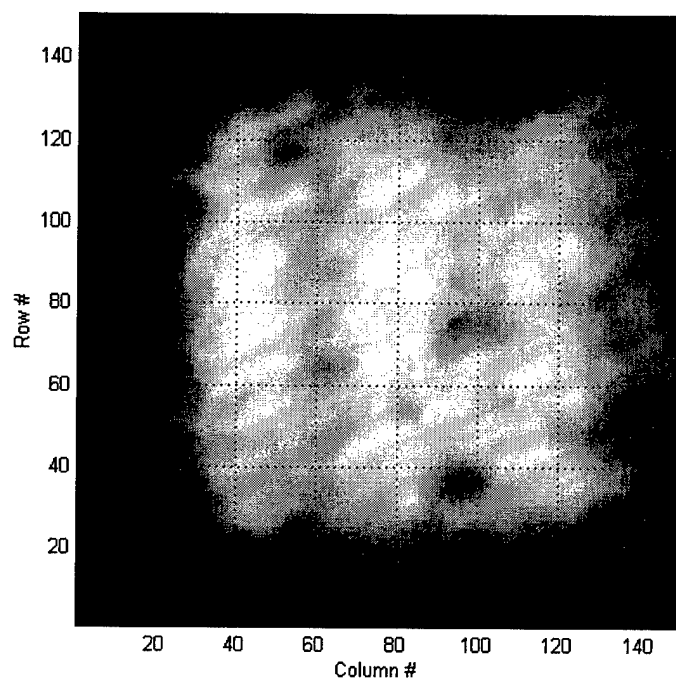


Figure 25. Original Image of Group 12, 5.7 micron scan, tar66a.tif, 2D & 3D Views

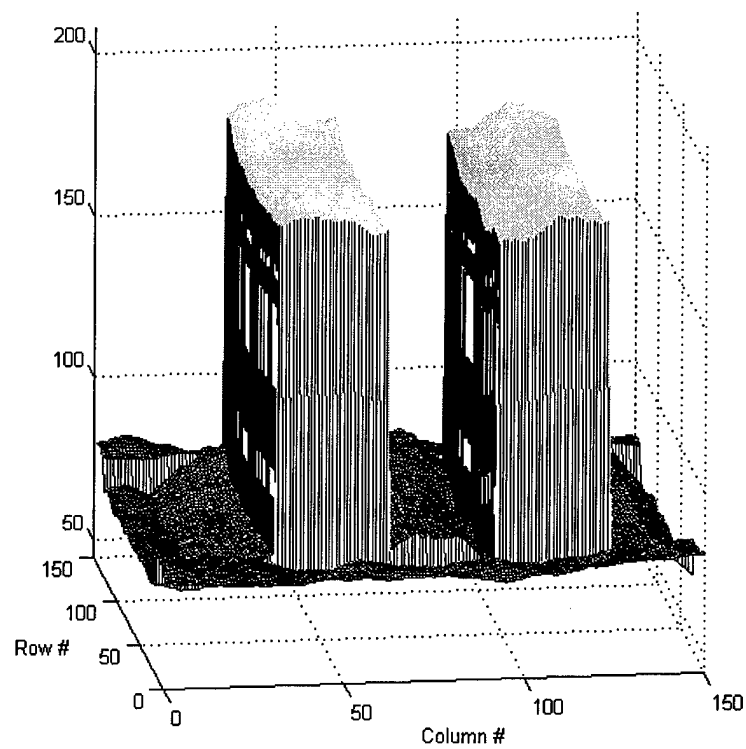
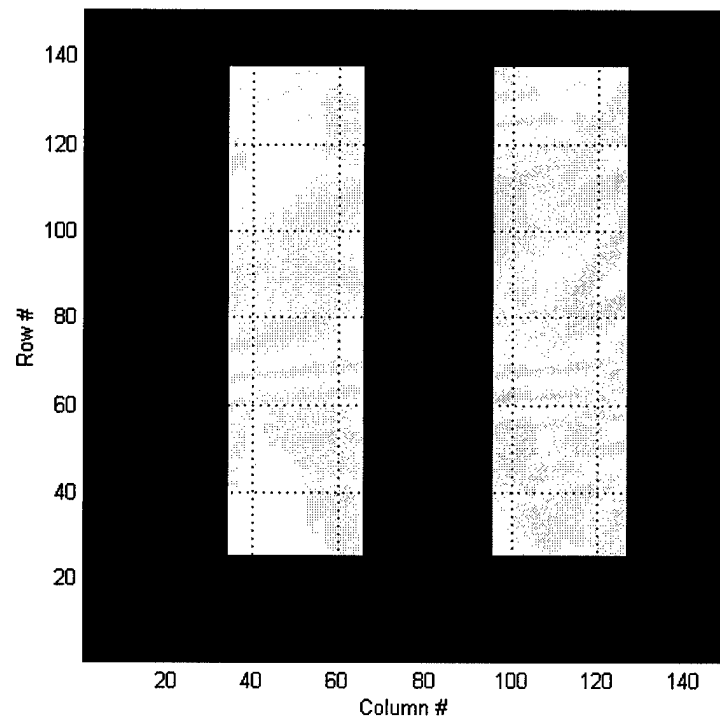


Figure 26. Optimized Image of Group 12, 2D & 3D Views

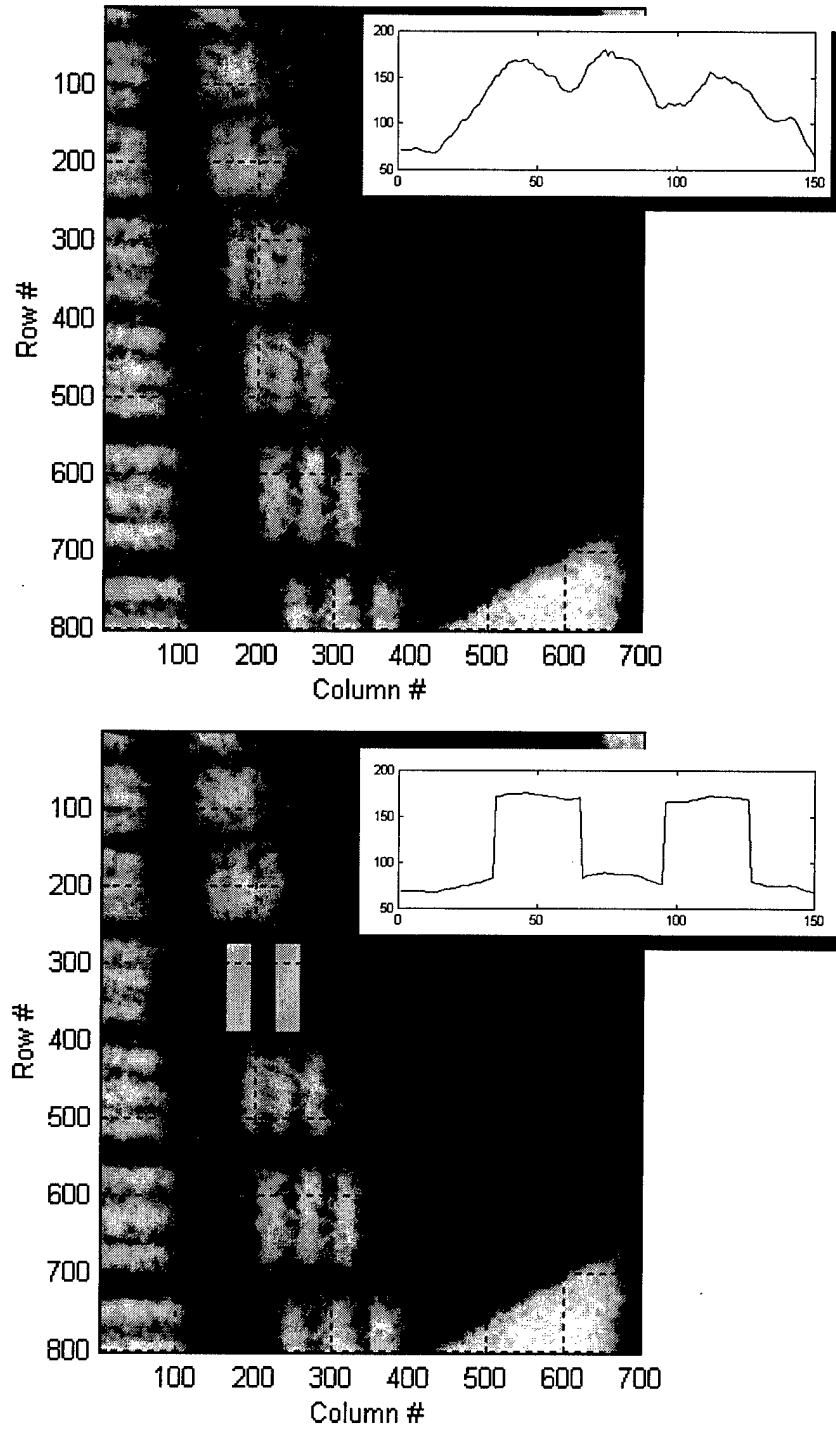


Figure 27. Original & Optimized Images of Group 12

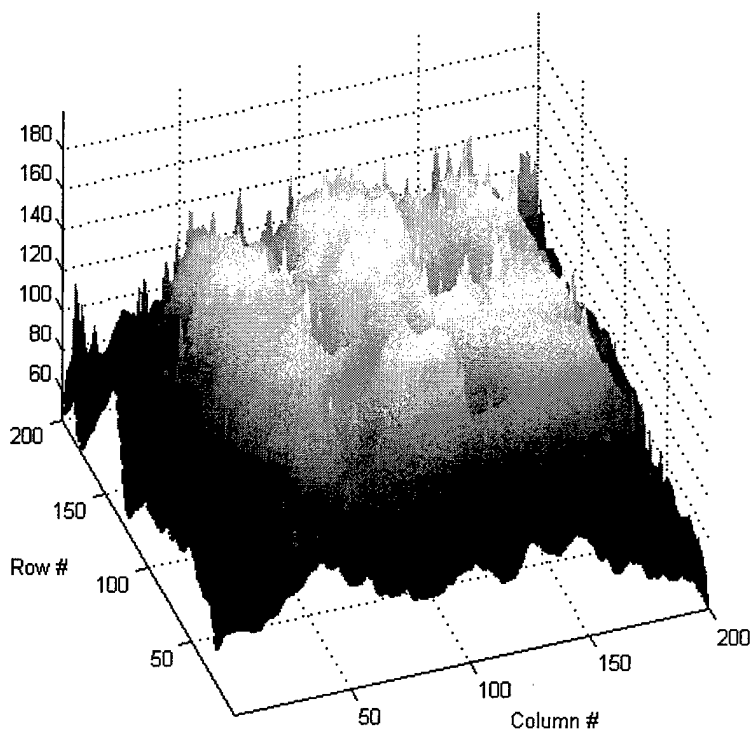
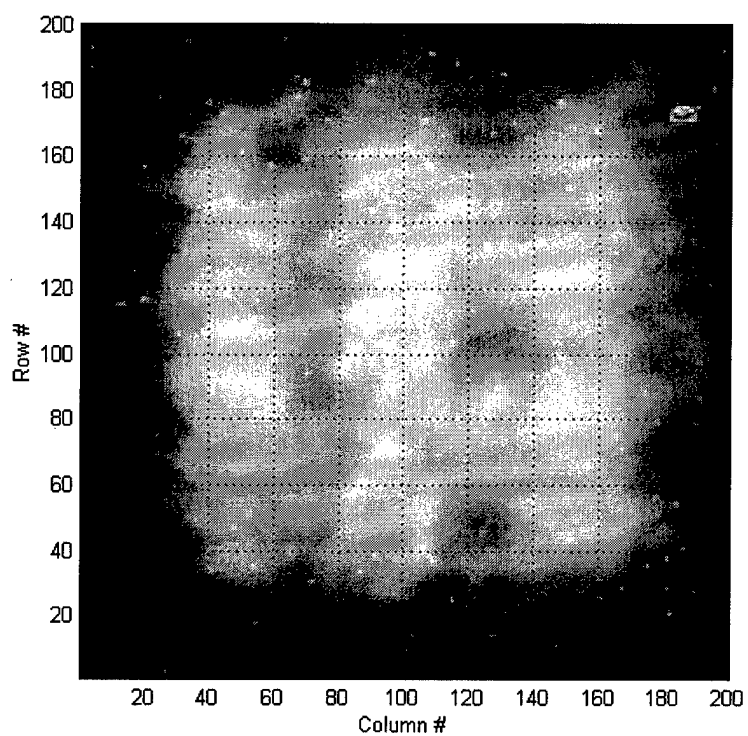


Figure 28. Original Image of Group 12, 4 micron scan, target66u.tif, 2D & 3D Views

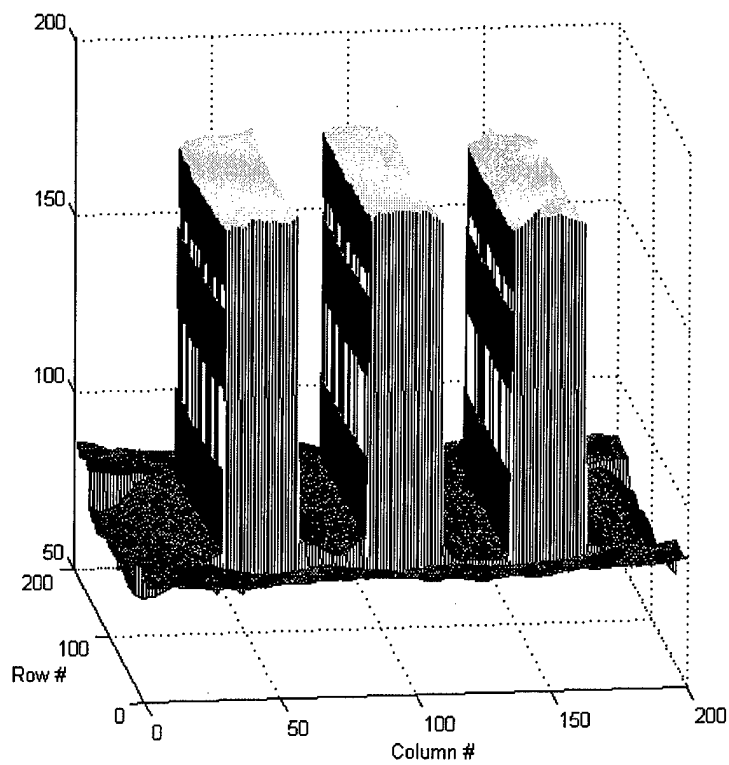
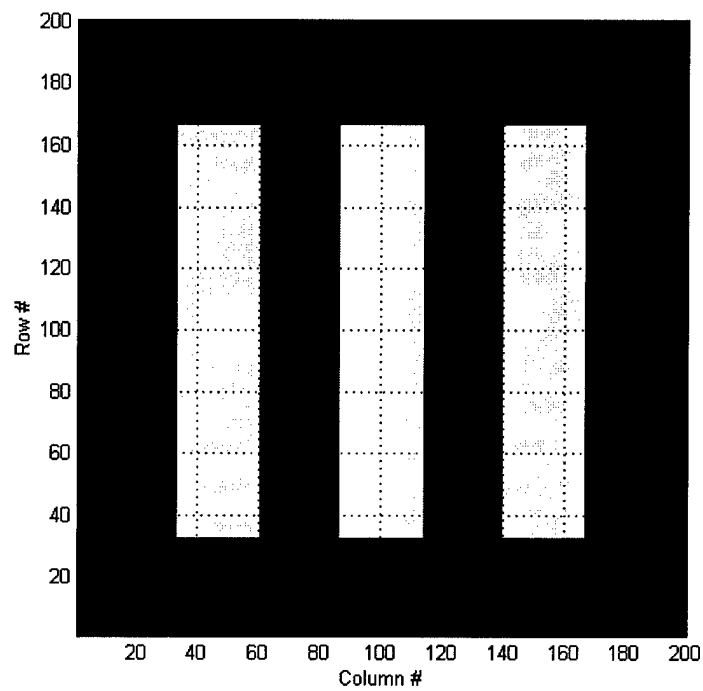


Figure 29. Optimized Image of Group 12, 2D & 3D Views

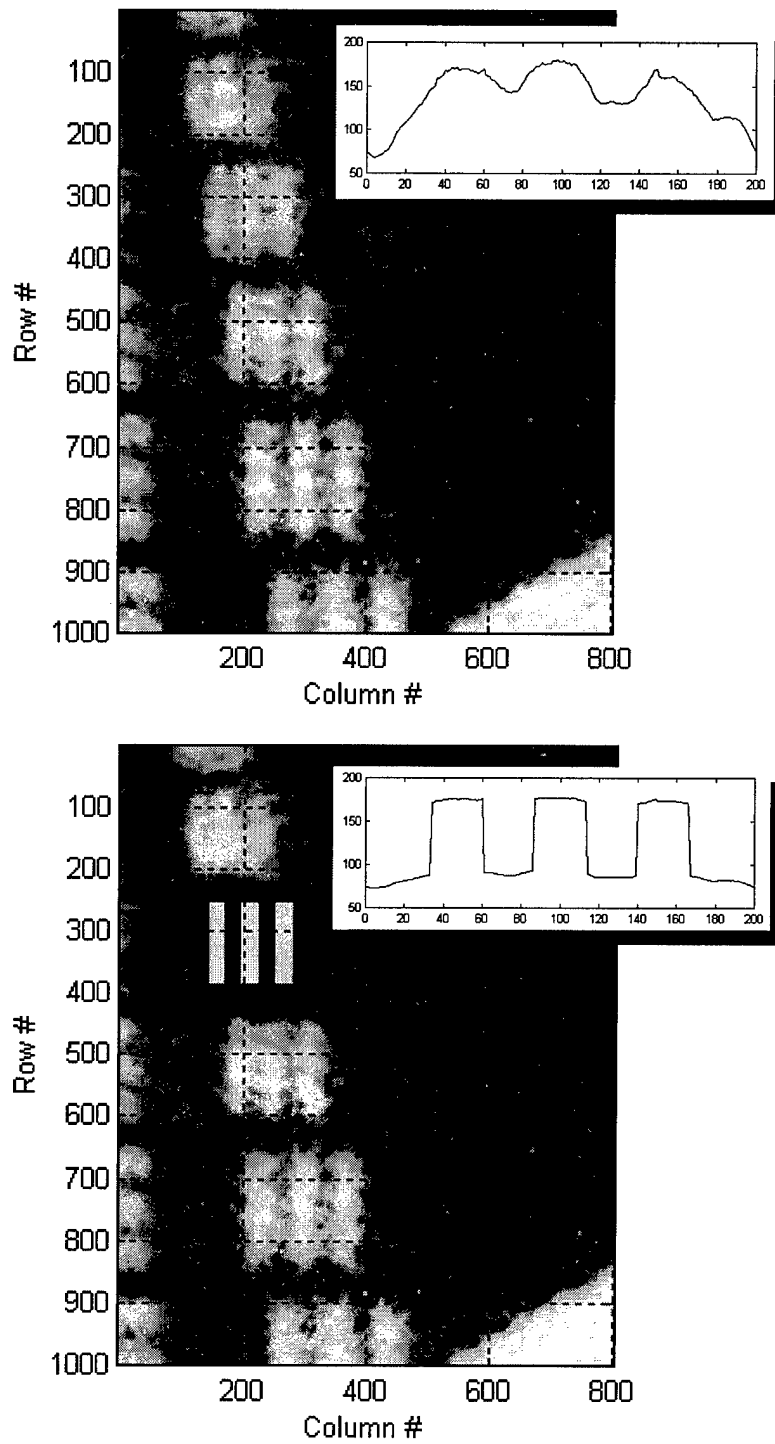


Figure 30. Original & Optimized Images of Group 12

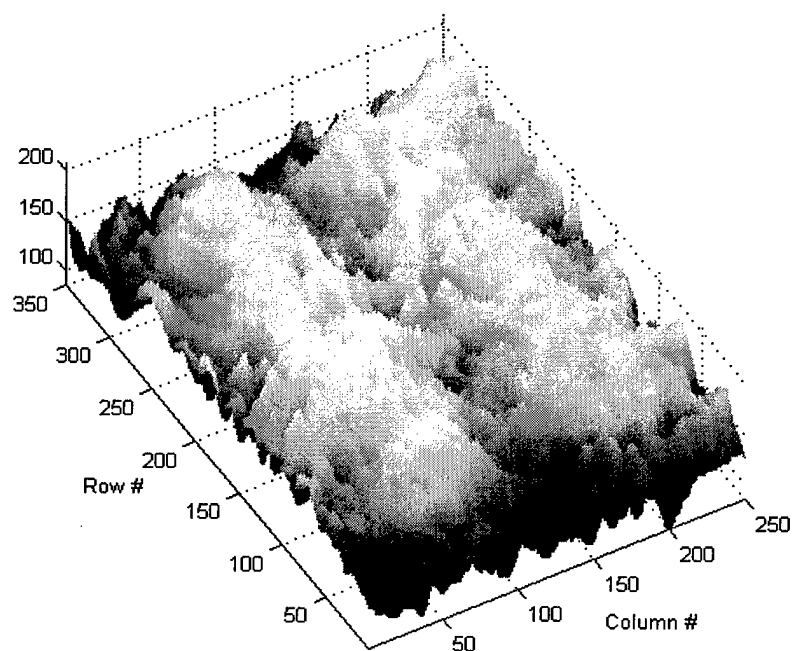
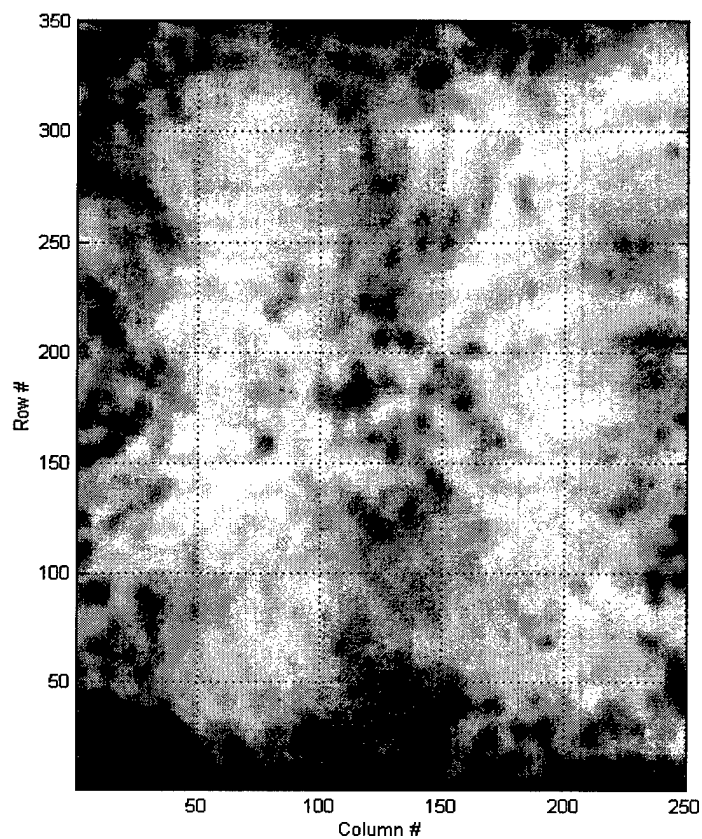


Figure 31. Original Image of 2-Bar Target, German S1 Filter, ges1a.tif,
2D & 3 D Views

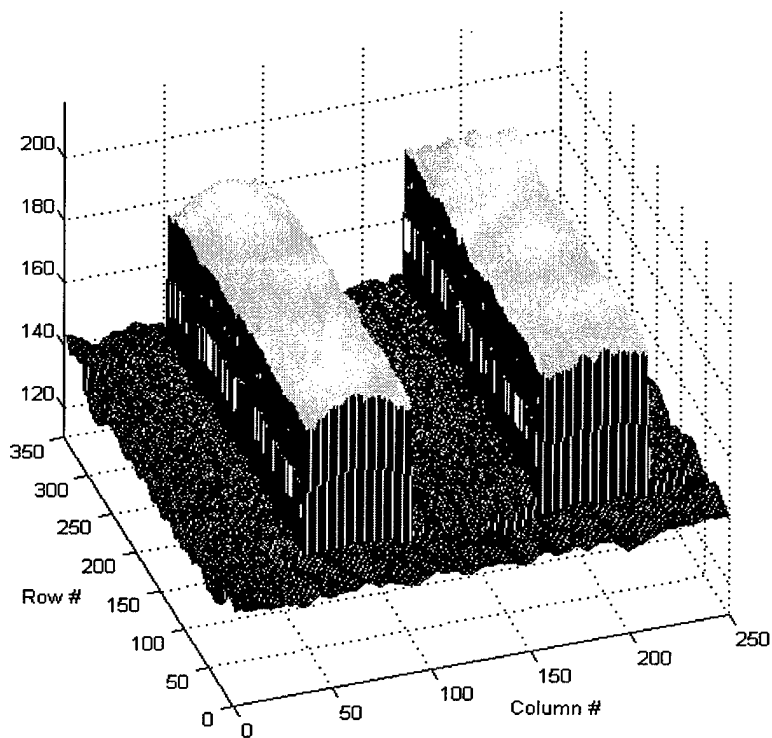
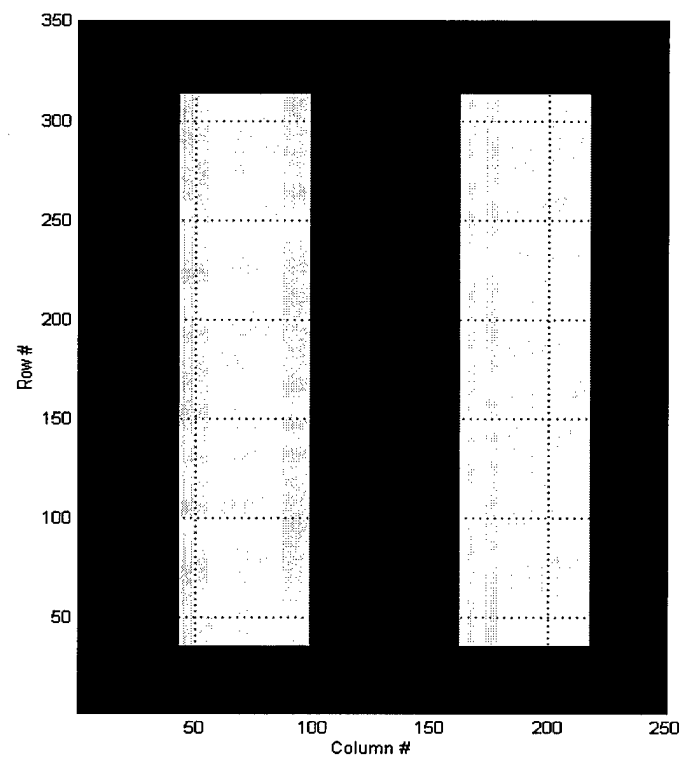


Figure 32. Optimized Image of 2-Bar Target, German S1 Filter,
2D & 3D Views

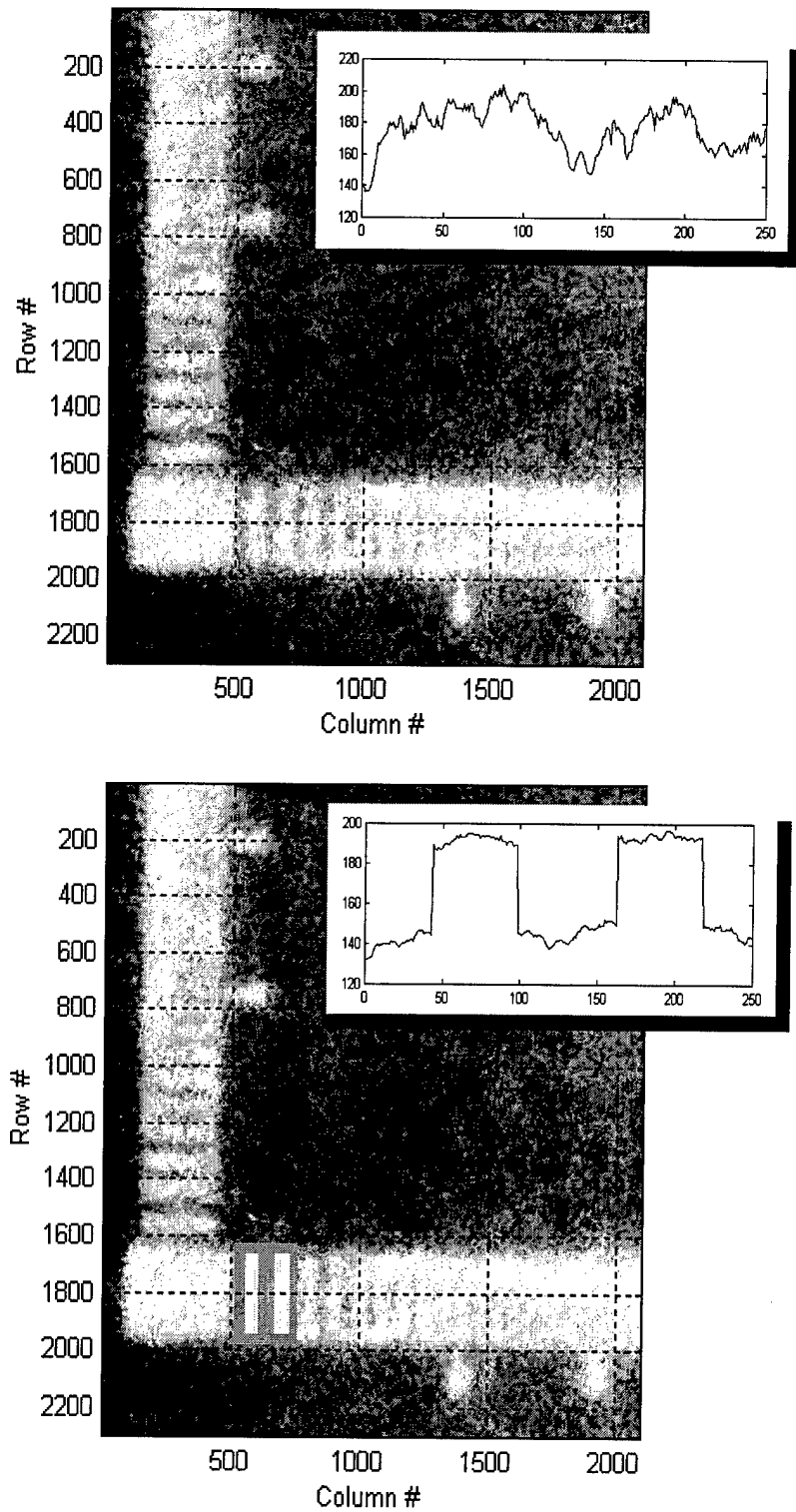


Figure 33. Original & Optimized Images of 2-Bar Target, German S1 Filter

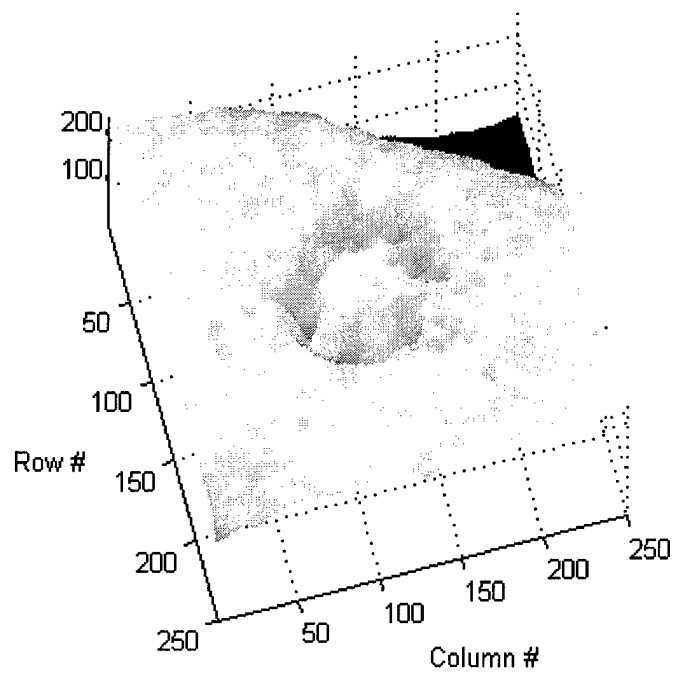
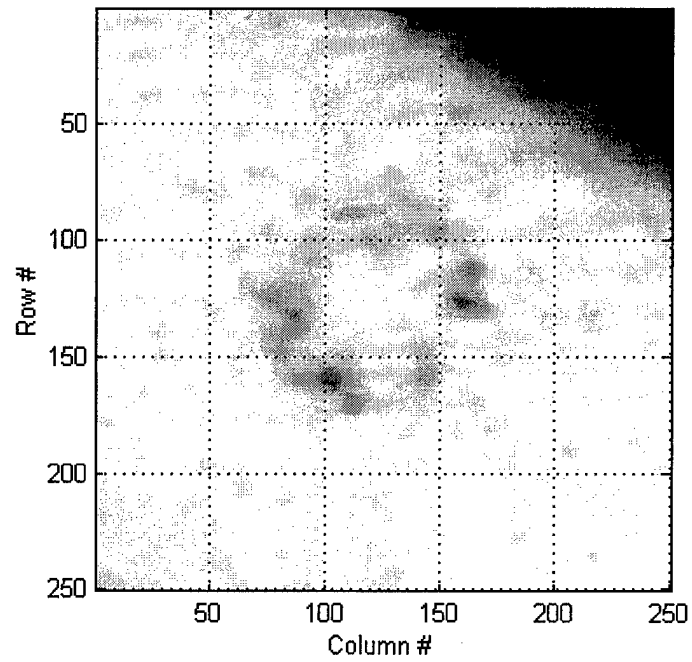


Figure 34. Original Airstar, B-1A Bomber, plane55b.tif, 2D & 3D Views

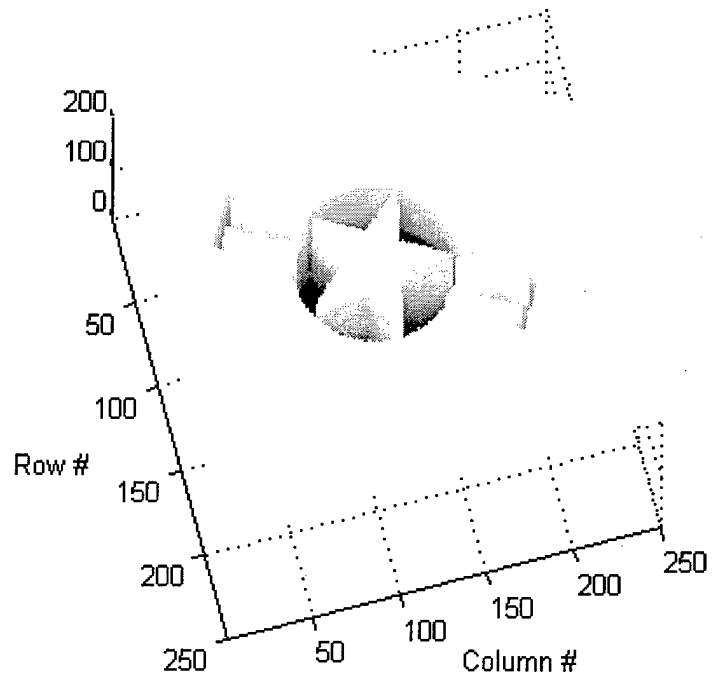
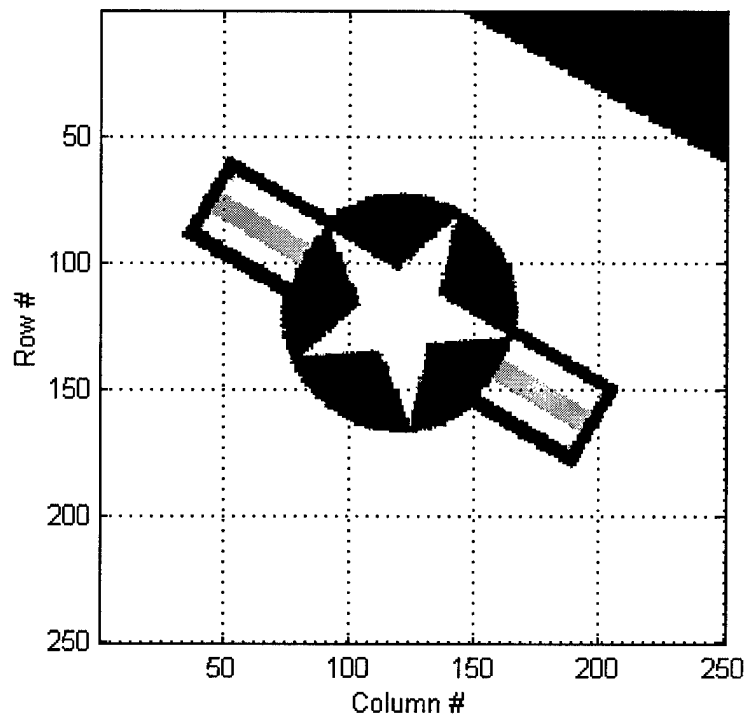


Figure 35. Model Airstar, B-1A Bomber, 2D & 3D Views

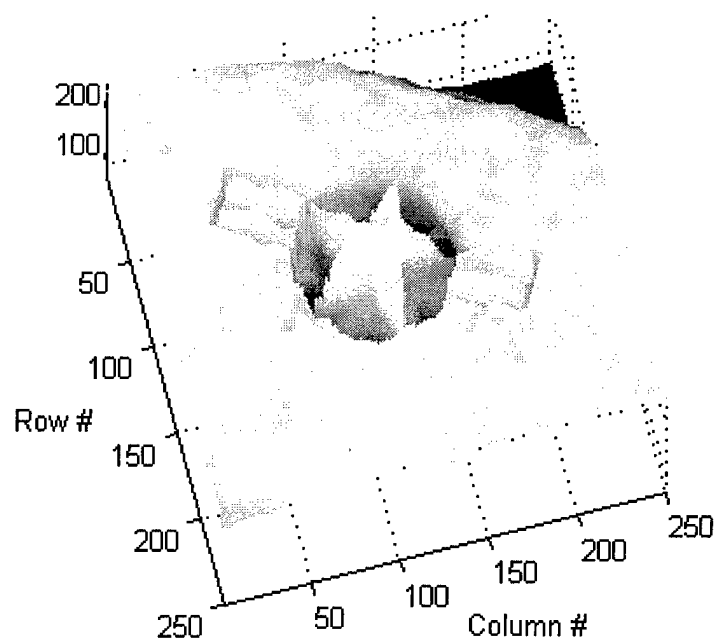
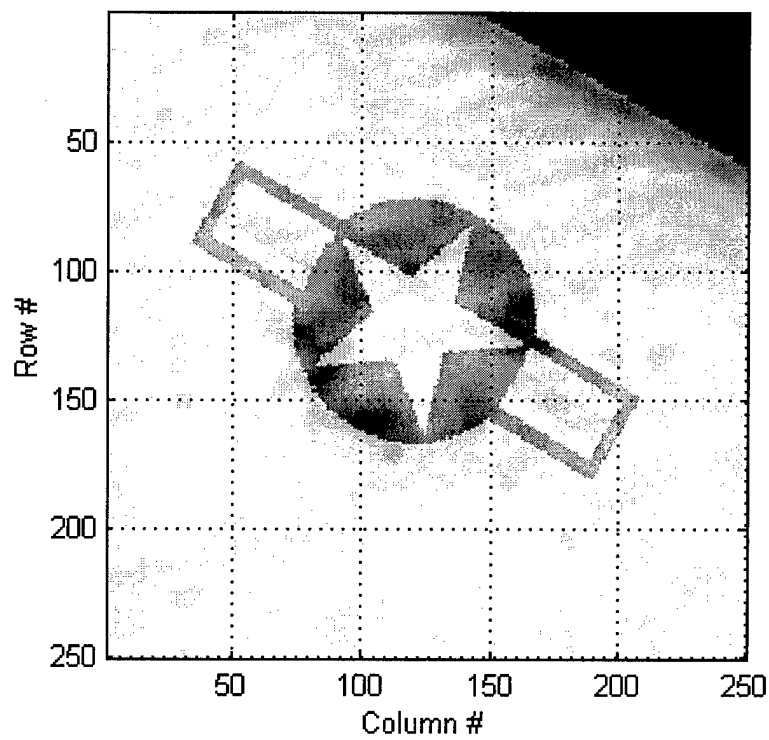


Figure 36. Optimized Airstar, B-1A Bomber, 2D & 3D Views

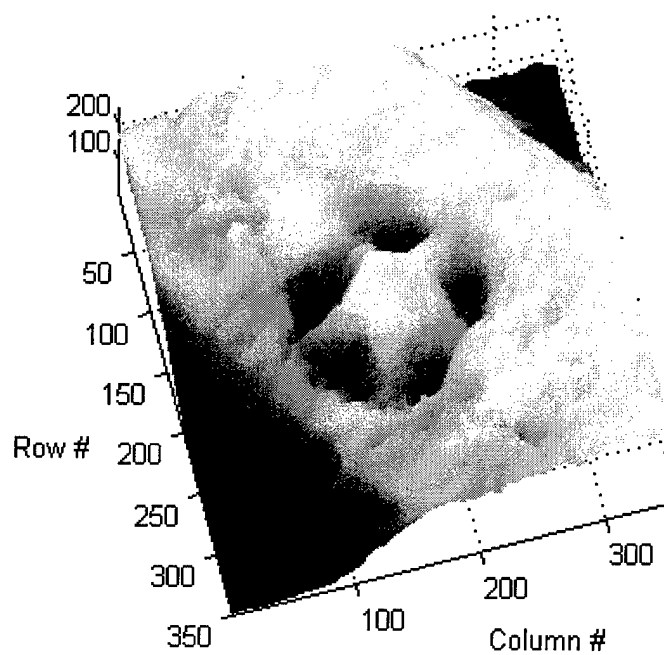
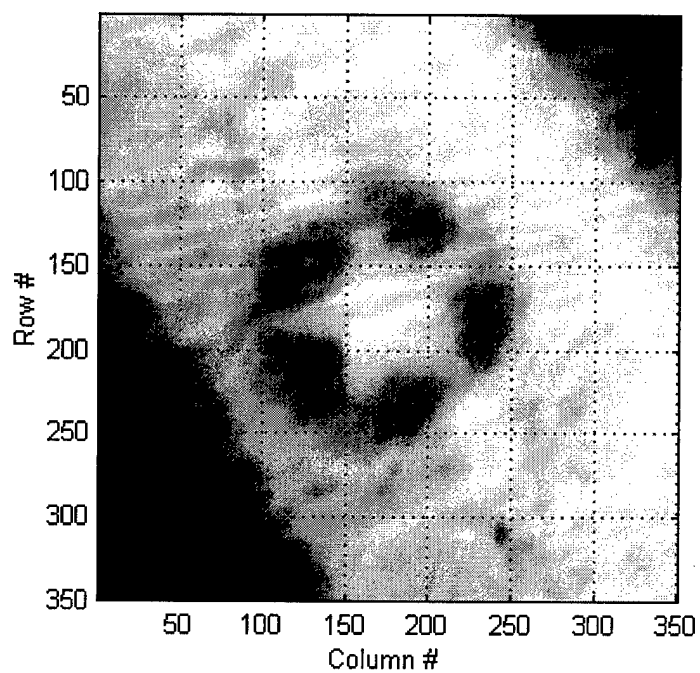


Figure 37. Original Airstar, C-119 Cargo Plane, plane55a.tif, 2D & 3D Views

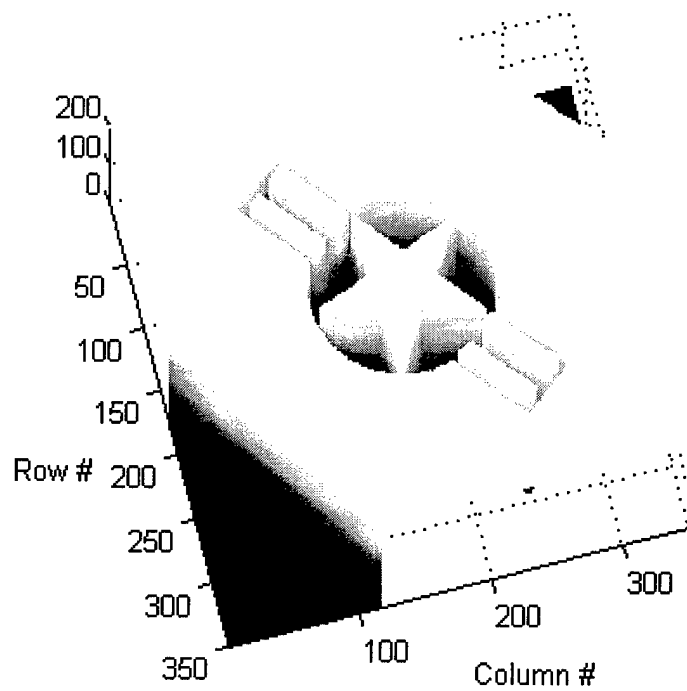
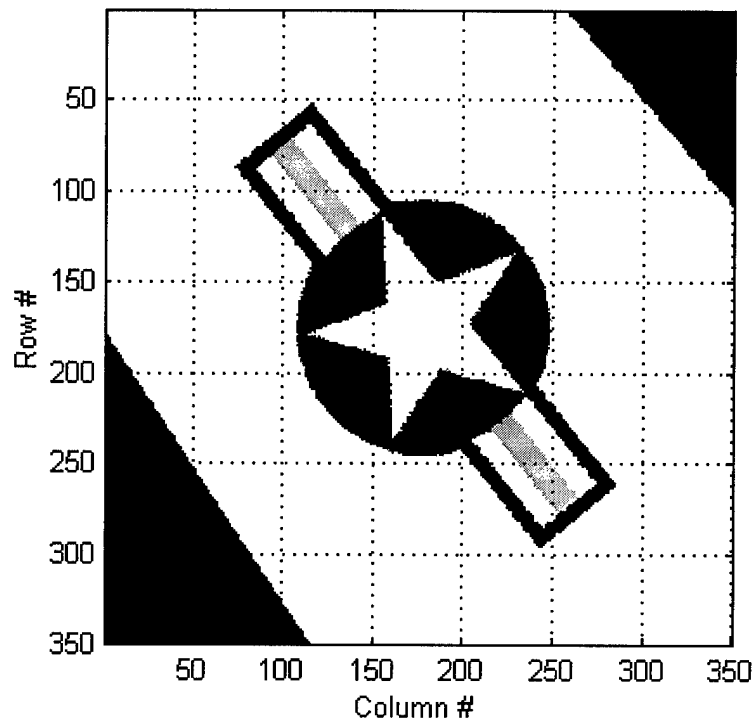


Figure 38. Model Airstar, C-119 Cargo Plane, 2D & 3D Views

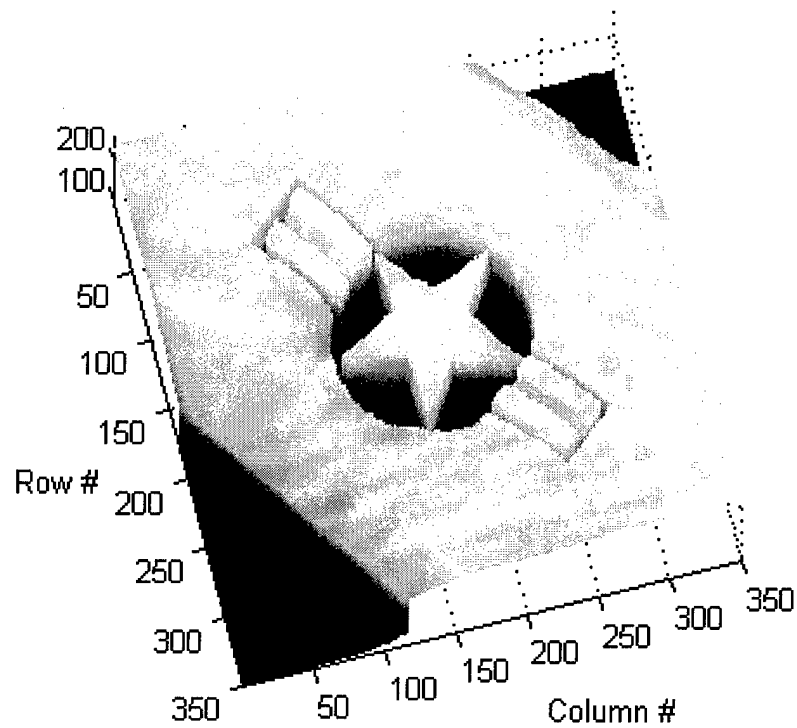
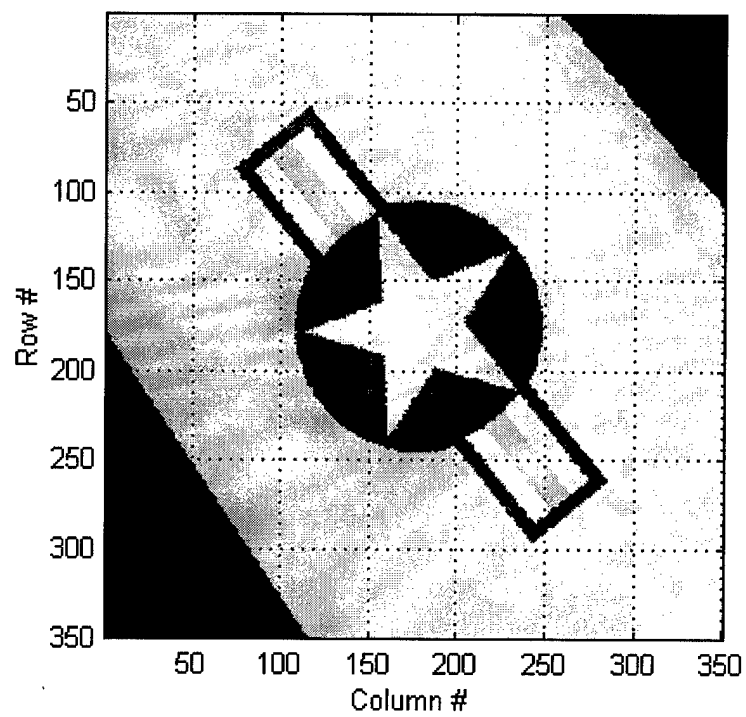


Figure 39. Optimized Airstar, C-119 Cargo Plane, 2D & 3D Views

VI. CONCLUSIONS and RECOMMENDATIONS

The results clearly show that using prior information to develop a model fit super-resolution algorithm *can increase the resolution of any* Open Skies aerial photographic image (including optically degraded images) by processing only in the spatial domain. This conclusion is evident from the sharp edges in the optimized images when compared to the original images. Also, use of a model fit algorithm can produce results that are almost perfect compared to the original or compared to the results achievable with commercially available photograph editing software. Furthermore, this research shows that increasing the resolution of OS photographs is dependent upon sampling: if the original images were not optically enlarged, there would have been insufficient samples for processing. For example, using the 5.7 micron scanner on group 9, the original negative produced a 21 by 21 pixel matrix, while scanning the enlarged negative produced a 200 by 200 pixel matrix. Scanning group 12 at 5.7 microns produced a 150 by 150 pixel matrix (Figure 25), while scanning at 4 microns produced a 200 by 200 pixel matrix (Figure 28). For group 12, the algorithm successfully optimized a 4 micron scan, but failed when applied to the 5.7 micron scan. The algorithm also increased the resolution of the airstar emblem present on the B-1A and the C-119 aircraft found outside the USAF Museum by 84 and 68 percent respectively. In both cases the optimized images show less noise (e.g., due to speckling) and more feature definition. In addition, the results indicate that sampling limits the amount of increased resolution.

The robustness of the model fit method is tied to prior knowledge (i.e., the better

the prior knowledge, the better the results). In this application, prior knowledge allows generation of specific models for specific images. When these models are applied to the wrong object (i.e., 3-Bar target model applied to an airstar image), the algorithms fail and the finished product may be nonsensical. For example, due to prior knowledge the 3-Bar target model is coded to find the first bar in a 3-Bar target within the first third of the image, while the 2-Bar target model finds the first bar within the first half of the image. Since the first third in a 2-Bar target image should not contain a bar (or at best, should contain only a portion of a bar), the 3-Bar target model fails when applied to a 2-Bar target image. Likewise, the 2-Bar target model fails when applied to a 3-Bar target image.

Follow-on research could easily extend this spatial domain prior knowledge model fit method by incorporating wavelet-based noise reduction, the error reduction technique developed by Matson [33], and developing additional models. Another area of research could develop methods that limit the amount of increased resolution achievable using prior knowledge.

APPENDIX A. Matlab Code

Table 3. List of Matlab Code and Data Files

Models	Input Data	Output Data	
BarModel_3d.m	group9_tar66a.mat group12_tar66a.mat group12_target66u.mat tar66a.mat target66u.mat	tar66a1_group9.mat tar66a1_group12.mat target66u_group12.mat	
astar_model_plane55.m	airstar.mat plane55a.mat plane55b.mat	astar_plane55b_B1.mat astar_plane55a_C119.mat	
BarModel_GE_S1.m	ges1.mat	ges1_vbar.mat	
Functions			
makemodelc.m	rect3.m	scale_intensity.m	line_MSE.m
minmize.m	minmize_2bar.m	suptitle.m	roundoff.m*
makemodelc_2bar.m	rect_2bar.m	line_MSE_2bar.m	fmins.m**
shiftu.m*	shiftl.m*	shiftr.m*	shiftd.m*
* Files are available at www.matlab.com			
** Matlab built-in function			

```
%-----
%-----
% program astar_model_plane55.m
% By Dan Sperl
% AFIT/GEO/ENG/00M-03
%-----
% subroutines called
% suptitle.m  fmins.m  roundoff.m
% shiftd.m   shiftu.m  shiftl.m  shiftr.m
% scale_intensity.m
%-----
% This program compares the airstar extracted from an image of a C-119 or a B-1A to a airstar model.
% The program begins by estimating the degree of rotation in the original, then resizes the model
% until it is smaller than the extracted section. Then the algorithm slides and rotates the model
% until the MSE is minimized. Finally, the results are plotted.
%-----
clear all
close all
format compact
% Uncomment selection, either C-119 (default) or B-1A
% Comment the others
plane='C-119';
%plane='B-1A';
```

```

load airstar.mat
if strcmp(plane,'C-119')
    load plane55a.mat
    fig1_tit='C-119 Cargo Plane';
    fig_tit='C-119 Airstar';
    data_out='astar_plane55a_C119';
    test_rat=.1; rat=0.9; ratio=1.5;
    MSE=1E100; MSE3=4E100; qt=20; MSE_count=1;
    scale_test=0; count=20; count_y=5;
    angle=0; scale=0; adjust=0.04;
    b1=.2; b2=.4; a1=-2; a2=2;
else strcmp(plane,'B-1A')
    load plane55b.mat
    cargo=B1A;
    fig1_tit='B-1A Bomber';
    fig_tit='B-1A Airstar';
    data_out='astar_plane55b_B1';
    test_rat=0.16; rat=0.9; ratio=1.5;
    MSE=1E100; MSE3=4E100; qt=20; MSE_count=1;
    scale_test=0; count=20; count_y=3;
    angle=0; scale=0; adjust=0.03;
    b1=.1; b2=.15; a1=-1; a2=1;
end; % if
%-----
airstar=airstar.*255;
star_wing=double(star_wing);
k=double(star_wing);
p4=k;
%-----
%determine spacing for x and y axis
[yk,xt]=size(p4);
%-----
% Determine degree of rotation
[a,b]=size(k);
angle=-atan((row2-row1)/(col2-col1));
angle_deg=angle*180/pi
%-----
% Begin main program
'Performing Best Fit'

while ((MSE_count>0)&(b1>=.08)&(rat<=ratio))
    x=linspace(b1,b2,count); y=linspace(a1,a2,3);
    MSE_count=0;
    for scale=length(x):-1:1
        for angle=1:length(y)
            test_sc=x(scale)
            test_angle=(angle_deg+y(angle))
            air=zeros(yk,xt)+max(max(airstar));
            airstar_test=imresize(airstar,(test_sc));
            [a,b]=size(airstar_test);
            ax=floor(yk/2-a/2); bx=floor(xt/2-b/2);
            if ((ax+a-1>yk)|(bx+b-1>xt)|ax<1|bx<1)% test size
                'do nothing' %move on to next case
            else % test size
                air(ax:ax+a-1,bx:bx+b-1)=airstar_test;
                airstar_rotate=shiftn(air,0,25,1);
            end
        end
    end
    MSE_count=MSE_count+1;
    MSE=MSE/MSE_count;
    MSE3=MSE3/MSE_count;
    MSE_count=0;
end

```

```

airstar_rot=imrotate(airstar_rotate,test_angle,'crop');
[a,b]=find(airstar_rot==0);
air=abs(airstar_rot);
clear airstar_rotate airstar_test
k=max(max(airstar));
for q=1:length(a)
    if air(a(q),b(q))==0, air(a(q),b(q))=k; end;    % if
end;    % for q
p4=air;
for s=1:9    % shifting procedure
    for t=1:4:qt
        switch s
            case 1, if t==1    % 'No shift'
                p4a=p4; end;
            case 2 %,['Shift ',num2str(t),' row(s) up']
                p4a=shifu(p4,0,t,1);
            case 3 %,['Shift ',num2str(t),' row(s) down']
                p4a=shiftd(p4,0,t,1);
            case 4 %,['Shift ',num2str(t),' columns(s) left']
                p4a=shifl(p4,0,t,1);
            case 5 %,['Shift ',num2str(t),' columns(s) right']
                p4a=shifr(p4,0,t,1);
            case 6 %,['Shift ',num2str(t),' row(s) up & column(s) left']
                p5=shifu(p4,0,t,1); p4a=shifl(p5,0,t,1);
            case 7 %,['Shift ',num2str(t),' row(s) up & column(s) right']
                p5=shifu(p4,0,t,1); p4a=shifr(p5,0,t,1);
            case 8 %,['Shift ',num2str(t),' row(s) down & column(s) left']
                p5=shiftd(p4,0,t,1); p4a=shifl(p5,0,t,1);
            case 9 %,['Shift ',num2str(t),' row(s) down & column(s) right']
                p5=shiftd(p4,0,t,1); p4a=shifr(p5,0,t,1);
        end;    % case
        air1=p4a;
        %-----
        % Redo the banding for trailing edge
        if strcmp(plane,'C-119')
            rise=length(rowt1:rowt2);
            run=length(col1:colt2);
            xcol=length(run:rise);    %number or column adjustments
            shift=run/xcol;
            count=0; col=1;
            for q=rowt1:rowt2
                count=count+1;
                col=col+1;
                if count>shift, col=col-1; count=shift-round(shift); end;
                air1(q,1:col)=0;
            end;
        end;    % if
        %-----
        % Redo the banding for leading edge
        rise=length(row1:row2); run=length(col1:col2);
        count=0; col=col1;
        if strcmp(plane,'C-119')
            xcol=length(run:rise);
            for q=1:length((row1):row2)
                count=count+1;
                if count==xcol

```



```

        airl(q,col:end)=0; col=col-1; count=0;
    else
        col=col+1; airl(q,col:end)=0;
    end
end; % for
else
    xcol=rise/length(rise:run);
    for q=1:length((row1):row2)
        count=count+1;
        if count>=xcol
            airl(q,col:end)=0; col=col+2; count=count-xcol;
        else
            col=col+1; airl(q,col:end)=0;
        end
    end; % for
end; % if C-119
[a1,a2]=size(star_wing);
%-----
% Calculate MSE between given data and model
MSE2=sum(sum((airl-star_wing).^2))/(a1*a2);
qrms=sqrt(MSE2);
model_diff=(airl-star_wing);
%-----
% scale intensity of model_diff if greater than 255 or less than 0
model_diff=scale_intensity(model_diff);
%-----
mean_given=(sum(sum(star_wing)))/(a1*a2);
std_given=sqrt(sum(sum((star_wing-mean_given).^2))/(a1*a2));
ratio=(qrms/std_given);
y_minz=(star_wing+ratio);
%-----
% scale intensity of y_minz if greater than 255 or less than 0
y_minz=scale_intensity(y_minz);
%-----
% Calculate MSE between given data and modified image
MSE1=sum(sum((y_minz-star_wing).^2))/length(star_wing);
rat=MSE1/MSE2;
if (((MSE1<MSE2)|(MSE2<MSE3))&(abs(rat-ratio))>=test_rat)
    MSE=MSE1;
    MSE3=MSE2;
    ratio_test=rat;
    ratio;
    airstar_new=y_minz;
    airstar_model=airl;
    shift_angle=test_angle;
    scale_new=test_sc;
    qrms_min=sqrt(MSE1);
    MSE_count=MSE_count+1;
end; % if
%-----
end; % test size
end; % for t
end; % for s
end; % for angle
end; % for scale
if MSE_count>0

```

```

        b1=scale_new-adjust;
        b2=scale_new+adjust;
        count=20;
    end; % if
end; % while
%-----
% Save variables
variables=' star_wing airstar_model airstar_new MSE MSE3 shift_angle scale_new ratio_test';
eval(strcat('save ',data_out,variables))
%-----
% Plotting routines
%-----
eval(strcat('load ',data_out))
az=75; el=78;
figure(11), set(gcf,'color',[1 1 1])
subplot(121)
imagesc(star_wing),axis image, grid on;
title('2D View'),ylabel('Row #'),xlabel('Column #')
subplot(122)
surf(star_wing),axis image, grid on, view(az,el), shading interp;
title('3D View'),ylabel('Row #'),xlabel('Column #')
set(gcf,'PaperType','usletter'), set(gcf,'PaperOrientation','landscape');
set(gca,'ZTick',[0;100;200])
set(gcf,'PaperPosition',[.25, .25, 10.5, 8]);
                        % left bottom width height
colormap(gray(256))
suptitle(strcat(fig_tit,' - Original Image'));
%-----
figure(12), set(gcf,'color',[1 1 1])
subplot(121)
imagesc(airstar_model),axis image,grid on
title('2D View'),ylabel('Row #'),xlabel('Column #')
subplot(122)
surf(airstar_model),axis image, grid on, view(az,el),shading interp;
title('3D View'),ylabel('Row #'),xlabel('Column #')
set(gcf,'PaperType','usletter'), set(gcf,'PaperOrientation','landscape');
set(gca,'ZTick',[0;100;200])
set(gcf,'PaperPosition',[.25, .25, 10.5, 8]);
                        % left bottom width height
colormap(gray(256))
suptitle(strcat(fig_tit,' - Model'));
%-----
az=75; el=78;
figure(13), set(gcf,'color',[1 1 1])
subplot(121)
imagesc(airstar_new),axis image, grid on;
title('2D View'),ylabel('Row #'),xlabel('Column #')
subplot(122)
surf(airstar_new),axis image, grid on, view(az,el),shading interp;
title('3D View'),ylabel('Row #'),xlabel('Column #')
set(gcf,'PaperType','usletter'), set(gcf,'PaperOrientation','landscape');
set(gca,'ZTick',[0;100;200])
set(gcf,'PaperPosition',[.25, .25, 10.5, 8]);
                        % left bottom width height
colormap(gray(256))
suptitle(strcat(fig_tit,' - Modified Image'));

```

```

%-----
%-----
% Program BarModel_3d.m
% By Dan Sperl
% AFIT/GEO/ENG/00M-03
%-----
% subroutines called
% makemodelc_2bar.m      rect_2bar.m      suptitle.m      fmins.m
% line_MSE_2bar.m       roundoff.m      shiftd.m       scale_intensity.m
% minimize_2bar.m       shiftu.m      shiftd.m       shiftr.m
%-----
% This program compares an extracted square matrix from the 3-Bar Target to a model.
% The program begins by scanning three rows to get an average estimate of the bar width and the
% the starting position. Using these estimates, the program calls subroutine 'makemodel.m'
% to create a model. The program then tries to minimize the mean square error (MSE) by varying the
% placement of the model by shifting the matrix (left, right, up, & down), width, starting
% position, as well as adjusting the minimum and maximum gray levels in the given matrix..
% The results are then plotted.
%-----
clear all
format compact
% Uncomment selection, either Group 9, tar66a.tif (default), Group 12, tar66a.tif, or Group 12, target66u.tif
% Comment the others
test_bar='Group 9, tar66a.tif';
%test_bar='Group 12, tar66a.tif';
%test_bar='Group 12, target66u.tif';
if strcmp(test_bar,'Group 9, tar66a.tif')
    fig_tit=' Group 9, tar66a.tif';
    data_in_1=' tar66a.mat';
    data_in_2=' grp9_tar66a.mat';
    data_out=' tar66a1_group9';
    av=1200; bv=2000; cv=1400; dv=2100;
    eval(strcat('load ',data_in_1))
    eval(strcat('load ',data_in_2))
    k=bar;
    b_width_est=[40];
elseif strcmp(test_bar,'Group 12, tar66a.tif')
    fig_tit=' Group 12, tar66a.tif';
    data_in_1=' tar66a.mat';
    data_in_2=' grp12_tar66a.mat';
    data_out=' tar66a1_group12';
    av=800; bv=2000; cv=1400; dv=2100;
    eval(strcat('load ',data_in_1))
    eval(strcat('load ',data_in_2))
    k=bar;
    b_width_est=[];
elseif strcmp(test_bar,'Group 12, target66u.tif')
    fig_tit=' Group 12, target66u.tif';
    data_in_1=' target66u.mat';
    data_in_2=' grp12_target66u.mat';
    data_out=' target66u_group12';
    av=1; bv=1300; cv=350; dv=1100;
    eval(strcat('load ',data_in_1))
    eval(strcat('load ',data_in_2))
    k=bar;
    b_width_est=[];

```

```

else
    'do nothing'
end; % if
%-----
% Declare global variables
global max_gray_floor min_gray_ceil x yk xt yt min_gray max_gray p1 ab_max_p ab_min_p ...
    scale_factor max_gray_floor min_gray_ceil p4 p4a y2 x0 b_width
%-----
% setup initial conditions
s1=a; % Start Row
s2=c+a; % End Row
x1=b; % Start Column
x2=c+b; % End Column

p=double(k(s1:s2,x1:x2));
p4=p; xx=x1:x2; beta=0.05;
y_min1=[]; y_rms=[]; bf=[]; x0_rms=[]; y_min2=[];
ab_max_p=max(max(p)); % maximum gray scale value
ab_min_p=min(min(p)); % minimum gray scale value

%determine spacing for x and y axis
[yk,xt]=size(p4);
x=linspace(x1,x2,xt); %y axis spacing
yt=linspace(s1,s2,xt); %x axis spacing
%-----
% determine min and max gray levels
max_gray_floor=round(ab_max_p-beta*ab_max_p); %determine floor and ceiling values
min_gray_ceil=round(ab_min_p+beta*1.5*ab_max_p); %for gray scale threshold
%-----
% Perform the linescan of the three rows to obtain estimate
% Pass variables row data
'Performing Line Scan to Determine Estimate of Width and Starting Position'
rows=[round(yk/3) round(yk/2) 2*round(yk/3)];
p1=p4(rows,:); x0_est=[];
for t=1:length(rows)
    p1=p4(rows(t,:),:);
    [b_width,x0,MSE,qrms,y_min]=line_MSE(p1); % data to estimate bar width & starting position
    b_width_est=cat(2,b_width_est,b_width);
    x0_est=cat(1,x0_est,x0);
end;
% determine estimate for bar width & starting position
if (strcmp(test_bar,'Group 12, tar66a.tif')|strcmp(test_bar,'Group 12, target66u.tif'))
    if mean(b_width_est(1:2))>mean(b_width_est(2:3))
        b_width=mean(b_width_est(2:3));
        x0=mean(x0_est(2:3,1));
    elseif mean(b_width_est(2:3))>mean(b_width_est(1:2))
        b_width=mean(b_width_est(1:2));
        x0=mean(x0_est(1:2,1));
    else
        b_width=mean(b_width_est);
        x0=mean(x0_est(:,1));
    end; % inner if
else
    b_width=mean(b_width_est);
    x0=mean(x0_est(:,1));
end; % outer if

```

```

p1=p4(rows(2),:);
%-----
% Begin main program
'Performing Best Fit'
MSE=1E12; q=10;
for s=1:9
    for t=1:q
        switch s
            case 1, if t==1 % 'No shift'
                p4a=p4; end;
            case 2 %,['Shift ',num2str(t),' row(s) up']
                p4a=shifu(p4,0,t,1);
            case 3 %,['Shift ',num2str(t),' row(s) down']
                p4a=shiftd(p4,0,t,1);
            case 4 %,['Shift ',num2str(t),' columns(s) left']
                p4a=shifl(p4,0,t,1);
            case 5 %,['Shift ',num2str(t),' columns(s) right']
                p4a=shifr(p4,0,t,1);
            case 6 %,['Shift ',num2str(t),' row(s) up & column(s) left']
                p5=shifu(p4,0,t,1); p4a=shifl(p5,0,t,1);
            case 7 %,['Shift ',num2str(t),' row(s) up & column(s) right']
                p5=shifu(p4,0,t,1); p4a=shifr(p5,0,t,1);
            case 8 %,['Shift ',num2str(t),' row(s) down & column(s) left']
                p5=shiftd(p4,0,t,1); p4a=shifl(p5,0,t,1);
            case 9 %,['Shift ',num2str(t),' row(s) down & column(s) right']
                p5=shiftd(p4,0,t,1); p4a=shifr(p5,0,t,1);
        end; % case

        count=11; b1=b_width-.5; b2=b_width+.5;
        MSE_count=1;

        while (MSE_count>0&(b1<b2))
            MSE_count=0;
            lam=[b_width, x0(1)];
            MSE1=double(fmins('minimize',lam));
            b_test=MSE1(1);
            x0=MSE1(2);

            [y2,x0]=makemodelc(b_test,x0,p4a);
            MSE1=sum(sum((y2-p4).^2))/(xt*yk); %Determine MSE
            if (MSE1<MSE)
                MSE=MSE1
                y_min=y2;
                x0_min=x0;
                b_min=b_test;
                qrms_min=sqrt(MSE1);
                MSE_new=qrms_min+MSE;
                MSE_count=MSE_count+1;
            end; %if
            if MSE_count>0'MSE Lowered'; end; % if
        end; % while
    end; % for t
end; % for s
%-----
% Collect variables
bf=cat(2,bf,b_min);
x0_rms=cat(1,x0_rms,x0_min);
mean_given=sum(sum(p4))/(xt*yk);

```

```

        std_given=sqrt(sum(sum((p4-mean_given).^2))/(xt*yk));
        ratio=(y_min-p4).*(qrms_min/std_given);
        y_minz=p4+ratio;
    end; %for t
end; %for s

bf=roundoff(bf,4);
x0_rms=roundoff(x0_rms,4);
%-----
% Replace optimized section in Original matrix
k_up=k;
k_up(s1:s2,x1:x2)=y_minz;
%-----
% Save variables
var1=' y_min1 y_rms x0_rms bf p1 x xx y_min y_minz y_min2';
var2=' ab_min_p ab_max_p s1 s2 qrms_min k_up p4 xt yk b_min';
eval(strcat('save ',data_out,var1,var2))
%-----
% Plotting routines
%-----
eval(strcat('load ',data_in_1))    % Load data file
eval(strcat('load ',data_out))    % Load data file

if strcmp(test_bar,'Group 12, target66u.tif')
    k=target;
else
    k=bar;
end;
% Display upsampled image
az=-20; el=38;
figure(12), set(gcf,'color',[1 1 1])
subplot(121)
imagesc(p4),grid on,axis image,ylabel('Row #'),xlabel('Column #');
set(gca,'ydir','normal');
subplot(122)
surf(p4),shading interp,view(az,el),axis image,ylabel('Row #'),xlabel('Column #');
colormap(bone),axis square
set(gcf,'PaperType','usletter'), set(gcf,'PaperOrientation','landscape');
set(gcf,'PaperPosition',[.25, .25, 10.5, 8]);
% left bottom width height
suptitle(strcat(fig_tit,' - Original Image'));
%-----
az=-7.5; el=14;
y_minz1=y_minz;
%scale intensity if greater than 255 or less than 0
if max(max(y_minz1))>255
    y_minz1=y_minz1-(max(max(y_minz1))-255);end;
if min(min(y_minz1))<0
    [a,b]=find(y_minz1<0);
    for q=1:length(a), y_minz1(a(q),b(q))=0; end
end;
z1=min(min(y_minz1))-20; if z1<0, z1=0; end;
z2=max(max(y_minz1))+20; if z2>255, z2=255; end;
figure(2), set(gcf,'color',[1 1 1])
subplot(121)
imagesc(y_minz1),grid on,axis image,ylabel('Row #'),xlabel('Column #');

```

```

set(gca,'ydir','normal')
subplot(122)
mesh(y_minz1),view(az,el),axis square,axis([0 yk 0 xt z1 z2]);
ylabel('Row #'),xlabel('Column #')
set(gcf,'PaperType','usletter'), set(gcf,'PaperOrientation','landscape');
set(gcf,'PaperPosition',[.25, .25, 10.5, 8]);
% left bottom width height
colormap(bone)
%colormap(copper)
suptitle(strcat(fig_tit,' - Optimized Image'));
%-----
figure(4), set(gcf,'color',[1 1 1])
subplot(121)
imagesc(k(av:bv,cv:dv)),colormap(gray(256)),grid on,axis image,ylabel('Row #'),xlabel('Column #');
subplot(122)
imagesc(k_up(av:bv,cv:dv)),colormap(gray(256)),grid on,axis image,ylabel('Row #'),xlabel('Column #');
set(gcf,'PaperType','usletter'), set(gcf,'PaperOrientation','landscape');
set(gcf,'PaperPosition',[.25, .25, 10.5, 8]);
% left bottom width height
suptitle(strcat(fig_tit,' - Original and Optimized Images'));

%-----
% Line plots
figure(1), set(gcf,'color',[1 1 1])
subplot(211)
plot(p4(round(yk/2),:))
subplot(212)
plot(y_minz1(round(yk/2),:))

```

```

%-----
%-----
% Program BarModel_GE_S1.m
% By Dan Sperl
% AFIT/GEO/ENG/00M-03
%-----
% subroutines called
% makemodelc_2bar.m      rect_2bar.m      suptitle.m      fmins.m
% line_MSE_2bar.m       roundoff.m      shiftd.m        scale_intensity.m
% minimize_2bar.m       shiftu.m        shiftl.m        shiftr.m
%-----
% This program compares an extracted square matrix from the 2-Bar Target to a model.
% The program begins by scanning five rows to get an average estimate of the bar width and the
% the starting position. Using these estimates, the program calls subroutine 'makemodel.m'
% to create a model. The program then tries to minimize the mean square error (MSE) by varying the
% placement of the model by shifting the matrix (left, right, up, & down), width, starting
% position, as well as adjusting the minimum and maximum gray levels in the given matrix..
% The results are then plotted.
%-----
clear all
format compact
load ges1.mat      % necessary data file
%-----
% Declare global variables
global max_gray_floor min_gray_ceil x yk xt yt min_gray max_gray p lab_max_p ab_min_p ...
scale_factor max_gray_floor min_gray_ceil p4 p4a y2 x0 b_width
%-----
% Setup initial conditions

k=bar;
% Uncomment selection, either v_bar (default) or h_bar
% Comment the others
test_bar='v_bar';
%test_bar='h_bar';
if strcmp(test_bar,'v_bar')
    fig1_tit='Vertical Bars';
    fig_tit='German S1 Filter';
    data_out='ges1_vbar';
    a=av; b=bv; c=cv; d=dv;
    p=double(v_bar);
else strcmp(test_bar,'h_bar')
    fig1_tit='Horizontal Bars';
    fig_tit='German S1 Filter';
    data_out='ges1_hbar';
    a=ah; b=bh; c=ch; d=dh;
    p=double(h_bar); % transpose data to calculate
end; % if

s1=a; % Start Row
s2=c+a; % End Row
x1=b; % Start Column
x2=d+b; % End Column
p4=p; xx=x1:x2; beta=0.05;

y_min1=[]; y_rms=[]; bf=[]; x0_rms=[]; y_min2=[];
ab_max_p=max(max(p));

```



```

ab_min_p=min(min(p));

%determine spacing for x and y axis
[yk,xt]=size(p);
x2a=x1+xt;
x=linspace(x1,x2,xt);    %y axis spacing
s2a=s1+yk;
yt=linspace(s1,s2,xt);    %x axis spacing

%-----
%determine min and max gray levels
max_gray_floor=round(ab_max_p-beta*ab_max_p);    %determine floor and ceiling values
min_gray_ceil=round(ab_min_p+beta*1.5*ab_max_p);    %for gray scale threshold

%-----
% Perform the linescan of the five rows to obtain estimate
% Pass variables row data
'Performing Line Scan to Determine Estimate of Width and Starting Position'
rows=[round(yk/6) 2*round(yk/6) 3*round(yk/6) 4*round(yk/6) 5*round(yk/6)];
p1=p(rows,:);
x0_est=[];
b_width_est=[];
for t=1:length(rows)
    strcat('row ',num2str(t))
    p1=p(rows(t,:),:);
    [b_width,x0,MSE,qrms,y_min]=line_MSE_2bar(p1);
    b_width_est=cat(2,b_width_est,b_width);
    x0_est=cat(1,x0_est,x0);
end;
b_width=mean(b_width_est)
x0=mean(x0_est(:,1))

%-----
% Begin main program
'Performing Best Fit'
MSE=1E12; q=10;
for s=1:9
    for t=1:q
        switch s
            case 1, if t==1 'No shift'
                p4a=p4; end;
            case 2, ['Shift ',num2str(t),' row(s) up']
                p4a=shiftu(p4,0,t,1);
            case 3, ['Shift ',num2str(t),' row(s) down']
                p4a=shiftd(p4,0,t,1);
            case 4, ['Shift ',num2str(t),' column(s) left']
                p4a=shifl(p4,0,t,1);
            case 5, ['Shift ',num2str(t),' column(s) right']
                p4a=shiftr(p4,0,t,1);
            case 6, ['Shift ',num2str(t),' row(s) up & column(s) left']
                p5=shiftu(p4,0,t,1); p4a=shifl(p5,0,t,1);
            case 7, ['Shift ',num2str(t),' row(s) up & column(s) right']
                p5=shiftu(p4,0,t,1); p4a=shiftr(p5,0,t,1);
            case 8, ['Shift ',num2str(t),' row(s) down & column(s) left']
                p5=shiftd(p4,0,t,1); p4a=shifl(p5,0,t,1);
            case 9, ['Shift ',num2str(t),' row(s) down & column(s) right']

```

```

        p5=shiftd(p4,0,t,1); p4a=shiftr(p5,0,t,1);
    end; % case

    count=11; b1=b_width-.5; b2=b_width+.5;
    MSE_count=1;

    while (MSE_count>0&(b1<b2))
        MSE_count=0;
        lam=[b_width, x0(1)];
        MSE1=double(fmins('minimize_2bar',lam));
        b_test=MSE1(1);
        x0=MSE1(2);

        [y2,x0]=makemodelc_2bar(b_test,x0,p4a);
        MSE1=sum(sum((y2-p4).^2))/(xt*yk);
        if (MSE1<MSE)
            MSE=MSE1
            y_min=y2;
            x0_min=x0;
            b_min=b_test;
            qrms_min=sqrt(MSE1);
            MSE_new=qrms_min+MSE;
            MSE_count=MSE_count+1;
            end; %if
            if MSE_count>0'MSE Lowered'; end; % if
        end; %while
        %-----
        % Collect variables
        bf=cat(2,bf,b_min);
        x0_rms=cat(1,x0_rms,x0_min);
        mean_given=sum(sum(p4))/(xt*yk);
        std_given=sqrt(sum(sum((p4-mean_given).^2))/(xt*yk));
        ratio=(y_min-p4).*(qrms_min/std_given);
        y_minz=p4+ratio;
    end; %for t
end; %for s

bf=roundoff(bf,4);
x0_rms=roundoff(x0_rms,4);
%-----
% Replace optimized section in Original matrix
k_up=k;
k_up(x1:x2,s1:s2)=y_minz;
%-----
% Save variables
var1=' y_min1 y_rms x0_rms bf p1 x xx y_min y_minz y_min2';
var2=' ab_min_p ab_max_p s1 s2 qrms_min k_up p4 xt yk b_min';
eval(strcat('save ',data_out,var1,var2))
%-----
% Plotting routines
%-----
eval(strcat('load ',data_out))
load ges1.mat

k=bar;
% Display upsampled image

```

```

az=-30; el=50;
figure(12), set(gcf,'color',[1 1 1]),subplot(121)
imagesc(p4),grid on,axis image,ylabel('Row #'),xlabel('Column #');
set(gca,'ydir','normal')
subplot(122)
surf(p4),shading interp,view(az,el),axis image,ylabel('Row #'),xlabel('Column #');
%colormap(copper)
colormap(bone)
set(gcf,'PaperType','usletter'), set(gcf,'PaperOrientation','landscape');
set(gcf,'PaperPosition',[.25, .25, 10.5, 8]);
% left bottom width height
suptitle(strcat(fig_tit,' - Original Image'));
%-----
az=-19; el=40;
y_minz1=y_minz;
% scale intensity if greater than 255 or less than 0
if max(max(y_minz1))>255
    y_minz1=y_minz1-(max(max(y_minz1))-255);end;%(255-ab_max_p); end;
if min(min(y_minz1))<0
    [a,b]=find(y_minz1<0);
    for q=1:length(a), y_minz1(a(q),b(q))=0; end
end;
z1=min(min(y_minz1))-20; if z1<0, z1=0; end;
z2=max(max(y_minz1))+20; if z2>255, z2=255; end;
figure(2), set(gcf,'color',[1 1 1])
subplot(121)
imagesc(y_minz1),grid on,axis image,ylabel('Row #'),xlabel('Column #');
set(gca,'ydir','normal')
subplot(122)
mesh(y_minz1),view(az,el),axis square,axis([0 xt 0 yk z1 z2]);
ylabel('Row #'),xlabel('Column #')%set(gca,'ydir','rev')
set(gcf,'PaperType','usletter'), set(gcf,'PaperOrientation','landscape');
set(gcf,'PaperPosition',[.25, .25, 10.5, 8]);
% left bottom width height
%colormap(bone)
colormap(copper)
suptitle(strcat(fig_tit,' - Optimized Image'));
%-----
figure(4), set(gcf,'color',[1 1 1])
a=2000; b=4300; c=1000; d=3100;
subplot(121)
imagesc(k(a:b,c:d)),colormap(gray(256)),grid on,axis image,ylabel('Row #'),xlabel('Column #');
subplot(122)
imagesc(k_up(a:b,c:d)),colormap(gray(256)),grid on,axis image,ylabel('Row #'),xlabel('Column #');
set(gcf,'PaperType','usletter'), set(gcf,'PaperOrientation','landscape');
set(gcf,'PaperPosition',[.25, .25, 10.5, 8]);
% left bottom width height
suptitle(strcat(fig_tit,' - Original and Optimized Images'));
%-----
% Line plots
figure(1), set(gcf,'color',[1 1 1])
subplot(211),plot(p4(round(yk/2),:))
subplot(212),plot(y_minz1(round(yk/2),:))

```

```

%-----
%-----
function [B_MIN,X0_MIN,MSE,qrms_min,y_min]=line_MSE(P1)
% Program line_MSE
% by Dan Sperl
% AFIT/GEO/ENG/00M-03
%-----
global max_gray_floor min_gray_ceil x yk xt yt
%-----
% Begin main program
PX=sort(P1);MSE=1E12;      MSE2=0;
count=5;    b1=1; b2=60;    MSE_count=1; b_min=b2;

% determine zz
zz=1; aa=1; bb=1;
max_gray=255; min_gray=0; % initialize gray levels for while loop
while max_gray>max_gray_floor&min_gray<min_gray_ceil
    max_gray=round(mean(PX(length(PX)-aa:length(PX))));
    min_gray=round(mean(PX(1:bb)));
    zz=zz+1; aa=aa+1; bb=bb+1;
end;

kz=linspace(1,zz,count);
y2x=zeros(count^4,length(x)); MSE1x=zeros(1,count^4); b_x=zeros(1,count^4); y_minx=[];
qrms_x=zeros(1,count^4); min_gray_x=zeros(1,count^4);
aa_count=1; bb_count=1; y_count=1; y1=[];
max_gray_x=zeros(1,count^4);
t1=find(P1==max(P1(1:round(yk/3)+2)));
t2=x(t1(1)); % starting point for rectangle
x1a=linspace(t2-1,t2+1,count);

while (MSE_count>0&(b1<b2)) %&(b_min<b2)
    z_count=1;
    MSE_count=0;
    %use 'for loops aa and bb' to minimize MSE for min_gray and max_gray
    for aa=1:length(kz)
        for bb=1:length(kz)
            max_gray=round(mean(PX(length(PX)-aa:length(PX))));
            min_gray=round(mean(PX(1:bb))); %detrmine min/max gray scale for each iteration

            % find desired square wave that minimizes the MSE with P1
            b=linspace(b1,b2,count); % set width dimensions for rectangle
            %use 'for loops y and z' to minimize MSE for rectangle width
            for y=1:length(x1a)
                for z=1:length(b)
                    z_count=z_count+1;
                    [y2,x0]=rect3(x1a(y),b(z),x); % rectangle function
                    y2xb=find(y2==1); y2(y2xb)=max_gray; % replace one values with max_gray values
                    y2xa=find(y2==0); y2(y2xa)=min_gray; % replace zero values with min_gray values
                    y2=y2+(P1-y2)/(sqrt(std(P1)));

                    MSE1=sum((y2-P1).^2)/length(y2);
                    qrms=sqrt(MSE1); % calculate root mean square error

                    if ((MSE1<MSE))
                        MSE=MSE1;

```

```

        y_min=y2;
        x0_min=x0;
        b_min=b(z)
        gray_min=min_gray;
        gray_max=max_gray;
        qrms_min=qrms;
        MSE_new=qrms+MSE;
        MSE_count=MSE_count+1;
    end; % if
end; % for z
end; % for y
end; % for bb
end; % for aa
mk=abs((b2-b1)/8);
if MSE_count>0
'MSE Lowered'
    b1=((b_min))-mk-0.2;      % reduce rectangle testing width
    b2=((b_min))+mk+0.2;    % reduce rectangle testing width
    if (b2-b1)<3, count=21; end;
    if (b2-b1)<=1.5, count=41; end;
end; % if
end; % while
B_MIN=b_min;
X0_MIN=x0_min;

```

```

%-----
%-----
function [B_MIN,X0_MIN,MSE,qrms_min,y_min]=line_MSE_2bar(P1)
% by Dan Sperl
% AFIT/GEO/ENG/00M-03
%-----
global max_gray_floor min_gray_ceil x yk xt yt
%-----
% Begin main program
    PX=sort(P1);MSE=1E12;      MSE2=0;
    count=5;    b1=1; b2=60;    MSE_count=1; b_min=b2;

% determine zz
zz=1; aa=1; bb=1;
max_gray=255; min_gray=0; % initialize gray levels for while loop
while max_gray>max_gray_floor&min_gray<min_gray_ceil
    max_gray=round(mean(PX(length(PX)-aa:length(PX))));
    min_gray=round(mean(PX(1:bb)));
    zz=zz+1; aa=aa+1; bb=bb+1;
end;

kz=linspace(1,zz,count);
y2x=zeros(count^4,length(x)); MSE1x=zeros(1,count^4); b_x=zeros(1,count^4); y_minx=[];
qrms_x=zeros(1,count^4); min_gray_x=zeros(1,count^4);
aa_count=1; bb_count=1; y_count=1; y1=[];
max_gray_x=zeros(1,count^4);
t1=find(P1==max(P1(1:round(yk/3)+2)));
t2=x(t1(1)); % starting point for rectangle
x1a=linspace(t2-1,t2+1,count);

while (MSE_count>0&(b1<b2))
    z_count=1;
    MSE_count=0;
    %use 'for loops aa and bb' to minimize MSE for min_gray and max_gray
    for aa=1:length(kz)
        for bb=1:length(kz)
            max_gray=round(mean(PX(length(PX)-aa:length(PX))));
            min_gray=round(mean(PX(1:bb))); % determine min/max gray scale for each iteration

            % find desired square wave that minimizes the MSE with P1
            b=linspace(b1,b2,count); % set width dimensions for rectangle
            %use 'for loops y and z' to minimize MSE for rectangle width
            for y=1:length(x1a)
                for z=1:length(b)
                    z_count=z_count+1;
                    [y2,x0]=rect_2bar(x1a(y),b(z),x); % rectangle function
                    y2xb=find(y2==1); y2(y2xb)=max_gray; % replace one values with max_gray values
                    y2xa=find(y2==0); y2(y2xa)=min_gray; % replace zero values with min_gray values
                    y2=y2+(P1-y2)/(sqrt(std(P1)));

                    MSE1=sum((y2-P1).^2)/length(y2);
                    qrms=sqrt(MSE1); % calculate root mean square error

                    if ((MSE1<MSE))
                        MSE=MSE1;
                        y_min=y2;

```

```

        x0_min=x0;
        b_min=b(z)
        gray_min=min_gray;
        gray_max=max_gray;
        qrms_min=qrms;
        MSE_new=qrms+MSE;
        MSE_count=MSE_count+1;
    end; % if
end; % for z
end; % for y
end; % for bb
end; % for aa
mk=abs((b2-b1)/8);
if MSE_count>0
'MSE Lowered'
    b1=((b_min))-mk-0.2;      % reduce rectangle testing width
    b2=((b_min))+mk+0.2;    % reduce rectangle testing width
    if (b2-b1)<3, count=21; end;
    if (b2-b1)<=1.5, count=41; end;
end; % if
end; % while
B_MIN=b_min;
X0_MIN=x0_min;

```

```

%-----
%-----
function [Y,X0]=makemodelc(B_ROWS,B_X0,Y_MIN1)
% by Dan Sperl
% AFIT/GEO/ENG/00M-03
%-----
global x yk xt yt min_gray max_gray p1 ab_max_p ab_min_p scale_factor ...
max_gray_floor min_gray_ceil
%-----
X=x; YK=yk; XT=xt; MIN_GRAY=ab_min_p;%min_gray;
MAX_GRAY=ab_max_p;%max_gray;
P1=p1;
start_row=1; end_row=1;
[QQ,RR]=size(Y_MIN1);

% Scan each to find beginning and ending row above threshold
for t=1:QQ
    PX=sort(Y_MIN1(t,:));
    aa=1; bb=1;
    max_gray=255; min_gray=0; % initialize gray levels for while loop
    while max_gray>max_gray_floor&min_gray<min_gray_ceil
        max_gray=round(mean(PX(length(PX)-aa:length(PX))));
        min_gray=round(mean(PX(1:bb)));
        aa=aa+1; bb=bb+1;
    end
end; %for
start_row;
end_row;

% determine # of rows and average starting position
K1=round(YK/2-1); %use middle row
NUM_ROWS=round(B_ROWS*5);
% calculate values for optimum square wave
MIN_GRAY=round(min(Y_MIN1(K1,:)));
MAX_GRAY=round(max(Y_MIN1(K1,:)));
[Y2,X0]=rect3(B_X0,B_ROWS,X); % rectangle function
Y2xb=find(Y2==1); Y2(Y2xb)=MAX_GRAY; % replace one values with max_gray values
Y2xa=find(Y2==0); Y2(Y2xa)=MIN_GRAY; % replace zero values with min_gray values
Y2=Y2+(P1-Y2)/(sqrt(std(P1)));
Y_min2=zeros(YK,XT)+min(Y2)+10;

for t=round(K1-NUM_ROWS/2+1):round(K1+NUM_ROWS/2)
    Y_min2(t,:)=Y2;
end;

Y=Y_min2;

```



```

%-----
%-----
function [Y,X0]=makemodelc_2bar(B_ROWS,B_X0,Y_MIN1)
% by Dan Sperl
% AFIT/GEO/ENG/00M-03
%-----
global x yk xt yt min_gray max_gray p1 ab_max_p ab_min_p scale_factor ...
max_gray_floor min_gray_ceil
%-----
X=x; YK=yk; XT=xt; MIN_GRAY=ab_min_p;%min_gray;
MAX_GRAY=ab_max_p;%max_gray;
P1=p1;
start_row=1; end_row=1;
[QQ,RR]=size(Y_MIN1);

% Scan each to find beginning and ending row above threshold
for t=1:QQ
    PX=sort(Y_MIN1(t,:));
    aa=1; bb=1;
    max_gray=255; min_gray=0; % initialize gray levels for while loop
    while max_gray>max_gray_floor&min_gray<min_gray_ceil
        max_gray=round(mean(PX(length(PX)-aa:length(PX))));
        min_gray=round(mean(PX(1:bb)));
        aa=aa+1; bb=bb+1;
    end;
end; %for
start_row;
end_row;

% determine # of rows and average starting position
K1=round(YK/2-1); %use middle row
NUM_ROWS=round(B_ROWS*5);
% calculate values for optimum square wave
MIN_GRAY=round(min(Y_MIN1(K1,:)));
MAX_GRAY=round(max(Y_MIN1(K1,:)));
[Y2,X0]=rect_2bar(B_X0,B_ROWS,X); %rectangle function
Y2xb=find(Y2==1); Y2(Y2xb)=MAX_GRAY; % replace one values with max_gray values
Y2xa=find(Y2==0); Y2(Y2xa)=MIN_GRAY; % replace zero values with min_gray values
Y2=Y2+(P1-Y2)/(sqrt(std(P1)));
Y_min2=zeros(YK,XT)+min(Y2)+10;

for t=round(K1-NUM_ROWS/2+1):round(K1+NUM_ROWS/2)
    %for t=start_row:end_row
    Y_min2(t,:)=Y2;
end;

Y=Y_min2;

```

```

%-----
%-----
function MSE1=minimize(lam)
% By Dan Sperl
% AFIT/GEO/ENG/00M-03
% This function is called by the Matlab command 'fmins' to minimize the mean
% squared error

global x yk xt yt min_gray max_gray p1 ab_max_p ab_min_p scale_factor ...
max_gray_floor min_gray_ceil p4 p4a y2

b_width=lam(1);
x0=lam(2);
y2=makemodelc(b_width,x0(1),p4a);
MSE1=sum(sum((y2-p4).^2))/(xt*yk); %Determine MSE

%-----
%-----
function MSE1=minimize_2bar(lam)
% By Dan Sperl
% AFIT/GEO/ENG/00M-03

global x yk xt yt min_gray max_gray p1 ab_max_p ab_min_p scale_factor ...
max_gray_floor min_gray_ceil p4 p4a y2
b_width=lam(1);
x0=lam(2);

y2=makemodela_2bar(b_width,x0(1),p4a);
MSE1=sum(sum((y2-p4).^2))/length(y2); %Determine MSE

%-----
%-----
function [Y]=scale_intensity(X)
% By Dan Sperl
% AFIT/GEO/ENG/00M-03

% This function scales the intensity of an matrix to values between 0 and 255
if min(min(X))<0
    X=X+abs(min(min(X)));
end;
if max(max(X))>255
    scale_X=max(max(X))/255;
    X=X/scale_X;
end;

```

```

%-----
%-----
function [YY,X0]=rect3(X1A,B,X)
% By Dan Sperl
% AFIT/GEO/ENG/00M-03

X0=[];
for w=1:3% this for loop determines the placement of the 3 rectangles
    X01=double(X1A+2*B*(w-1));
    X0=cat(2,X0,X01);
end; % for w

% Optimum Rectangle Function
Y2=zeros(1,length(X));
for t=1:length(X0)
    q=(X-X0(t))/B;
    for r=1:length(q)
        if abs(q(r))>0.5
            Y1(r)=0;
        else
            Y1(r)=1;
        end; % if
    end; % for r
    Y2=Y2+Y1; % sum the 3 iterations to get a vector with 3 rectangles
end; % for t
YY=Y2;

%-----
%-----
function [YY,X0]=rect_2bar(X1A,B,X)
% By Dan Sperl
% AFIT/GEO/ENG/00M-03

X0=[];
for w=1:2% this for loop determines the placement of the 3 rectangles
    X01=round(double(X1A+3*B*(w-1)));
    X0=cat(2,X0,X01);
end; % for w
%X0=x(X0);
adj=.2;
% Optimum Rectangle Function
Y2=zeros(1,length(X));
for t=1:length(X0)
    q=((X-X0(t))/B);
    q=roundoff(q,3);
    for r=1:length(q)
        if abs(q(r))>0.5+adj
            Y1(r)=0;
        else
            Y1(r)=1;
        end; % if
    end; % for r
    Y2=Y2+Y1; % sum the 2 iterations to get a vector with 2 rectangles
end; %for t
YY=Y2;

```

```

%-----
% This function was obtained from www.mathworks.com
%-----
function hout=suptitle(str)
%SUPTITLE Puts a title above all subplots. SUPTITLE('text') adds text to the top of the figure
% above all subplots (a "super title"). Use this function after all subplot commands.
% Drea Thomas 6/15/95 drea@mathworks.com
% Warning: If the figure or axis units are non-default, this will break.
% Parameters used to position the supertitle. Amount of the figure window devoted to subplots.

plotregion = .92;
titleypos = .95; % Y position of title in normalized coordinates
fs = get(gcf,'defaultaxesfontsize')+4; % Fontsize for supertitle
fudge=1; % Fudge factor to adjust y spacing between subplots
haold = gca;
figunits = get(gcf,'units');

% Get the (approximate) difference between full height (plot + title + xlabel) and bounding rectangle.
if (~strcmp(figunits,'pixels')),
    set(gcf,'units','pixels');
    pos = get(gcf,'position');
    set(gcf,'units',figunits);
else,
    pos = get(gcf,'position');
end
ff = (fs-4)*1.27*5/pos(4)*fudge;

% The 5 here reflects about 3 characters of height below
% an axis and 2 above. 1.27 is pixels per point.

% Determine the bounding rectangle for all the plots
% h = findobj('Type','axes');
% findobj is a 4.2 thing.. if you don't have 4.2 comment out
% the next line and uncomment the following block.

h = findobj(gcf,'Type','axes'); % Change suggested by Stacy J. Hills

% If you don't have 4.2, use this code instead
%ch = get(gcf,'children');
%h=[];
%for i=1:length(ch),
% if strcmp(get(ch(i),'type'),'axes'),
% h=[h,ch(i)];
% end
%end

max_y=0;
min_y=1;

oldtitle=0;
for i=1:length(h),
    if (~strcmp(get(h(i),'Tag'),'suptitle')),
        pos=get(h(i),'pos');
        if (pos(2) < min_y), min_y=pos(2)-ff/5*3;end;
        if (pos(4)+pos(2) > max_y), max_y=pos(4)+pos(2)+ff/5*2;end;
    else,

```

```

        oldtitle = h(i);
    end
end

if max_y > plotregion,
    scale = (plotregion-min_y)/(max_y-min_y);
    for i=1:length(h),
        pos = get(h(i),'position');
        pos(2) = (pos(2)-min_y)*scale+min_y;
        pos(4) = pos(4)*scale-(1-scale)*ff/5*3;
        set(h(i),'position',pos);
    end
end

np = get(gcf,'nextplot');
set(gcf,'nextplot','add');
if (oldtitle),
    delete(oldtitle);
end
ha=axes('pos',[0 1 1 1],'visible','off','Tag','suptitle');
ht=text(.5,titlepos-1,str);set(ht,'horizontalalignment','center','fontsize',fs);
set(gcf,'nextplot',np);
axes(haold);
if nargout,
    hout=ht;
end
end

```

```

%-----
% This function was obtained from www.mathworks.com
%-----
function y = shiftd(A,column,shift,type)

% PURPOSE: y = shiftd (A, column, shift) moves #column of matrix A downwards by #shift positions.
% INPUT ARGUMENTS:
% 'A' is the input matrix. ('A' can be a vector). 'column' is the number of the column to be shifted. If
% 'column' is zero, then all columns in the matrix are shifted. 'shift' is the number of positions by which the
% column is shifted down. 'type' is an optional argument. The shifted matrix-elements are discarded if
% this argument is 0 or is omitted, then vacated spaces at the top are filled with zeroes. The shifted
% matrix-elements are retained if 'type' is 1 or any other non-zero value, then vacated spaces at the top are
% filled with the shifted column-elements from the bottom (i.e. "wraparound").
%
[M,N] = size(A);
if column > N | column < 0, error('Invalid Column'); end
if shift < 0, error('Negative shift value - use "shifu" instead'); end
if shift > M, error('Shift value exceeds number of rows'); end

if column == 0
    if nargin == 4 & type ~= 0
        A = [A(M-shift+1:M,:); A(1:M-shift,:)];
    else
        A = [zeros(shift,N); A(1:M-shift,:)];
    end
end
else
    if nargin == 4 & type ~= 0
        A(:,column) = [A(M-shift+1:M,column); A(1:M-shift,column)];
    else
        A(:,column) = [zeros(shift,1); A(1:M-shift,column)];
    end
end
y = A;
Y=X;

```

```

%-----
% This function was obtained from www.mathworks.com
%-----
function y = shiftr(A,row,shift,type)

% PURPOSE:
% y = shiftr (A, row, shift) moves #row of matrix A to the right by #shift positions.
% INPUT ARGUMENTS:
% 'A' is the input matrix. ('A' can be a vector). 'row' is the number of the row to be shifted. If 'row' is zero,
% then all rows in the matrix are shifted. 'shift' is the number of positions by which the row is shifted
% to the right. % 'type' is an optional argument. The shifted matrix-elements are discarded if this
% argument is 0 or is omitted, then vacated spaces to the left are filled with zeroes. The shifted
% matrix-elements are retained if 'type' is 1 or any other non-zero value,
% then vacated spaces to the left are filled with the shifted row-elements from the right (i.e. "wraparound").
%
[M,N] = size(A);
if row > M | row < 0, error('Invalid Row'); end
if shift < 0, error('Negative shift value - use "shiftl" instead'); end
if shift > N, error('Shift value exceeds number of columns'); end

if row == 0
    if nargin == 4 & type ~= 0
        A = [A(:,N-shift+1:N) A(:,1:N-shift)];
    else
        A = [zeros(M,shift) A(:,1:N-shift)];
    end
end
else
    if nargin == 4 & type ~= 0
        A(row,:) = [A(row,N-shift+1:N) A(row,1:N-shift)];
    else
        A(row,:) = [zeros(1,shift) A(row,1:N-shift)];
    end
end
end
y = A;

```

```

%-----
% This function was obtained from www.mathworks.com
%-----
function y = shiffl(A,row,shift,type)

% PURPOSE:
% y = shiffl(A, row, shift) moves #row of matrix A to the left by #shift positions.
% INPUT ARGUMENTS: 'A' is the input matrix. ('A' can be a vector). 'row' is the number of the row to
% be shifted. If 'row' is zero, then all rows in the matrix are shifted. 'shift' is the number of positions by
% which the row is shifted to the right. 'type' is an optional argument. The shifted matrix-elements are
% discarded if this argument is 0 or is omitted, then vacated spaces to the right are filled with zeros.
% The shifted matrix-elements are retained if 'type' is 1 or any other non-zero value, then vacated spaces to
% the right are filled with the shifted row-elements from the left (i.e. "wraparound").
%
[M,N] = size(A);
if row > M | row < 0, error('Invalid Row'); end
if shift < 0, error('Negative shift value - use "shiftr" instead'); end
if shift > N, error('Shift value exceeds number of columns'); end

if row == 0
    if nargin == 4 & type ~= 0
        A = [A(:,1+shift:N) A(:,1:shift)];
    else
        A = [A(:,1+shift:N) zeros(M,shift)];
    end
else
    if nargin == 4 & type ~= 0
        A(row,:) = [A(row,1+shift:N) A(row,1:shift)];
    else
        A(row,:) = [A(row,1+shift:N) zeros(1,shift)];
    end
end
y = A;

```



```

%-----
% This function was obtained from www.mathworks.com
%-----
function y = shiftu(A,column,shift,type)

% PURPOSE:
% y = shiftu (A, column, shift) moves #column of matrix A upwards by #shift positions.
% INPUT ARGUMENTS: 'A' is the input matrix. ('A' can be a vector). 'column' is the number of the
% column to be shifted. If 'column' is zero, then all columns in the matrix are shifted. 'shift' is the number
% of positions by which the column is shifted vertically. 'type' is an optional argument. The shifted
% matrix-elements are discarded if this argument is 0 or is omitted, then vacated spaces on the bottom are
% filled with zeroes. The shifted matrix-elements are retained if 'type' is 1 or any other non-zero value,
% then vacated spaces on the bottom are filled with the shifted column-elements from the top (i.e.
% "wraparound").
%
[M,N] = size(A);
if column > N | column < 0, error('Invalid Column'); end
if shift < 0, error('Negative shift value - use "shiftd" instead'); end
if shift > M, error('Shift value exceeds number of rows'); end
if column == 0
    if nargin == 4 & type ~= 0
        A = [A(1+shift:M,:); A(1:shift,:)];
    else
        A = [A(1+shift:M,:); zeros(shift,N)];
    end
else
    if nargin == 4 & type ~= 0
        A(:,column) = [A(1+shift:M, column); A(1:shift, column)];
    else
        A(:,column) = [A(1+shift:M, column); zeros(shift,1)];
    end
end
y = A;

```

```

%-----
% This function was obtained from www.mathworks.com
%-----
function y = roundoff(number,decimal_places)

% Rounds a number (vector) to a specified number of decimal places

decimals = 10.^decimal_places;
y = fix(decimals*number + 0.5)./decimals;

```

APPENDIX B. List of Scanned Negatives

3-Bar Targets	USAF Museum
55target.tif	55aircraft.tif ✓
56target.tif	56aircraft.tif
57target.tif	56aircraft.tif
58target.tif	57aircraft.tif
59target.tif	58aircraft.tif
60target.tif	59aircraft.tif
61target.tif	60aircraft.tif
62target.tif	61aircraft.tif
63target.tif	62aircraft.tif
64target.tif	63aircraft.tif
65target.tif	64aircraft.tif
66target.tif ✓	65aircraft.tif
67target.tif	Enlarged Negatives
68target.tif	tar66a.tif ✓
69target.tif	target66u.tif ✓
70target.tif	plane55a.tif ✓
71target.tif	plane55b.tif ✓
72target.tif	ges1a.tif ✓ (7,283 feet)
73target.tif	
74target.tif	
75target.tif	
76target.tif	

BIBLIOGRAPHY

1. Alam, M. S., Bogнар, J. G., Hardie, R. C., Yashuda, B. J. "High Resolution Infrared Image Reconstruction using Multiple, Randomly Shifted, Low Resolution, Aliased Frames." *Proceedings of SPIE Aerosense, Orlando FL*, V3063, P102-112 (1997).
2. American Psychological Association. *Publication Manual of the American Psychological Association* (4th ed.). Washington, DC: Author (1994).
3. Banham, Mark R., & Katsaggelos, Aggelos, K. "Digital Image Restoration." *IEEE Signal Processing Magazine*, March, P24-41 (1997).
4. Barnard, Kenneth J., White, Carl E., & Absi, Anthony E. "Two-Dimensional Restoration of Motion-Degraded CCD Imagery." *Applied Optics*, V38, N10, P1942-1952 (1999).
5. Bishop, Christopher M. *Neural Networks for Pattern Recognition*. New York: Oxford University Press, Inc (1995).
6. Boyd, R.W. *Nonlinear Optics*. New York: Academic Press, Inc (1992).
7. Carrellas, P.T., & Fantone, S. D. "Lens Testing: the Measurement of MTF." *Photonics Spectra*, September, P133-138 (1989).
8. Chen, Q., Defrise, M., & Deconinck, F. "Symmetric Phase-Only Matched Filtering of Fourier-Mellin Transforms for Image Registration and Recognition." *IEEE Transactions on Pattern Analysis and Machine Intelligence*, V16, N12 (1994).
9. Condociu, Frank M., & Principe, Jose C. "Super-Resolution of Images Based on Local Correlations." *IEEE Transactions on Neural Networks*, V10, N2, P372-380 (1999).
10. Crane, R. *A Simplified Approach to Image Processing*. New Jersey: Prentice-Hall (1997).
11. Elad, M., & Feuer, Arie. "Super Resolution of an Image Sequence." *IEEE Transactions on Image Processing*, V8, N3, P387-395 (1999).
12. Gabriele, Mark David. *The Treaty on Open Skies and Its Practical Implications for the United States*. Ph.D. dissertation, Rand Graduate School, Santa Monica, California, 1998 (RGSD-143).
13. Gershenfeld, Neil. *The Nature of Mathematical Modeling*. New York: Cambridge University Press, Inc (1999).
14. Gonzalez, R., & Woods, R. *Digital Image Processing*. New York:

Addison-Wesley Publishing (1993).

15. Goodman, J. W. *Introduction to Fourier Optics*. New York: McGraw-Hill (1996).
16. Hanselman, D., & Littlefield, Bruce. *Mastering Matlab 5: A Comprehensive Tutorial and Reference*. New Jersey: Prentice-Hall (1998).
17. Hardie, R. C., Cain, S., Barnard, K. J., Bogнар, J. G., Armstrong, E. E., & Watson, E. A. "High-Resolution Image Reconstruction from a Sequence of Rotated and Translated Infrared Images." *Proceedings of SPIE Aerosense, Orlando FL*, V3063, P113-124 (1997).
18. Hardie, Russell C., Tuinstra, Timothy R., Bogнар, John G., Barnard, Kenneth J., & Armstrong, Ernest E. "High-Resolution Image Reconstruction from Digital Video with Global and Non-Global Scene Motion." *IEEE Transactions on Image Processing*, V3063, P153-156 (1997).
19. Hardie, Russell C., Barnard, Kenneth J., Armstrong, Ernest E., Bogнар, John G., & Watson, Edward A. "High-Resolution Image Reconstruction from a Sequence of Rotated and Translated Frames and its Application to an Infrared Imaging System." *Optical Engineering*, V37, N1, P247-260 (1998).
20. Hardie, Russell C., Barnard, Kenneth J., & Armstrong, Ernest E. "Joint MAP Registration and High-Resolution Image Estimation Using a Sequence of Undersampled Images." *IEEE Transactions on Image Processing*, V6, N12, P1621-1633 (1997).
21. Hunt, Bobby R., Overman, T. L., & Gough, Peter. "Image Reconstruction from Pairs of Fourier-transform Magnitude." *Optics Letters*, V23, N14, P1123-1125 (1998).
22. Hunt, Bobby R. "Super-Resolution of Images: Algorithms, Principles, Performance." *International Journal of Imaging Systems and Technology*, V6, P297-304 (1995).
23. Irani, M. & Peleg, S. "Improving Resolution by Image Registration." *CVGIP: Graphical Models and Image Processing*, V53, N3, P231-239 (1991)..
24. Jacquemod, G., Odet, C., & Goutte, R. "Image Resolution Enhancement Using Subpixel Camera Displacement." *Elsevier Signal Processing*, V26, P136-146 (1992).
25. Kaltenbacher, E. & Hardie, R. "High-Resolution Infrared Image Reconstruction Using Multiple, Low Resolution, Aliased Frames." *Proceedings of the IEEE NAECON Conference*, V2, P702-709 (1996).

26. Kim, S. P., Bose, N. K., & Valenzuela, H. M. "Recursive Reconstruction of a High Resolution Image from Noisy Undersampled Multiframe." *IEEE Transactions on Acoustics, Speech, and Signal Processing*, V38, N6, P1013-1027 (1990).
27. Kim, S. P. & Su, Wen-Yu. "Recursive High-Resolution Reconstruction of Blurred Multiframe Images." *IEEE Transactions on Image Processing*, V2, N4, P534-539 (1993).
28. Kundur, Deepa, & Hatzinakos, Dimitrios. "A Novel Blind Deconvolution. Scheme for Image Restoration Using Recursive Filtering." *IEEE Transactions on Signal Processing Magazine*, V46, N2, P375-390 (1998).
29. Kundur, Deepa, & Hatzinakos, Dimitrios. "Blind Image Deconvolution." *IEEE Signal Processing Magazine*, May, P43-64 (1996).
30. Mango, Steve (personal communication) Kodak Corporation, Subject: Grain size of Kodak 3404 film (January 4, 2000).
31. Mathworks Inc. *Matlab: Users Manual. (Release 11)*. Massachusetts: (1997).
32. Mathworks Inc. *Matlab: Image Processing Toolbox. (Version 2)*. Natick, Massachusetts (1997).
33. Matson, Charles L. "Error Reduction in Images using High-Quality Prior Knowledge." *Optical Engineering*, V336, N10, P3233-3236 (1994).
34. Miller, Casey, Hunt, Bobby R., Marcellin, Michael W., & Neifield, Mark A. "Image Restoration with the Viterbi Algorithm." *Journal of the Optical Society of America A*, V17, N2, P265-275 (2000).
35. National Air Intelligence Center. *German Open Skies Certification Document (Draft). TU-154 M Mission Equipment Sensors and Accessories (Trans.)*. Section 2.4, Wright-Patterson AFB, OH (1997).
36. National Air Intelligence Center: Open Skies Media Processing Facility. *Target Baseline Report*. Appendix A, para. 4.2.7. Wright-Patterson AFB, OH (1998).
37. Navy International Programs Office. Open Skies Treaty Web page: http://www.nawcwpns.navy.mil/~treaty/Open_Skies.html. Naval Air Warfare Center Weapons Division, China Lake, CA (1999).
38. Park, S. T., S and Schowengerdt, R., & Kaczynski, M. "Modulation-transfer-function analysis for sampled image systems." *Applied Optics*, V23, N15, P2572-2582 (1984).
39. Pratt, W. K. *Digital Image Processing*. New York: John Wiley & Sons (1978).

40. Redfern, D., & Campbell, C. *The Matlab 5 Handbook*. New York: Springer - Verlag (1998).
41. Roggeman, Michael C., & Tyler, David C. "Model-Based Image Reconstruction by Means of a Constrained Least-Squares Solution." *Applied Optics*, V36, N11, P2360-2369 (1997).
42. Sementilli, P. J., Hunt, Bobby R., & Nadar, M. S. "Analysis of the Limit to Super-resolution in Incoherent Imaging." *Journal of the Optical Society of America*, V10, N11, P2265-2276 (1993).
43. Sheppard, David G., Hunt, Bobby R., & Marcellin, Michael W. "Iterative Multiframe Super-Resolution algorithms for Atmospheric-Turbulence Degraded Imagery." *Journal of the Optical Society of America A*, V15, N, P978-992 (1998).
44. Stadtmiller, T. "Pixel Registration for Super Resolution Enhancement in Staring Infrared Imagers." Master's Thesis, University of Dayton (1996).
45. Tsai, R.Y., & Huang, T. S. "Multiframe Image Restoration and Registration." *Advances in Computer Vision and Image Processing*, V1, P317-339 (1984).
46. Walsh, David O., & Nielsen-Delaney, Pamela A. "Direct Method for Super-Resolution." *Journal of the Optical Society of America A*, V11, N2, P572-579 (1994).
47. Wang, Zhou, Yu, Yinglin, & Zhang, David. "Best Neighborhood Matching: An Information Loss Restoration Technique for Block-Based Image Coding Systems." *IEEE Transactions on Image Processing*, V7, N7, P1056-1061 (1998).

Vita

Captain Daniel E. Sperl was born on 29 September 1965 in Homestead, Florida. He graduated from Grace Baptist Academy in 1986. He entered undergraduate studies at Florida International University in Miami, Florida, where he graduated with a Bachelor of Science degree in Electrical Engineering. The USAF commissioned him through Detachment 155, AFROTC, at the University of Miami, Florida.

His first assignment was at the Ballistic Missile Organization (BMO) in September 1991. In October 1994, BMO disbanded and became Detachment 10, Space and Missile Systems Center. In August 1995, after acceptance into the AFIT Education with Industry Program (EWI) at Long Beach, California, he worked at McDonnell Douglas (now Boeing) on the C-17 Globemaster III program. Following Squadron Officer School at Maxwell AFB, Alabama, he transferred to Edwards AFB, California, where he managed flight tests. In August 1998, he entered the Electro-Optics program, School of Engineering, Air Force Institute of Technology. Upon graduation, his follow on assignment is the National Air Intelligence Center, Wright-Patterson AFB, Ohio.

Permanent Address: 1224 Winterhawk Drive
St. Augustine, FL 32086

REPORT DOCUMENTATION PAGE			Form Approved OMB No. 0704-0188	
Public reporting burden for this collection of information is estimated to average 1 hour per response, including the time for reviewing instructions, searching existing data sources, gathering and maintaining the data needed, and completing and reviewing the collection of information. Send comments regarding this burden estimate or any other aspect of this collection of information, including suggestions for reducing this burden, to Washington Headquarters Services, Directorate for Information Operations and Reports, 1215 Jefferson Davis Highway, Suite 1204, Arlington, VA 22202-4302, and to the Office of Management and Budget, Paperwork Reduction Project (0704-0188), Washington, DC 20503.				
1. AGENCY USE ONLY (Leave blank)		2. REPORT DATE Mar 2000		3. REPORT TYPE AND DATES COVERED Master's Thesis
4. TITLE AND SUBTITLE POST-PROCESSING RESOLUTION ENHANCEMENT OF OPEN SKIES PHOTOGRAPHIC IMAGERY			5. FUNDING NUMBERS	
6. AUTHOR(S) Daniel E. Sperl, Captain, USAF				
7. PERFORMING ORGANIZATION NAME(S) AND ADDRESS(ES) Air Force Institute of Technology Graduate School of Engineering and Management (AFIT/EN) 2950 P Street, Building 640 Wright-Patterson AFB OH 45433-7765			8. PERFORMING ORGANIZATION REPORT NUMBER AFIT/GEO/ENG/00M-03	
9. SPONSORING/MONITORING AGENCY NAME(S) AND ADDRESS(ES) NAIC/GTN Attn: Mr. Steve Hayden 4180 Watson Way Wright-Patterson AFB, OH 45433-5648 DSN:787-7048			10. SPONSORING/MONITORING AGENCY REPORT NUMBER	
11. SUPPLEMENTARY NOTES Dr. Steven C. Gustafson, ENG, DSN: 785-3636, ext. 4598				
12a. DISTRIBUTION AVAILABILITY STATEMENT APPROVED FOR PUBLIC RELEASE; DISTRIBUTION UNLIMITED.			12b. DISTRIBUTION CODE	
13. ABSTRACT (Maximum 200 words) The Treaty on Opens Skies allows any signatory nation to fly a specifically equipped reconnaissance aircraft anywhere over the territory of any other signatory nation. For photographic images, this treaty allows for a maximum ground resolution of 30 cm. The National Air Intelligence Center (NAIC), which manages implementation of the Open Skies Treaty for the US Air Force, wants to determine if post-processing of the photographic images can improve spatial resolution beyond 30 cm, and if so, determine the improvement achievable. Results presented in this thesis show that standard linear filters (edge and sharpening) do not improve resolution significantly and that super-resolution techniques are necessary. Most importantly, this thesis describes a prior-knowledge model fitting technique that improves resolution beyond the 30 cm treaty limit. The capabilities of this technique are demonstrated for a standard 3-Bar target, an optically degraded 2-Bar target, and the USAF airstar emblem.				
14. SUBJECT TERMS Super-Resolution, Model Fit, Spatial Domain, Error Reduction, Open Skies			15. NUMBER OF PAGES 97	
			16. PRICE CODE	
17. SECURITY CLASSIFICATION OF REPORT UNCLASSIFIED	18. SECURITY CLASSIFICATION OF THIS PAGE UNCLASSIFIED	19. SECURITY CLASSIFICATION OF ABSTRACT UNCLASSIFIED	20. LIMITATION OF ABSTRACT UL	